



January 2019

SPARC, A Matricellular Protein, In A Cell Culture Model Of Heavy Metal Cadmium Induced Bladder Urothelial Carcinoma

Emily Rae Biggane

Follow this and additional works at: <https://commons.und.edu/theses>

Recommended Citation

Biggane, Emily Rae, "SPARC, A Matricellular Protein, In A Cell Culture Model Of Heavy Metal Cadmium Induced Bladder Urothelial Carcinoma" (2019). *Theses and Dissertations*. 2546.
<https://commons.und.edu/theses/2546>

This Dissertation is brought to you for free and open access by the Theses, Dissertations, and Senior Projects at UND Scholarly Commons. It has been accepted for inclusion in Theses and Dissertations by an authorized administrator of UND Scholarly Commons. For more information, please contact zeinebyousif@library.und.edu.

SPARC, A MATRICELLULAR PROTEIN, IN A CELL CULTURE MODEL OF
HEAVY METAL CADMIUM INDUCED BLADDER UROTHELIAL CARCINOMA

by

Emily Rae Biggane
Bachelor of Arts, Minot State University, 2013

A Dissertation

Submitted to the Graduate Faculty

of the

University of North Dakota

in partial fulfillment of the requirements

for the degree of

Doctor of Philosophy


Grand Forks, North Dakota

August
2019

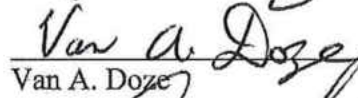
Copyright 2019 Emily Biggane

This dissertation, submitted by Emily Rae Biggane in partial fulfillment of the requirements for the degree of Doctor of Philosophy from the University of North Dakota, has been read by the Faculty Advisory Committee under whom the work has been done and is hereby approved.


Jane R. Dunlevy, Chairperson


David S. Bradley


Holly M. Brown-Borg


Van A. Doze


Scott H. Garrett


Seema Somji

This dissertation is being submitted by the appointed advisory committee as having met all of the requirements of the School of Graduate Studies at the University of North Dakota and is hereby approved.


Dr. Chris Nelson, Associate Dean
School of Graduate Studies

7/19/19
Date

PERMISSION

Title SPARC, a matricellular protein, in a cell culture model of heavy metal
 cadmium induced bladder urothelial carcinoma

Department Biomedical Sciences

Degree Doctor of Philosophy

In presenting this dissertation in partial fulfillment of the requirements for a graduate degree from the University of North Dakota, I agree that the library of this University shall make it freely available for inspection. I further agree that permission for extensive copying for scholarly purposes may be granted by the professor who supervised my dissertation work or, in her absence, by the Chairperson of the department or the dean of the School of Graduate Studies. It is understood that any copying or publication or other use of this dissertation or part thereof for financial gain shall not be allowed without my written permission. It is also understood that due recognition shall be given to me and to the University of North Dakota in any scholarly use which may be made of any material in my dissertation.

Emily Biggane
June, 20, 2019

TABLE OF CONTENTS

LIST OF FIGURES.....	xi
LIST OF TABLES.....	xiv
ACKNOWLEDGEMENTS.....	xv
ABSTRACT.....	xvii
CHAPTER	
I. INTRODUCTION.....	1
II. SPARC AND BLADDER UROTHELIAL CARCINOMA CELL ATTACHMENT, SPREADING, AND MIGRATION	34
Introduction.....	34
Materials and Methods.....	38
Cell Culture.....	38
Wound Closure Assay.....	38
Cell Attachment and Spreading Under Normal Tissue Culture Conditions.....	39
Fiji and PHANTAST Image Pre-Processing.....	39
Leica LASX Image Analysis.....	41
Cell Attachment and Spreading Assay on Collagen I Matrix.....	43
Modified Cell Attachment and Spreading Assay on a Collagen I Matrix.....	44

Immunofluorescent Microscopy during Cell Spreading.....	44
SPARC siRNA Transfection in the Cd #1-SPARC Transfected Cell Line.....	45
RNA and Protein Isolation from Cd #1-SPARC Transfected Cell Line.....	46
RT-qPCR Analysis of SPARC siRNA Transfected Cd #1-SPARC Cells.....	47
Western Blot Analysis of SPARC siRNA Transfected Cd #1-SPARC Cells.....	48
Statistics.....	49
Results.....	50
Wound Closure of SPARC ⁺ UROtsa Parent, Cd #1, and the Respective Cd #1-SPARC Transfected Cell Lines.....	50
Cell Attachment and Spreading Under Normal Tissue Culture Conditions.....	53
FIJI PHANTAST Cell Attachment and Spreading Image Processing.....	54
Leica LASX Cell Attachment and Spreading Image Analysis.....	56
Preliminary Cell Attachment and Spreading of SPARC Expressing and Non-SPARC Expressing Urothelial Cells on a Collagen I Matrix.....	60
Cell Attachment and Spreading of SPARC Expressing and Non-SPARC Expressing Urothelial Cells on a Collagen I Matrix.....	63
Immunofluorescent Microscopy of F-actin during Cell Spreading.....	68

	SPARC siRNA Knockdown in Cd #1-SPARC Transfected Cell Line.....	69
	Cell Attachment and Spreading Following SPARC siRNA Knockdown in Cd #1-SPARC Cells.....	71
	Discussion.....	75
III.	TRANSCRIPTION FACTOR BINDING AND SPARC REPRESSION IN CD-TRANSFORMED UROTHELIAL CARCINOMA CELLS.....	79
	Introduction.....	79
	Materials and Methods.....	85
	Cell Culture.....	85
	RNA and Protein Isolation from SPARC ⁺ UROtsa Parent and Cd #1 Cell Lines.....	85
	RT-qPCR Analysis of Sp1, Sp3 and SOX5 Transcription Factors in SPARC ⁺ UROtsa Parent and Cd #1 Cell Lines.....	85
	Western Blot Analysis of Sp1, Sp3 and SOX5 Transcription Factors in SPARC ⁺ UROtsa Parent and Cd #1 Cell Lines.....	86
	PCR Primer Design Using NCBI Genome Browser and Oligo7 for Transcription Factor Binding to SPARC Promoter.....	87
	Genomic DNA Isolation from SPARC ⁺ UROtsa Parent Cell Line.....	89
	Conventional PCR and Gel Electrophoresis of Genomic DNA from SPARC ⁺ UROtsa Parent Cell Line.....	89
	Chromatin ImmunoPrecipitation Assay for Sp1, Sp3, and SOX5 Transcription Factors in SPARC ⁺ UROtsa Parent and Cd #1 Cell Lines.....	91

Conventional PCR and Gel Electrophoresis of Sp1, Sp3 and SOX5 ChIP DNA in SPARC ⁺ UROtsa Parent and Cd#1 Cell Lines.....	94
Sp1, Sp3, and SOX5 siRNA Transfection of SPARC ⁺ UROtsa Parent and Cd#1 Cell Lines.....	95
RNA Isolation of Sp1, Sp3, and SOX5 siRNA Transfected SPARC ⁺ UROtsa Parent and Cd#1 Cell Lines.....	96
RT-qPCR Analysis of Sp1, Sp3, and SOX5 Transcription Factors in siRNA Treated SPARC ⁺ UROtsa Parent and Cd#1 Cell Lines.....	96
RT-qPCR Analysis of SPARC mRNA Expression in siRNA Treated SPARC ⁺ UROtsa Parent and Cd#1 Cell Lines.....	96
Statistics.....	97
Results.....	97
Sp1 mRNA and Protein Expression in SPARC ⁺ UROtsa Parent and Cd #1 Cell Lines.....	97
Sp3 mRNA and Protein Expression in SPARC ⁺ UROtsa Parent and Cd #1 Cell Lines.....	98
SOX5 mRNA and Protein Expression in SPARC ⁺ UROtsa Parent and Cd #1 Cell Lines.....	99
ChIP Analysis of Sp1 and/or Sp3 Transcription Factor Binding to the SPARC Gene Promoter in UROtsa Parent and Cd #1 Cell Lines.....	100
ChIP Analysis of SOX5 Transcription Factor Binding to the SPARC Gene Promoter in UROtsa Parent and Cd #1 Cell Lines.....	102
Sp1, Sp3, and SOX5 mRNA Expression in siRNA Treated SPARC ⁺ UROtsa Parent and Cd #1 Cell Lines.....	103

	SPARC mRNA Expression in siRNA Treated SPARC ⁺ UROtsa Parent and Cd #1 Cell Lines.....	107
	Discussion.....	109
IV.	SPARC AND TUMOR INITIATION IN SERIALY TRANSPLANTED BLADDER UROTHELIAL TUMORS.....	113
	Introduction.....	113
	Materials and Methods.....	118
	Cell Culture.....	118
	RNA and Protein Isolation From SPARC ⁺ UROtsa Parent, Cd #1, and Cd #1-SPARC Cell Lines.....	119
	RT-qPCR Analysis of SPARC mRNA Expression in SPARC ⁺ UROtsa Parent, Cd #1, and Cd #1-SPARC Cell Lines.....	119
	Secreted SPARC Protein Purification from Media of SPARC ⁺ UROtsa Parent, Cd #1, and Cd #1-SPARC Cell Lines.....	119
	Visualization of SPARC Expression in SPARC ⁺ UROtsa Parent, Cd #1, and Cd #1-SPARC Cell Lines via Immunofluorescent Microscopy.....	120
	Serial Heterotransplant Tumors in Nude Mice.....	121
	Immunohistochemical Localization of SPARC Protein Expression in Serial Heterotransplant Tumors.....	122
	Immunohistochemical Localization of α -Smooth Muscle Actin Protein Expression in Serial Heterotransplant Tumors.....	123
	RNA Isolation from Serial Heterotransplant Tumors....	123
	RT-qPCR Analysis of hSPARC and mSPARC mRNA Expression in Serial Heterotransplant Tumors.....	124

Recombinant hSPARC or mSPARC Treatment of Cd #1-SPARC Cell Line.....	124
RNA Isolation of Cd #1-SPARC Cell Line Following Recombinant SPARC Treatment.....	125
RT-qPCR Analysis of SPARC Expression in Cd #1-SPARC Cell Line Following Recombinant SPARC Treatment.....	126
Statistics.....	126
Results.....	126
SPARC mRNA and Secreted Protein Expression in SPARC ⁺ UROtsa Parent, Cd #1, and Cd #1-SPARC Cell Lines.....	126
Immunofluorescent Microscopy of SPARC Expression in SPARC ⁺ UROtsa Parent, Cd #1, and Cd #1-SPARC Cell Lines.....	128
Immunohistochemical Localization of SPARC Protein Expression in Serial Heterotransplants.....	131
Human SPARC and Mouse SPARC mRNA Expression in Serial Heterotransplants.....	136
SPARC mRNA Expression in Cd #1-SPARC Cell Line Following Recombinant SPARC Treatment.....	139
Discussion.....	141
V. DISCUSSION.....	148
REFERENCES.....	164

LIST OF FIGURES

Figure		Page
I-1.	Histology of the Urinary Bladder.....	2
I-2.	Urothelial Tumor Progression.....	4
I-3	Cadmium Cellular Transport.....	11
I-4	SPARC Ribbon Structure and Proposed Cellular Functions.....	20
I-5	Various Roles for SPARC in Cancer.....	28
II-1.	Attachment and Spreading of Adherent Cells.....	36
II-2.	Phase Contrast Images of Wound Closure.....	52
II-3.	Percent Wound Closure and SPARC Expression.....	53
II-4.	Preliminary Cell Attachment and Spreading Assay under Normal Tissue Culture Conditions.....	54
II-5.	Cell Attachment and Spreading Assay Image Processing.....	55
II-6.	LASX Classifier Image.....	57
II-7.	Classification Comparison of SPARC ⁺ UROtsa Parent Cells.....	59
II-8.	Preliminary Cell Spreading Assay Quantitation on a Collagen I Matrix.....	61
II-9.	Preliminary Relative Surface Area Comparison of Attached Cells	62
II-10.	Preliminary Total Cell Attachment on a Collagen I Matrix.....	63
II-11.	Quantitation of Cell Spreading on a Collagen I Matrix.....	65
II-12.	Relative Surface Area Comparison of Attached Cells.....	67
II-13.	Total Cell Attachment on a Collagen I Matrix.....	68

II-14.	F-Actin Localization during Cell Spreading on a Collagen I Matrix.....	69
II-15.	siRNA Knockdown of SPARC in Cd #1-SPARC Cells.....	70
II-16.	Quantitation of Cell Spreading Following SPARC siRNA Knockdown.....	72
II-17.	Relative Surface Area Comparison of Attached Cells Following SPARC siRNA Knockdown.....	74
II-18.	Total Cell Attachment on a Collagen I Matrix Following SPARC siRNA Knockdown.....	75
III-1.	Sp1 mRNA and Protein Expression in SPARC ⁺ UROtsa Cells and Non- SPARC Expressing Cd #1 Cells.....	98
III-2.	Sp3 mRNA and Protein Expression in SPARC ⁺ UROtsa Cells and Non- SPARC Expressing Cd #1 Cells.....	99
III-3.	SOX5 mRNA and Protein Expression in SPARC ⁺ UROtsa Cells and Non-SPARC Expressing Cd #1 Cells.....	100
III-4.	Chromatin ImmunoPrecipitation Analysis of Sp1/Sp3 Binding at the SPARC Promoter.....	101
III-5.	Chromatin ImmunoPrecipitation Analysis of SOX5 Binding at the SPARC Promoter.....	102
III-6.	Sp1 mRNA Expression in SPARC ⁺ UROtsa Cells and Non-SPARC Expressing Cd #1 Cells Following siRNA Knockdown of Sp1.....	104
III-7.	Sp3 mRNA Expression in SPARC ⁺ UROtsa Cells and Non-SPARC Expressing Cd #1 Cells Following siRNA Knockdown of Sp3.....	105
III-8.	SOX5 mRNA Expression in SPARC ⁺ UROtsa Cells and Non-SPARC Expressing Cd #1 Cells Following siRNA Knockdown of SOX5.....	106
III-9.	SPARC mRNA Expression in SPARC ⁺ UROtsa Cells and Non-SPARC Expressing Cd #1 Cells Following siRNA Knockdown of Sp1, Sp3, or SOX5.....	108
IV-1.	SPARC mRNA and Secreted Protein Expression in SPARC ⁺ UROtsa Parent, Non-SPARC Expressing Cd #1, and Cd #1-SPARC Transfected Cells.....	128
IV-2.	Visualization of SPARC Expression in UROtsa Parent, Cd #1, and Cd #1-SPARC using Confocal Microscopy.....	130

IV-3. Immunohistochemistry Images of SPARC Expression in Serial Bladder Heterotransplant Tumors.....	132
IV-4. Immunohistochemistry Images of SPARC Expression within Tumor cells of Serial Bladder Heterotransplant Tumors.....	135
IV-5. Human and Mouse SPARC mRNA Expression in Serial Bladder Heterotransplant Tumors.....	138
IV-6. SPARC mRNA Expression in Cd #1-SPARC Cells Exposed to Recombinant hSPARC or Recombinant mSPARC.....	140

LIST OF TABLES

Table	Page
1. LASX Classification Measurements.....	57
2. Sp1/Sp3 and SOX5 Primer Sequences.....	88
3. Summary of Immunohistochemistry Staining for SPARC Expression in Serial Bladder Heterotransplant Tumors.....	133

ACKNOWLEDGEMENTS

First and foremost, I would like to extend my sincerest thank you to my advisor Dr. Jane Dunlevy. She graciously welcomed me into her lab and has supported me 100% in my time with her. Her guidance, support, passion, and dedication has been instrumental to my training as well as my all-around experience as a graduate student. I cannot possibly express my gratitude in enough words to thank her for everything she has done for me. Although my time in her lab is nearing the end, I will cherish the memories and know that I will always have her guidance and support as I move into my career.

I would also like to thank my committee members: Dr. Jane Dunlevy, Dr. Scott Garrett, Dr. David Bradley, Dr. Holly Brown-Borg, Dr. Van Doze, and Dr. Seema Somji for their advice and support. I want to extend an additional thank you to Dr. Don Sens for his collaboration and financial support throughout my time here. Thank you to Dr. Xu Dong and Yan Wang for helping me with the immunohistochemistry experiments. Yan's smile is infectious and I will never forget the excitement from successful staining.

Thank you to the Biomedical Sciences faculty for their overall support at seminars and interest in my success. A special thank you to Dr. Catherine Brissette and the Biomedical Sciences Graduate Admissions Committee for making me feel welcome and for valuing my opinion. Additionally, I want to extend a special thank you to Michelle Montgomery for her support and guidance. I am exceptionally grateful to have met her and have her become an important part of my life.

I want to extend a very special thank you to my lab mates who have become lifelong friends. They have made my time in the lab enjoyable and I will miss seeing them across the bench. Dr. Swojani Shrestha, Dr. Bethany Davis, Zach, Ashlee, and Danielle I will especially miss our volleyball nights. Thank you to Dr. Andrea Nore for her overall guidance and support as well as her help with the heterotransplant study. Thank you to the Biomedical Sciences graduate students and especially my cohort of students. I am so grateful for their friendship and support throughout the years, and I look forward to seeing everyone's success.

A special thank you to my family and my dear friend Mia. Thank you to my mom, Rhonda, and dad, Scott, for their love and support from the very beginning and seeing the potential in everything I do. To my sister, Erin, and my brother, Easton, for their support and continuously bringing a smile to my face. And, thank you to Mia for her friendship, utmost support, and listening ear. I could not have made it without her.

To my husband Joe, who has seen me at my worst and at my best. His love, patience, and support have been my rock throughout my graduate school career. He has helped me realize my potential and I would not be where I am today without him. We have been through more than most and I cannot thank him enough for never giving up on me.

Last, but not least, my dearest Eleanor Louise. She has been a blessing in disguise and an inspiration for me to be the best I can be. I could not imagine doing this without her. Her smiles, hugs, kisses, and two year old conversations bring so much joy to my life and help keep me motivated. One day I hope she can understand how important she was to my success in graduate school. Eleanor, this is for you.

ABSTRACT

Bladder cancer, the most common urinary tract malignancy, has environmental toxicant exposure as one of its biggest risk factors. This lab examines potential biomarkers employing an *in vitro* model of urothelial carcinoma using a normal bladder cell line and its malignantly transformed cells transformed counterpart, transformed by exposure to long term, low doses of cadmium (Cd^{2+}). Initial microarray analysis determined that Secreted Protein Acidic and Rich in Cysteine (SPARC) was the most repressed gene across all transformed cell lines compared to its normal counterpart (Garrett et al., 2014, Larson et al., 2010).

SPARC, an extracellular matrix glycoprotein, functions by regulating cell-matrix interactions. It has both oncogene and tumor suppressor actions depending upon the cancer with its role in bladder carcinoma remaining unclear. Previous lab results identified three key findings regarding the role of SPARC: 1) SPARC was significantly repressed following short term, low dose cadmium exposure; 2) SPARC is expressed at moderate levels in the normal transitional epithelium, however, in urothelial carcinomas, SPARC expression is drastically repressed; and 3) when SPARC was transfected into Cd^{2+} transformed cells with expression being ‘forced’ via a CMV promoter, heterotransplant tumors again had very little, if any, SPARC expression (Larson et al., 2010; Slusser et al., 2016).

The current study is based on 3 overarching hypotheses: 1) SPARC plays a critical role in urothelial cell proliferation, migration, attachment, and spreading; 2)

Cadmium transformation significantly decreases SPARC expression by silencing the promoter early in the malignant transformation process; and 3) that in urothelial tumors generated from Cd²⁺-transformed cell lines, SPARC is prohibitive to tumor initiation.

The results of this study advance the understanding of SPARC in transformed cells by showing that SPARC promotes cell spreading which may be inhibitory to tumor initiation, necessitating its repression; preferential transcription factor binding of SOX5 compared to Sp1/Sp3 contributing to SPARC repression; and that in serial heterotransplant tumors, repression of human tumor SPARC continues along with an increase in mouse stromal SPARC. Overall, the conclusion from this research is that SPARC acts as a tumor suppressor in the UROtsa model system requiring repression for malignant transformation and tumor initiation.

CHAPTER I

INTRODUCTION

The bladder is an organ located in the bowl of the pelvis and is part of the urinary tract. The urinary tract is comprised of the kidneys, ureters, bladder, and urethra. The kidneys function to filter waste products from cellular processes into urine that then travels down to the bladder through the ureters. The bladder is a muscular organ that distends acting as a reservoir for urine, and contracts to expel the urine out through the urethra.

Histologically, the urinary tract, from the renal pelvis of the bladder to the proximal urethra, is lined with transitional epithelium, called urothelium. The urothelium contains umbrella-like cells on the apical surface that are in direct contact with the urine (Anderson, 2018; Pawlina, 2016). They are flexible cells that flatten when the bladder distends in order to keep the epithelial barrier intact and maintain separation between the urine and vulnerable underlying tissue. The urothelial plaques and hinges help to make the urothelium one of the most flexible and impermeable membranes in the human body (Wu et al., 2009, Negrete et al., 1996). Urothelial plaques are aggregates of uroplakin proteins interrupted by small plasma membrane hinge regions that cover nearly 90% of the apical surface of the urothelium (Lewis, 2000, Wu et al., 2009). The N-terminal luminal regions of the uroplakin proteins are heavily glycosylated creating a “sticky” glycocalyx that is important for the physical and chemical barrier between concentrated waste products and the underlying tissue (Kałtnik-Prastowska et al., 2014). The lamina

propria is the layer of connective tissue situated below the epithelial layer and superficial to the muscularis layer. This layer contains necessary immune cells and the vasculature that supplies the superficial epithelial layer with important nutrients. The muscle of the bladder is termed the Detrusor muscle and is comprised of three alternating layers of muscle. This layering of muscle increases the contractile strength of the bladder to adequately expel urine. The outer most surface of the bladder is surrounded by a connective tissue capsule that helps to preserve the integrity of the layers of the bladder and protect it from physical injury. Figure I-1 depicts the thickness of the bladder at the cellular and molecular level emphasizing the importance of isolating the waste products from the rest of the body and properly expelling the toxic waste.

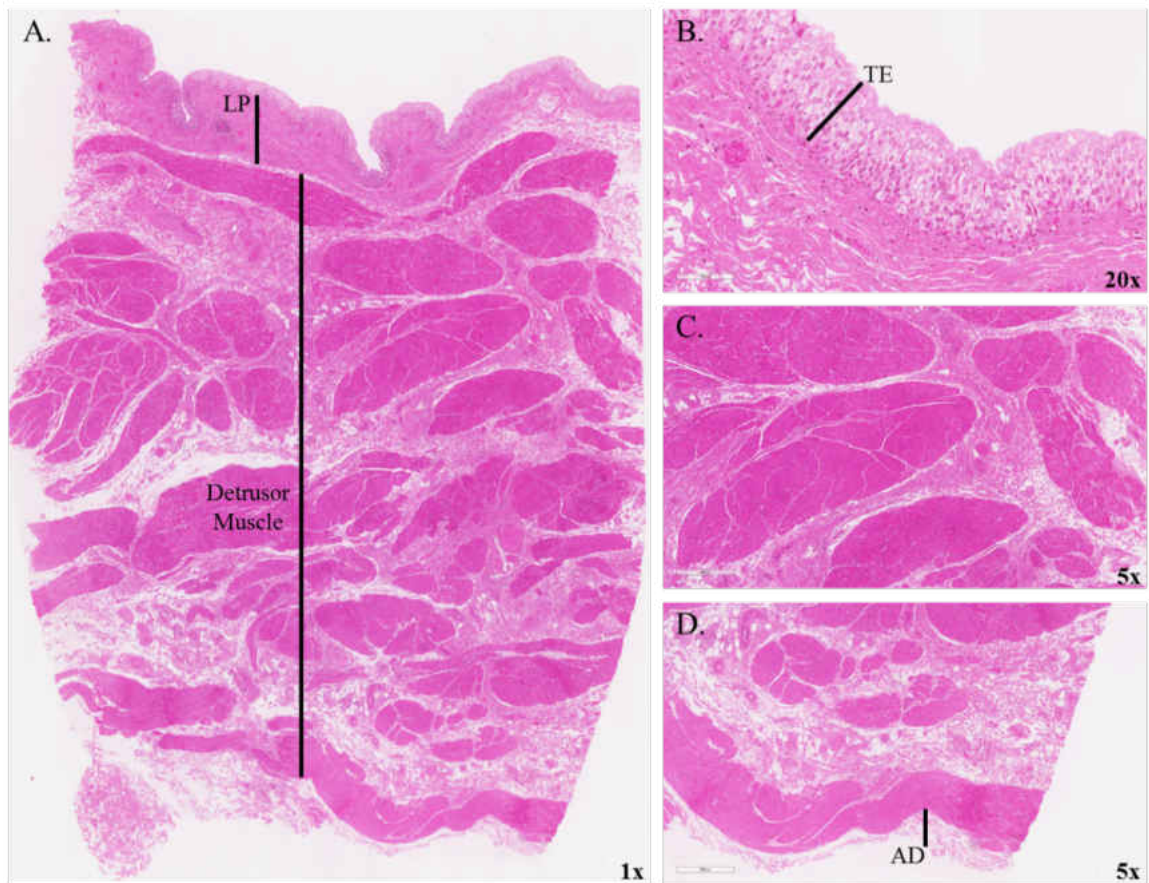


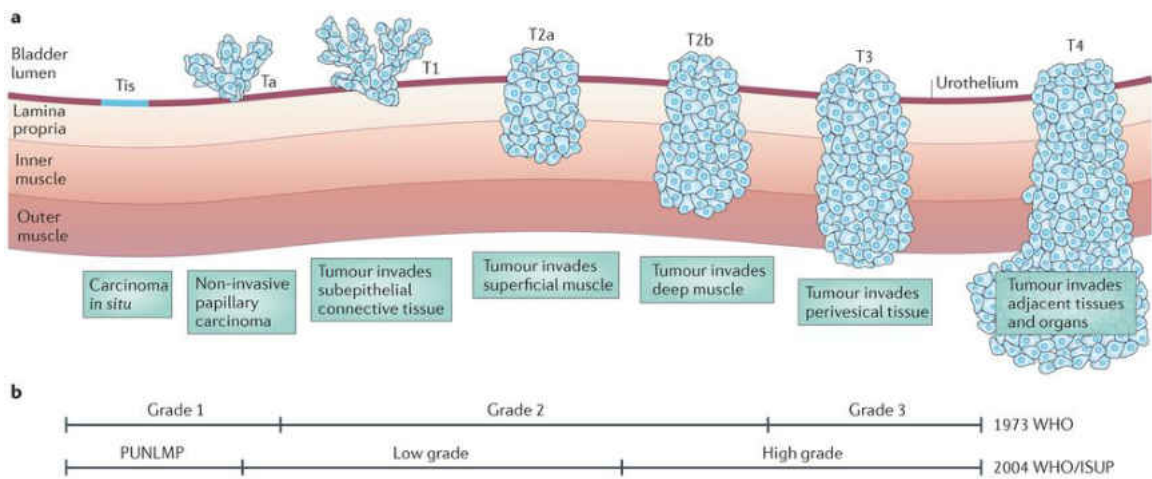
Figure I-1. Histology of the Urinary Bladder. Histological layers of the bladder illustrating: the transitional epithelium, lamina propria (LP), thick Detrusor muscle, and

adventia. (A) 1x overview of the bladder, (B) 20x magnification of transitional epithelium (TE) and lamina propria, (C) 5x magnification of Detrusor muscle, (D) 5x magnification of outer muscle layer, and adventitia (AD). [UND SMHS Virtual Slide Collection]

The bladder, like the majority of organs in the body, is not immune to the devastating disease of cancer. Bladder cancer is the most commonly diagnosed cancer of the urinary tract (Anderson, 2018). It is diagnosed in approximately 400,000 new patients each year around the world making it one of the most prevalent types of cancer (Inamura, 2018). In 2019 it is estimated that over 80,000 new cases of bladder cancer will be diagnosed in the United States with over 17,000 patients succumbing to this disease. Men are approximately three to four times more likely to be diagnosed with bladder cancer than are women (ACS Facts and Figures 2019). However, women are older, on average, at the time of diagnosis, present in the clinic with more advanced disease, and tend to have a poorer survival rate than men (Anderson, 2018). It is the most expensive cancer to treat per patient lifetime due to a high rate of recurrence that requires long-term treatment and monitoring (Kaffenberger et al., 2018, Jung et al., 2018).

There are multiple types of bladder cancer with urothelial carcinoma or transitional cell carcinoma being the most common type, affecting the transitional epithelial layer of cells in direct contact with the urine (Jacobs et al., 2010, Kamat et al. 2016). Like other cancers, the specific type of bladder cancer determines the form of treatment needed to manage the disease as best as possible (Kamat et al., 2016). 75% of bladder cancer diagnoses are urothelial carcinomas which are non-muscle invasive tumors (Kamat et al., 2016, Kaffenberger et al., 2018). The majority of the non-muscle invasive bladder cancers (NMIBC) are low-grade papillary tumors that do not have a high rate of progression (10-30%) but they have an alarmingly high rate of recurrence at

50-70% (Kamat et al, 2016, Anderson, 2018, Inamura, 2018). The low- and intermediate-risk papillary NMIBC tumor type protrudes into the lumen of the bladder compared to the high-risk NMIBC carcinoma *in situ* (CIS) that is flat within the urothelium as seen in Figure I-2. CIS is considered high-risk because it has been shown to progress to muscle-invasive bladder cancer (MIBC) in many cases (Barth et al., 2018). MIBCs progressively invade through the thick Detrusor muscle and into adjacent organs as well as the peritoneal cavity, ultimately increasing the chances of metastasis (Knowles and Hurst, 2015).



Nature Reviews | Cancer

Figure I-2. Urothelial Tumor Progression. Urothelial tumor progression from carcinoma *in situ* to T4 metastatic tumor and associated grading represented by the 1973 WHO grading system as well as the updated 2004 WHO/ISUP system. [Reprinted from Knowles and Hurst, 2015, with © permission from Springer Nature Publishing]

The most common and most correlated symptom of bladder cancer that presents in the clinic is haematuria which warrants further diagnostic testing (Kamat et al., 2016). In these patients, various forms of imaging are used to evaluate the urinary tract. The upper urinary tract is examined using computed tomography (CT) urography and the lower urinary tract is examined using cystoscopy (Kamat et al., 2016). CIS is inherently

difficult to detect via cystoscopy because it is flat and incorporated into the urothelium presenting a disadvantage to this imaging technique (Jacobs et al., 2010).

Once diagnosed, the standard of care is to remove the tumor via TransUrethral Resection of the Bladder Tumor (TURBT) (Kamat et al, 2016, Anderson, 2018, Kaffenberger et al., 2018). However, there are issues that arise from this procedure including increased recurrence rates, in part, due to tumor cells breaking off during resection increasing the possibility of cells implanting elsewhere in the bladder and establishing a potential recurrence site (Anderson, 2018).

Currently, intravesical chemotherapy or immunotherapy treatments are in place to help reduce recurrence attributed to TURBT to slightly less than 40% (Kaffenberger et al., 2018). For low- and intermediate-risk non-muscle invasive bladder carcinomas it is recommended to administer a chemotherapeutic agent, most commonly mitomycin-C, directly into the bladder immediately following a TURBT procedure. This treatment appears more beneficial for intermediate-risk NMIBC patients when administering follow-up maintenance doses for one year (Kamat et al., 2016). Although proven efficacious, treatment of bladder cancer with mitomycin-C has been slow to be incorporated into the clinic due to its expense, its availability, and most importantly, its potential toxicity (Kaffenberger et al., 2018). High-risk non-muscle invasive bladder cancer has been shown to respond better to intravesical immunotherapy compared to chemotherapy. Most commonly, Bacillus Calmete-Guerin (BCG) is used in these cases (Kamat et al., 2016). It is a live strain of mycobacterium that recruits and activates the patient's own immune cells to attack the tumor (American Cancer Society, 2016, Anderson, 2018). As with chemotherapy treatment, BCG immunotherapy has been

shown to be most effective when followed up with maintenance treatment for one to three years (Kamat et al., 2016, Anderson, 2018). Due to the high recurrence rate of bladder tumors, surveillance cystoscopy is recommended four times per year for one to two years followed by annual scans (Jacobs et al., 2010). Although the majority of bladder cancer diagnoses will not progress to muscle-invasive bladder cancers, studies show that repeated scans, procedures, and treatments have a substantial impact on patient quality of life (Jung et al., 2018). This illustrates the desperate need for a therapeutic target to help decrease the high recurrence rate and increase patient quality of life.

Biomarkers are researched and used for many conditions and diseases, including cancer. Generally, a biomarker is defined as a substance that is measurable and able to be used to indicate normal function as well as the potential and/or presence of disease (Strimbu and Tavel, 2010). There are numerous categories of biomarkers utilized by researchers and clinicians to further understand: disease risk, prediction, diagnosis, treatment, and even safety of a medical therapeutic or environmental agent (FDA-NIH, 2016, Mayeux, 2004). Traditionally, clinical condition or disease has allowed researchers to better identify a key missing or over-active component of a biological process, as well as the safety of a substance (Mayeux, 2004). Therefore, a majority of known biomarkers when absent or present, functional or non-functional can result/predict a range of abnormalities. These biomarkers can then be used to: implement preventative strategies to minimize disease, determine the best course of treatment, as well as create laws for public safety (FDA-NIH, 2016). Researchers are continually aimed at identifying and developing new therapeutic targets or biomarkers to advance medicine. However, a complicating factor emerges when a lab-based biomarker does not succeed in clinical

settings (Strimbu and Tavel, 2010). There is extensive and necessary testing to be done prior to a biomarker reaching the clinical setting to minimize failure and better predict success; but, the true potential therapeutic benefit can only be determined in the clinic (FDA-NIH, 2016). The ultimate end goal of biomedical research is to positively impact human health, making biomarker research important to the scientific community as well as the general public.

Numerous cancer types have at least one biomarker associated with them; however, some are more well-known than others. BRCA 1/2 gene mutations can be used as susceptibility biomarkers to predict a patient's risk of developing breast or ovarian cancer; which, can be followed by preventative intervention to reduce or minimize clinical outcome (FDA-NIH, 2016). Estrogen receptor (ER), progesterone receptor (PR), and human epidermal growth factor receptor 2 (HER2) status can be used as predictive biomarkers to determine the best course of treatment for breast cancer patients (Clark et al., 2019). Many molecules have been studied as potential biomarkers for transitional cell carcinoma, including: p53 status, ERCC2 and other DNA damage response genes, programmed death ligand-1 (PD-L1), fibroblast growth factor receptor 3 (FGFR3), as well as alterations in epidermal growth factor receptor (EGFR) and human epidermal growth factor receptor 2 and 3 (HER2 and 3). Unfortunately, there remains to be a reliable biomarker utilized in the clinic for bladder cancer (Cheng and Iyer, 2018, Miremami and Kyprianou, 2014, Tabayoyong and Kamat, 2018). Invasive cystoscopy and non-invasive cytology are the recognized diagnosis tools for bladder cancer; however, both have limitations in regards to accurate visualization and sensitivity, respectively (Tabayoyong and Kamat, 2018). The FDA has approved a select few

markers to be used in conjunction with, not in place of, cystoscopy and cytology due to lower sensitivity (Tabayoyong and Kamat, 2018). However, there are no biomarkers approved for standard of care guided urinary bladder cancer treatment (Cheng and Iyer, 2018). Therefore, there is a desperate need for bladder cancer biomarkers to decrease recurrence rates and increase patient quality of life by providing less invasive long-term monitoring.

Bladder cancer has a number of known risk factors, including age and environmental exposure to toxicants (Anderson, 2018, Inamura, 2018, Kaffenberger, et al., 2018). It has a strong link to environmental toxicant exposure; in part, due to the body filtering toxicants into the urine that is then stored and concentrated in the bladder. Toxicant exposure has also been proposed to address the increased frequency of bladder cancer in men; stating that men held occupations in industrial settings and were more likely to smoke increasing exposure to toxicants (Dobruch et al., 2016, Kirkali et al., 2005). Animal research by Reid et al. (1984), also suggests a role for sex-specific hormones in either promoting, or not inhibiting, oncogenesis (androgen), and conversely, inhibiting, or not promoting, oncogenesis (estrogen) (Dobruch et al., 2016, Kirkali et al., 2005). However, this does not fully address the disparity between men and women in regards to bladder cancer and should be further researched.

A particular environmental toxicant studied in our lab is cadmium. Cadmium is a heavy metal element that is naturally occurring in the Earth's crust (Bernhoft, 2013). In the periodic table it falls near zinc (Zn) and mercury (Hg) and takes on chemical similarities to zinc (Bernhoft, 2013). Humans can be exposed to cadmium through a variety of different mechanisms. Non-smokers are mainly exposed to cadmium through

ingestion of contaminated food and water, either naturally from the soil or from industrial pollutants; and, inhalation of cigarette smoke is the major source of cadmium exposure in smokers (Bernhoft, 2013, Bertin and Averbek, 2006, Rani et al., 2014, Satarug et al., 2010). Although it exists in the Earth's crust at low levels of 0.1 ppm, certain areas can have higher concentrations of cadmium in the soil (Bernhoft, 2013). This becomes important when the areas containing higher levels of cadmium are agricultural farmlands in the upper Midwest that can be further contaminated with cadmium from fertilizers (Page et al., 1987, Vacchi-Suzzi et al., 2016). Cadmium can be readily taken up and bioaccumulated by plants and subsequently ingested as food or inhaled as tobacco smoke leading to human exposure of higher concentrations of cadmium (Bernhoft, 2013, Rani et al., 2014).

Higher concentrations of cadmium exposure are concerning because of its extremely long biological half-life of greater than 20 years; as well as, its deposition and accumulation within tissues of the body (Bernhoft, 2013, Rani et al., 2014). Cadmium has been studied for its ability to cause or contribute to various diseases as early as the late 1800's and early 1900's (Nordberg, 2009, Rani et al., 2014). Most notably, environmental contamination of cadmium was described to be a major contributing factor to *Itai-Itai* disease, or ouch-ouch disease, that affected Japanese people (Bernhoft, 2013, Nordberg et al., 2009, Rani et al., 2014). The rice fields irrigated using the Jinzu River became contaminated when cadmium was released from a mine into the river (Nordberg et al., 2009). Following this described strong link between environmental cadmium exposure and disease, cadmium became a main area of research resulting in its classification as a priority pollutant by the Environmental Protection Agency (EPA) and

Type I human carcinogen by the International Agency for Cancer Research (IARC) (Rani et al., 2014, Waisberg et al., 2003, EPA, 2014, IARC, 1993).

Cadmium can enter cells and various tissues using different mechanisms and ultimately elicit an adverse effect on multiple cellular processes. Several studies have shown that the main organs for deposition and potential subsequent toxicity are the liver and kidney in part due to metallothionein synthesis in these tissues (Bernard, 2008, Bernhoft, 2013, Rani et al., 2014, Yang and Shu, 2015). Under normal conditions, mechanisms are in place to mediate the toxic effect of metals by binding to the metal and reducing the reactivity of free cadmium. Following exposure, cadmium in the circulation is bound by albumin and readily endocytosed into hepatocytes, inducing metallothionein expression and production (Yang and Shu, 2015). Metallothioneins are small proteins with high affinity for metal ions resulting in sequestration of cadmium and other potentially toxic metals (Nordberg, 2009, Waisberg et al., 2003, Yang and Shu, 2015). This small metallothionein-cadmium complex is then released back into the circulation to the kidney where it is readily filtered through the glomerulus and endocytosed into the proximal tubule (Yang and Shu, 2015). The complex is quickly dissociated and the free cadmium induces metallothionein expression within renal cells and is taken up to reduce toxicity (Waisberg et al., 2003, Yang and Shu, 2015). However, cadmium deposition has been shown to be cumulative, resulting in high concentrations of cadmium and a saturation of metallothionein-cadmium complex formation leading to potential toxicity from reactive cadmium (Bernard, 2008, Waisberg et al., 2003, Yang and Shu, 2015).

There are other transport mechanisms cadmium has been shown to utilize to gain entry into the cell; however, these are mainly *in vitro* studies and are not as fully

understood. All of the transport mechanisms hypothesize the use of mimicry by cadmium to take the place of a similar molecule, as cadmium has no known benefit within human cells (Zalups and Ahmad, 2003). Cadmium has been described to utilize: zinc transporters (ZIP8 and ZIP14) and calcium transient receptor potential channels (TRP) competing with zinc and calcium, respectively, for binding, organic-anion, -cation, and amino acid transporters shielded by thiol-containing molecules; as well as, divalent metal transporters and metal transport proteins (Zalups and Ahmad, 2003, Yang and Shu, 2015). Figure I-3 illustrates potential cadmium transport mechanisms into the cell. As with metallothionein sequestration, these transport mechanisms can also contribute to cadmium accumulation within the cell and subsequent potential toxicity.

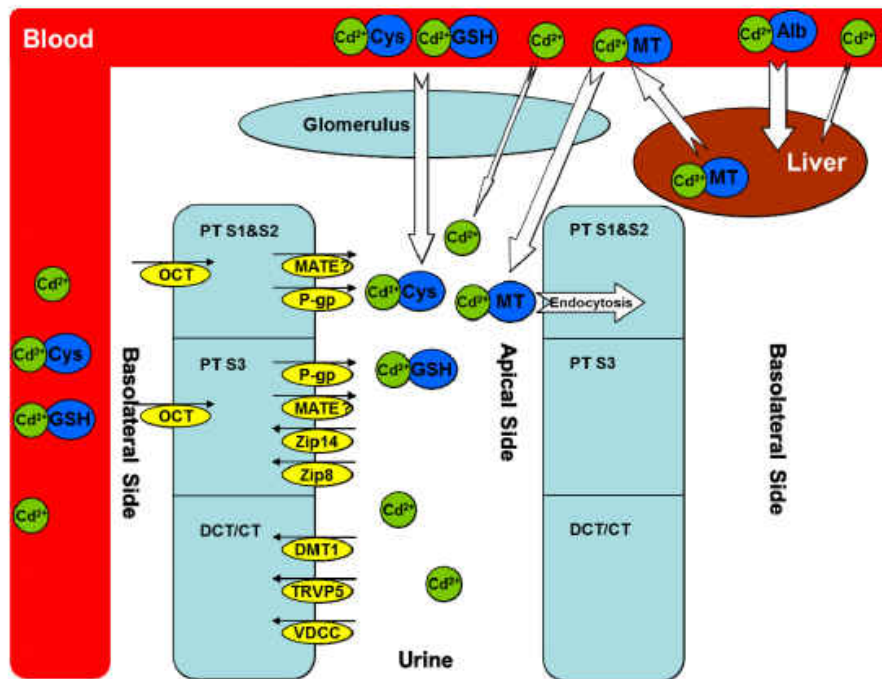


Figure I-3. Cadmium Cellular Transport. Proposed receptors and transporters utilized by cadmium (Cd^{2+}) to gain entry into the cell. Also illustrates the flow of cadmium from the circulation to the liver, leaving the liver, re-entering the circulation and being filtered through the glomerulus, ultimately being endocytosed and accumulating in the kidney tubules. P-glycoprotein (P-gp) has been shown to aid in cellular excretion of cadmium and multidrug and toxin extrusion proteins (MATE) have been proposed to aid in this process as well. Metallothionein (MT), L-Cysteine (Cys), Glutathione (GSH), Zinc/iron-

regulated transporter (ZIP), Divalent metal-ion transporter (DMT), Organic cation transporter (OCT), Voltage-dependent calcium channel (VDCC), Transient receptor potential vanilloid (TRVP), Proximal tubular cells segment 1, 2, or 3 (PT S1, S2, S3), Distal convoluted tubular cells (DCT), Connected tubular cells (CT). [with © permission under Creative Commons Attribution License from Yang and Shu, 2015]

Free cadmium within the cell can have severely detrimental effects on numerous cellular processes including: proliferation, DNA replication and repair, cell cycle progression, and has been shown to induce malignant transformation of different cell types (Bertin and Averbeck, 2006, Chen and Costa, 2017, Luevano and Damodaran, 2014, Sens et al., 2004). Several studies have investigated potential mechanisms behind cadmium's negative effect on the cells, showing that cadmium can directly mimic similar metals resulting in protein distortion and inhibited function; and, that cadmium indirectly causes genomic instability via oxidative stress (Bertin and Averbeck, 2006, Rani et al., 2014, Waisberg et al., 2003) Cadmium's high affinity for thiol groups such as those in cysteine residues result in cadmium's ability to replace zinc in zinc-finger motifs rendering the protein inactive (Bertin and Averbeck, 2006). Although cadmium itself cannot elicit oxidative stress in the cell, its presence decreases availability of detoxifying enzymes such as glutathione and indirectly generates several types of reactive oxygen species (ROS) (Rani et al., 2014). This results in oxidative stress in the form of lipid peroxidation, DNA damage, chromosomal abnormalities, and potentially carcinogenesis (Bertin and Averbeck, 2006, Luevano and Damodaran, 2014, Rani et al., 2014).

Oxidative stress may play a central role; however, it most probably is a complex, combinatorial effect of multiple mechanisms resulting in cadmium toxicity. Prolonged exposure to oxidative stress, such as chronic cadmium exposure, can lead to cell adaptation and redox homeostasis shift along with priming the activation of signaling

molecules important for redox reactions (Luevano and Damodaran, 2014). Making cells more sensitive to stress could potentially abnormally initiate signaling pathways and ultimately promote carcinogenesis. Interestingly, cadmium has been associated with multiple types of cancers (Bertin and Averbeck, 2006, Luevano and Damodaran, 2014, Waisberg et al., 2003).

The majority of cadmium is retained in the cells of the body. As mentioned earlier, the liver and kidney have been shown to have the highest cadmium accumulation (Bernard, 2008, Bernhoft, 2013, Rani et al., 2014, Yang and Shu, 2015). However, when cadmium is excreted, it is in small amounts in the urine relative to the total cadmium in the body (Vacchi-Suzzi et al., 2016). Excreted cadmium could potentially have negative effects on downstream organs, including the bladder. Studies have shown that even chronic small amounts of cadmium can result in adverse biological effects (Rani et al., 2014). The bladder does express low levels of three functional isoform genes important for encoding metallothioneins 1 and 2 with two of the three showing upregulation in bladder cancers (Somji et al., 2001). ZIP8 has also been shown to be expressed on bladder and bladder cancer cells (Ajjimaporn et al., 2012). Ajjimaporn et al. (2012) also showed that ZIP8 could be internally localized near the nucleus of these cells. This, coupled with a strong association between environmental toxicant exposure and bladder cancer; as well as, numerous carcinogenesis research studies, support cadmium as a potential carcinogenic factor for transitional cell carcinoma of the bladder.

This lab exploits the strong link between environmental toxicant exposure, specifically cadmium, and bladder cancer to study potential biomarkers. This system uses urothelial cells from the lining of the ureter that were immortalized using the Simian

Virus-40 (SV-40) Large-T antigen (Petzoldt et al., 1994 and 1995). They maintain their normal morphology and basal epithelial cell characteristics as well as contact-inhibited growth when grown in serum containing media, and are non-tumorigenic (Sens et al., 2004). They are known as UROtsa cells and represent an adequate *in vitro* system to study the human bladder (Rossi et al., 2001).

Malignant transformation of the UROtsa cells by exposure to cadmium took place over several weeks. The cells were exposed to 1 μ M cadmium and showed minimal signs of toxicity in the first 30 days of exposure (Sens et al., 2004). However, more than 95% cell death occurred between 30-48 days after showing short-term signs of toxicity in the preceding 96 hours (Sens et al., 2004). Exposure to cadmium was continued and multiple clones of proliferating cells were observed 15-30 days later (Sens et al., 2004). After several passages, again, 95% cell death was observed; however, this time, proliferating clones appeared and subsequent confluency quickly developed (Sens et al., 2004). Once it was determined there was no further toxicity after several subsequent passages, it appeared the cells had been transformed, showing: increased growth rates, colony formation in soft agar, and heterotransplant tumor formation in nude mice (Sens et al., 2004). The heterotransplant tumors were similar to human transitional cell carcinoma tumors (Sens et al., 2004), providing further evidence as to cadmium's carcinogenic potential as well as increasing the value of this model system. Further testing of these transformed cells showed increased resistance to cadmium-induced cell death compared to non-transformed UROtsa parent cells (Somji et al., 2006).

Following the initial cadmium malignant transformation of UROtsa cells, Somji et al. (2010) wanted to determine if independent cadmium exposure resulted in

transformed cell lines with similar phenotypic characteristics. Another goal of the study was to address the disparity in the investigation of reproducible transformation of a cell line via exposure to a single environmental toxicant; thereby, further validating the model system (Somji et al., 2010). Eight identical UROtsa cell cultures were exposed to $1\mu\text{M}$ Cd^{2+} and the protocol from the initial transformation was followed (Somji et al., 2010). Results were similar to the initial transformation showing an initial round of cell death followed by regrowth in 6 of the 8 subcultures (Somji et al., 2010). These cells did not form colonies in soft agar; however, after a second round of cell death, the cultures reached confluency and did form colonies on soft agar (Somji et al., 2010). These 6 subcultures were combined with the initial transformed cell line resulting in 7 independent Cd^{2+} -transformed cell lines to be studied for phenotypic characteristics (Somji et al., 2010).

Doubling times were measured for the transformed cell lines to assess cell growth. Results showed decreased doubling times for 5 of the 7 transformed lines portraying increased growth rates compared to the non-transformed UROtsa parent cell line (Somji et al., 2010). A hallmark characteristic of a malignant cell is increased proliferation, which is observed in the majority of these cell lines providing evidence of malignant transformation. Additionally, light microscopy revealed similar epithelial morphology across all cell lines with continued contact-inhibited growth of the monolayers (Somji et al., 2010). Furthermore, subcutaneous injections of the transformed cell lines into nude athymic mice resulted in tumor formation in at least 2 of 5 mice for every cell line compared to no tumor formation after inoculation with non-transformed UROtsa parent cells (Somji et al., 2010). Overall histological analysis showed the

heterotransplants were similar to the initial transformation study and to human invasive transitional cell carcinoma (Somji et al., 2010). Subsequent characterization studies, using gene expression analysis, determined heterotransplant tumors generated from the transformed cell lines display more basal-like characteristics, similar to those observed in human muscle invasive urothelial carcinomas (Hoggarth et al., 2018).

The ability of these cell lines to colonize organs within the peritoneal cavity was investigated to determine metastatic potential of these transformed cell lines. Intraperitoneal tumor formation results showed only 1 of the 7 transformed cell lines formed tumor nodules with no nodules seen in the non-transformed UROtsa parent inoculated mice (Somji et al., 2010). In the Cd #1 group that did form peritoneal tumors, 4 of 6 mice had extensive tumor nodules on several organs throughout the peritoneum (Somji et al., 2010). Therefore, although all transformed cell lines developed subcutaneous tumors, variation was observed in the ability of the transformed cell lines to colonize organs within the peritoneal cavity (Somji et al., 2010). Overall, results from this study provided further evidence in support of cadmium's potential as a transitional cell carcinoma carcinogen. Following establishment of this Cd²⁺ transformed UROtsa model system, displaying minimal phenotypic variation, later studies used microarray analysis to determine a number of candidate genes to further investigate as potential biomarkers for transitional cell carcinoma (Garrett et al., 2014).

One gene of considerable interest was Secreted Protein Acidic and Rich in Cysteine (SPARC). It is a secreted extracellular matrix glycoprotein acting in the extracellular matrix environment (Yan and Sage, 1999). Extracellular matrix proteins are a family of proteins that were first studied in the mid-1990's by Paul Bornstein, PhD and his lab at the

University of Washington (Murphy-Ullrich and Sage, 2014). He defined matricellular proteins as, “modular, extracellular proteins whose functions are achieved by binding to matrix proteins as well as to cell surface receptors, or to other molecules such as cytokines and proteases that interact, in turn, with the cell surface” (Bornstein, 1995). He went on to describe a non-structural role for matricellular proteins in the extracellular matrix as opposed to the structural roles described for: fibrillar collagens, laminin, fibronectin, and vitronectin (Bornstein, 1995, Chiodoni et al., 2010, Murphy-Ullrich and Sage, 2014, Yan and Sage, 1999). This seminal research has resulted in several subsequent studies, performed in multiple labs, leading to a family of matricellular proteins that has expanded from the original: SPARC, thrombospondin, and tenascin members. Currently, the matricellular family of proteins includes: SPARC, hevin (SPARC-like Protein 1), testicans (SPOCK) 1-3, follistatin-like protein 1 (fstl-1), and secreted modular calcium binding protein (SMOC) 1 and 2 (Bradshaw, 2012). Interestingly, SPARC is the most well-known and well-characterized matricellular protein, in part due to its relatively simple structure (Murphy-Ullrich and Sage, 2014, Yan and Sage, 1999).

Most protein families are comprised of members with similar structure and somewhat similar function. Matricellular proteins are unique in that they are biologically non-homologous in structure; showing a high degree of structural divergence in the N-terminal acidic domain (Bradshaw, 2012). However, each member retains a conserved EF-hand motif, important for calcium-binding protein activity (Bradshaw, 2012, Murphy-Ullrich and Sage, 2014). Murphy-Ullrich and Sage (2014) reviewed the matricellular unifying characteristics, classifying them as secreted proteins, associated with, but not

necessarily part of, structural extracellular matrix. It was further stated that they display de-adhesive properties and are highly expressed during tissue remodeling events as well as mammalian and avian development. These proteins are highly expressed during development; however, in the adult, expression is much more regulated and limited to wound healing and tissue remodeling events (Chiodoni et al., 2010).

Matricellular proteins are important for cell-matrix interactions, either directly or indirectly, leading to potential influence of multiple downstream signaling pathways responsible for: cell proliferation, adhesion and migration, survival, cell death, cell senescence and extracellular matrix deposition, among others (Chiodoni et al., 2010, Murphy-Ullrich and Sage, 2014). Potential influence of several signaling pathways requires heavy regulation to keep homeostatic biological processes functioning correctly. When these processes are needed, such as in wound healing, matricellular protein expression increases to aid in successful wound closure (Chiodoni et al., 2010). Interestingly, knockout of a matricellular protein in mice is not lethal; but rather, results in subtle phenotype changes, namely alterations in wound response, as observed with SPARC (Bornstein and Sage, 2002). Furthermore, the variation in the alteration of wound responses suggests diverse biological functions for this family of proteins (Kyriakides and Bornstein, 2003). Consequently, dysregulation of matricellular proteins has been described for several diseases, including cancer (Murphy-Ullrich and Sage, 2014).

SPARC is a prototype matricellular protein and although it was not the first discovered, it is fairly well characterized, in part, due to its relatively simplistic structure as seen in Figure I-4 (Murphy-Ullrich and Sage, 2014, Yan and Sage, 1999). It is also known as osteonectin or basement membrane protein 40 (BM-40) (Bradshaw and Sage,

2001). Osteonectin was first described to be a bone-specific, 32kD protein that bound collagen, calcium, and hydroxyapatite, and was chemically distinct from other bone-proteins, as well as immunologically different from serum proteins (Terminé et al., 1981). Helene Sage, in Paul Bornstein's, laboratory described a similar glycoprotein with a molecular weight of 43kD, due to carbohydrate addition, that was secreted from endothelial cells (Sage et al., 1984). In 1986, a glycoprotein termed SPARC was described to be "structurally and antigenically closely related to" the glycoprotein described by Sage et al. (1984) determined by amino acid sequence and structure homology (Mason et al., 1986). It was also determined that removal of the carbohydrate from SPARC resulted in migration of a 32kD molecular weight protein under non-reducing conditions (Mason et al., 1986). Buttgerit et al. (1988) used partial sequence analysis, and determined a common identity between BM-40 and the newly described SPARC matricellular protein. Interestingly, BM-40 sequence had also been shown to have high homology to osteonectin (Buttgerit et al., 1988). It was concluded, in this publication, that SPARC, osteonectin, and BM-40 characterized the same protein (Buttgerit et al., 1988).

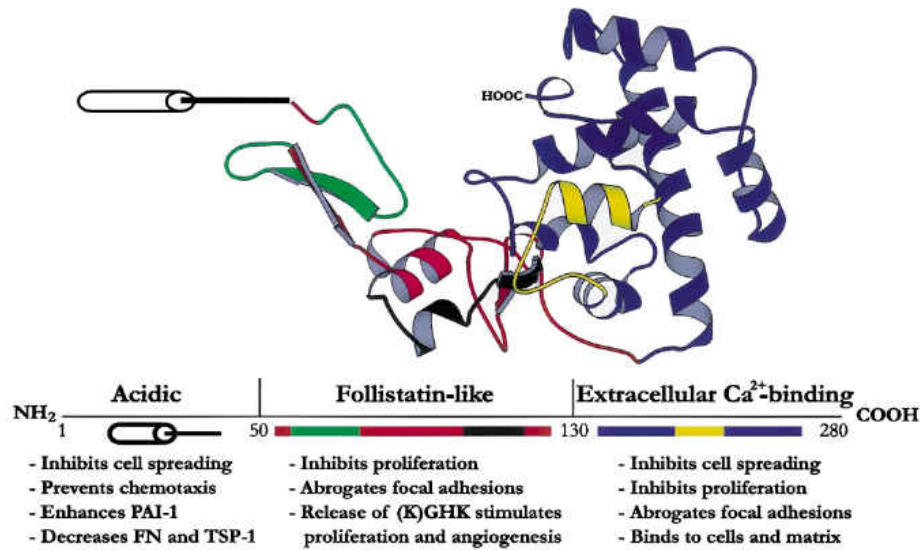


Figure I-4. SPARC Ribbon Structure and Proposed Cellular Functions. SPARC ribbon structure illustrating the three domains: Acidic, Follistatin-like, and Extracellular Ca²⁺-binding, along with the cellular functions that have been attributed to each domain. [Reprinted from Brekken, R. A., & Sage, E. H. (2001). SPARC, a matricellular protein: At the crossroads of cell-matrix communication. *Matrix Biology*, 19(8), 815-827, which was modified from Hohenester et al. (1997) and the Brookhaven Protein Database, with © permission from Elsevier]

The human SPARC gene is located on chromosome 5q31-33 and contains 9 coding exons (Brekken and Sage, 2001, UCSC Genome Browser [Kent et al., 2002]). The first exon remains untranslated and contains CCTG sequence repeats resulting in expression of a reporter gene while the 3' untranslated region resides entirely in exon 10 along with at least two functional polyadenylation sites (Lane and Sage, 1994). Synthesis of full length SPARC results in a protein that is 303 amino acids in length with the addition of the signaling sequence; which, is removed prior to secretion, resulting in a functional protein of 286 amino acids (Brekken and Sage, 2001, UCSC Genome Browser [Kent et al., 2002], Yan and Sage, 1999). SPARC shows a high degree of evolutionary conservation between species. Murine and human SPARC share 92% amino acid sequence homology, and bovine and human share 99% sequence homology (Brekken and

Sage, 2001). There are small differences; however, the substantial sequence homology observed indicates a necessary functional role for this protein for species to survive.

SPARC protein has been described to have three functional domains including: the acidic N-terminal domain, a follistatin-like domain, and an extracellular Ca^{2+} -binding C-terminal domain (Brekken and Sage, 2001, Clark and Sage, 2008). Proposed cellular functions have been described for each domain resulting in roles for SPARC in several biological processes such as: impeding cell adhesion, growth factor activity modulation, and inhibiting cell proliferation (Brekken and Sage, 2001). Several reviews summarize structure and proposed functions for each domain of the SPARC protein, in a succinct but descriptive manner, describing key findings that lead to the characterization of this protein (Brekken and Sage, 2001, Clark and Sage, 2008, Yan and Sage, 1999).

The acidic N-terminal domain I, comprised of amino acids 1-52, has low calcium-binding affinity and its structure is sensitive to Ca^{2+} changes in the environment (Brekken and Sage, 2001, Yan and Sage, 1999). Along with Ca^{2+} -binding, it has also been proposed as the interaction site with hydroxyapatite as well as contributing to collagen binding (Romberg et al., 1985). The major immunological epitopes to the SPARC protein can be found in the N-terminal domain (Brekken and Sage, 2001, Yan and Sage, 1999). This, in combination with structural diversity among family members, results in little, if any, antibody cross-reactivity between family members (Yan and Sage, 1999). There are also differences between human and nematode SPARC within this domain. Nematode SPARC lacks exon 3; however, studies showed functional SPARC protein with no effect on Ca^{2+} -binding nor collagen-binding due to the lack of exon 3 (Maurer et al., 1997, Schwarzbauer et al., 1994). An important post-translational modification affecting protein

function within this domain is disulfide crosslinking between SPARC and cysteine-rich proteins. For example, Aechlimann et al. (1995) described transglutaminase-mediated SPARC complexes in cartilage that were thought to contribute to extracellular matrix stability. Crosslinking with a variety of proteins in different tissues may support tissue-specific roles for SPARC. Some of the roles that the N-terminal domain has been proposed to participate in are cell spreading inhibition and preventing chemotaxis (Hohenester et al., 1997, Lane and Sage, 1994). Mechanistically, SPARC may be directly sequestering growth factors and chemokines away from cell surface receptors; or, it may be participating by competitively binding or blocking interaction with cell surface receptors and subsequent signaling.

The second domain of SPARC is the follistatin-like domain II, comprised of amino acids 53-137 (Yan and Sage, 1999). This is a cysteine-rich domain, containing disulfide bonds, and showing sequence and structure similar to follistatin (Patthy, 1991). One similarity within this domain is the potential for copper-binding. KGHK copper binding sites, at residues 119-122, have been proposed for SPARC in promoting cell proliferation and angiogenesis of endothelial cells (Funk and Sage, 1993, Lane et al., 1994). This is thought to act through a bioactive peptide created by proteolysis of this cationic region (Funk and Sage, 1993). A peptide comprising amino acids 113-130 and containing the KGHK copper-binding site as well as part of the Kazal protease inhibitor-like region stimulated endothelial cell proliferation and angiogenesis *in vitro* (Funk and Sage, 1993, Brekken and Sage, 2001). This study described a functional cell biological role for this region of the SPARC protein; although, the complete mechanism remains unknown. Another bioactive peptide comprised of amino acids 55-74 and containing a

portion of the EGF-like β hairpin, was found by Funk and Sage (1993) to bind copper with high affinity and inhibit endothelial cell proliferation but had no effect on angiogenesis.

Additionally, the follistatin-like domain contains the single glycosylation site of the SPARC protein at asparagine (Asn)99 (Yan and Sage, 1999). In endothelial cells this has been shown to be an N-linked oligosaccharide; however, in bone SPARC is glycosylated with a high mannose-type oligosaccharide (Yan and Sage, 1999). This contributes to the molecular weight difference observed in SDS-PAGE analysis between endothelial cells (43kD) and bone (32kD). It has also been proposed to contribute to tissue-specific SPARC protein function as well as collagen binding specificity (Kelm and Mann, 1991). Overall, the follistatin-like domain contains binding motifs for a variety of molecules, as well as post-translational modifications, important for SPARC function (Yan and Sage, 1999).

The final domain of the SPARC protein is the extracellular calcium binding domain III, comprised of amino acids 138-286 (Yan and Sage, 1999). It is largely composed of an α -helical structure with a canonical pair of EF-hands showing high affinity for calcium (Hohenester et al., 1996). This domain was originally defined as two separate domains; however, Pottgiesser et al. (1994) determined it to be a single domain with propensity for both extracellular calcium and collagen binding. Maurer et al. (1995) and (1997) determined that SPARC binds to basement membrane associated collagen IV with moderate affinity, as well as fibrillar collagens. It was discovered that interaction with the follistatin-like domain II stabilizes calcium-binding to domain III (Hohenester et al., 1997). It was also shown that SPARC binding to fibrillar collagens I, III, and VI and

basement membrane associated collagen IV is a Ca^{2+} dependent event (Sasaki et al., 1998). Crystal structure and site-directed mutagenesis studies determined the residues necessary for collagen binding and found that proteolytic cleavage at lysine (Lys)197 and Lys198 increased collagen affinity by 10-fold (Sasaki et al., 1998). These studies showed that protein cleavage by matrix metalloproteinases may be a regulatory mechanism utilized to increase SPARC activity (Sasaki et al., 1998). Matrix metalloproteinases are highly expressed in tissue injury and remodeling events, as is SPARC, making this a significant interaction for normal biological function (Tardáguila-García, et al., 2019). Other cell processes domain III has been proposed to impact are: deterring cell spreading, disrupting focal adhesions, and inhibiting cell proliferation (Brekken and Sage, 2001, Lane and Sage, 1994, Murphy-Ullrich et al., 1991). The exact mechanism behind the majority of SPARC's roles are not well understood; however, SPARC's interaction with collagens have been extensively studied and as a result is fairly well characterized.

Once SPARC-collagen binding was understood, studies began to identify SPARC binding sites on fibrillar collagens I, III, and VI as well as non-fibrillar collagen IV. The structure of collagen is important for its binding to various extracellular matrix molecules as well as to cells. It has a triple helical structure that is comprised of three α chains (Giudici et al., 2008). The α chains contain Glycine (Gly)-X-Y sequence repeats with X most often representing proline and Y most often representing hydroxyproline (Giudici et al., 2008). Although the X and Y repeat positions can vary, glycine is imperative at every third residue to allow for proper α chain interaction due to a lack of hindering side chains on glycine (Giudici et al., 2008). The X and Y residues contain side chains that are exposed on the triple helical structure providing potential binding epitopes for various

molecules and proteins (Giudici et al., 2008). Giudici et al. (2008) mapped SPARC binding sites on fibrillar collagens using a synthetic SPARC peptide and rotary shadowing. A conserved SPARC binding site on collagens I, II, and III at around 180nm from the C terminus was found (Giudici et al., 2008). Interestingly, there is some overlap of cell surface receptor binding and SPARC binding to collagen within this region (Giudici et al., 2008).

Collagens have been determined to bind to cells via integrin cell surface receptors $\alpha_1\beta_1$, $\alpha_2\beta_1$, and $\alpha_{11}\beta_1$ as well as discoidin domain receptors (Agarwal, et al., 2002, Giudici et al., 2008, Xu et al., 2000, Zhang et al., 2003). Synthetic peptides have been important for mapping active binding sites on both SPARC and its collagen binding partners resulting in a better understanding and characterization of SPARC. The mapping of SPARC binding sites on fibrillar collagens revealed a potential role for SPARC in collagen fibrillogenesis, further evidenced by later studies finding decreased collagen fibril diameter as well as a reduction in fibril size uniformity (Bradshaw et al., 2003, Giudici et al., 2008). Earlier studies, observing early onset cataractogenesis along with increased lens capsule basement membrane permeability in SPARC-null mice, implicated a role for SPARC in basement membrane formation and stability; potentially, via modulation of collagen IV transport and deposition into the basement membrane matrix (Chioran et al., 2017, Gilmour et al., 1998, Martinek et al., 2007, Norose et al., 1998, Yan et al., 2002). Additionally, SPARC binding to collagen may act to inhibit or block cell surface binding to collagen affecting downstream signaling pathways important for cell adhesion, proliferation, and survival, as well as modulating growth factor activity with the cell surface (Giudici et al., 2008).

Among the many roles described for SPARC, modulation of growth factor activity can result in significant alterations in cellular function. SPARC has been shown to modulate the activity of several growth factors and cytokines including: platelet derived growth factor (PDGF), vascular endothelial growth factor (VEGF), basic fibroblast growth factor (bFGF), and transforming growth factor (TGF)- β (Brekken and Bradshaw, 2010). Raines et al. (1992) found that SPARC domain III, separate from Ca^{2+} -dependent collagen-binding epitope (Göhring et al., 1998), bound to specific variants of PDGF (-AB and -BB) and prevented interaction with cell surface receptors, ultimately inhibiting proliferation of fibroblasts. Similarly, Kupprion et al. (1999) determined that the EC domain III of SPARC bound to VEGF, inhibiting its interaction with cell surface receptors on endothelial cells. This reduced cell proliferation via a proposed decrease in tyrosine phosphorylation of mitogen-activated protein kinases (MAPKs) (Kupprion et al., 1998). Another growth factor determined to be affected by SPARC is bFGF. Hasselaar and Sage (1992) showed a reduction in migration and proliferation of bovine endothelial cells in the presence of exogenous SPARC; however, SPARC's role did not appear to be direct and required a subsequent serum component. Additional mechanistic studies are needed to better understand the interaction between SPARC and bFGF.

TGF- β has several known homeostatic biological functions. TGF- β was shown by Lane and Sage (1994) to act as a regulator of SPARC expression in fibroblasts stimulating its expression. Both TGF- β and SPARC are expressed during wound healing and in tissue remodeling events providing a basis for investigation into potential interactions. Later studies using mesangial cells isolated from SPARC-null mice indicated decreased levels of TGF- β that could be increased by exposure to exogenous

SPARC (Francki et al., 1999). Therefore, these two studies indicate a potential positive feedback loop between SPARC and TGF- β ; however, more research is needed to determine the mechanism and if the interaction is direct or indirect. Growth factor interactions have the potential to affect several downstream signaling pathways resulting in aberrant cellular function. However, tight regulation including: tissue- and time-specific expression, proteolytic activation, transcription factor binding, miRNA, and feedback loops, among others, maintain the homeostatic activity of matricellular proteins such as SPARC (Murphy-Ullrich and Sage, 2014).

The regulated expression and function of SPARC and other matricellular proteins makes them ideal targets for disease. These proteins are critical for proper wound healing and tissue remodeling; however, dysregulation resulting in aberrant protein expression and function can have severely detrimental effects (Murphy-Ullrich and Sage, 2014). For the purpose of this study, cancer will be the disease of focus. Tumors have been described as, “wounds that do not heal” (Dvorak, 1986). SPARC plays an integral role in wound healing and therefore has been implicated in various types of cancer. However, as reviewed by several researchers, its expression and role is not consistent between cancers but instead is tissue-specific (Arnold and Brekken, 2009, Nagaraju et al., 2014, Said and Theodorescu, 2013). In general, SPARC has been described to act in an oncogene-like fashion promoting tumor progression in melanomas, and gliomas; however, it has been described to act in a tumor-suppressor-like fashion inhibiting tumor progression in many epithelial cancers such as lung, prostate, ovarian and colorectal (Arnold and Brekken, 2009, Brekken and Bradshaw, 2010, Said and Theodorescu, 2013). There are also cancers that have varying SPARC expression depending on the subtype and/or tumor grade

(Nagaraju et al., 2014, Said and Theodorescu, 2013). As seen in Figure I-5, SPARC's contradictory roles in either promoting cellular processes or inhibiting cellular processes through proposed mechanisms, along with tissue-specific expression of proteolytic molecules such as matrix metalloproteinases, could explain its dysregulation in particular cancer types (Nagaraju et al., 2014). The mechanisms behind SPARC's function in cancer are overwhelmingly thought to occur through modulation of signaling factors and interruptions in signaling pathways resulting in aberrant cellular function and, more recently, through weakening of the extracellular matrix via collagen IV interactions (Arnold and Brekken, 2009, Morrissey et al., 2016, Nagaraju et al., 2014). This is complicated by SPARC being a secreted protein making it necessary to consider SPARC expression by the tumor as well as the surrounding stromal environment.

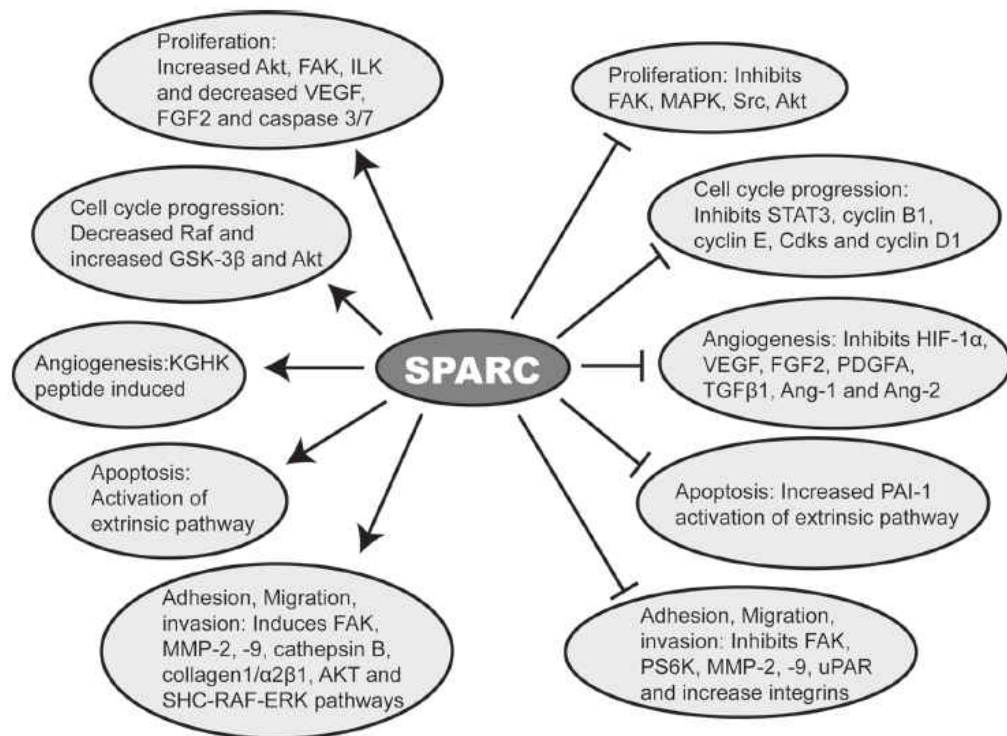


Figure I-5. Various Roles for SPARC in Cancer. Diagram depicting SPARC's contradictory roles in promoting cancer as well as inhibiting cancer. Mechanistic details determined from numerous studies describe tissue and cancer-specific functions for SPARC. [Nagaraju et al., 2014, by © permission of Oxford University Press]

Harold Dvorak (1986) explained the necessary, complex interplay between tumor and stroma, along with the potential role for aberrant wound healing in cancer. Tumor associated stroma is an environment conducive to: aberrant matricellular protein expression and function, inappropriate wound healing events, and ultimately tumor progression. It is important to consider that both tumor cells and supporting cancer-associated stromal cells can secrete matricellular proteins (Chiodoni et al., 2010). It has not been fully determined if the source of secreted matricellular proteins contributes differently to the overall outcome; however, this is of considerable interest as it may lead to potential therapeutic targets.

SPARC expression and function in urothelial carcinoma is limited; however, studies show expression appears to be negatively correlated with disease progression (Said et al., 2013, Said, 2016). SPARC is expressed in normal urothelium in the basal and luminal cells of the epithelial layer (Said et al., 2013). However, in urothelial carcinoma tumors, SPARC expression within the tumor cells is decreased while expression is maintained or increased in the supporting stromal cells (Larson et al., 2010, Said et al., 2013). The downregulation of SPARC within tumor cells was shown to promote carcinogenesis and tumor progression through ROS accumulation, increased cell proliferation, and increased carcinogen-induced inflammation (Said et al., 2013). Ovarian cancer studies report similar findings of increased stromal SPARC expression with decreased tumor cell expression (Brown et al., 1999). In this case, SPARC is thought to elicit its tumor suppressor functions through inhibition of cell adhesion, suppression of mitogen-activated protein kinase (MAPK) cell survival signaling, as well as tumor microenvironment neutralization (Said et al., 2007a, Said et al., 2007b). This, along with

tumor cell heterogeneity and the complex tumor-stroma cross-talk, further exemplify the importance of studying the origin of SPARC expression in regards to cancer and future therapeutics. SPARC's tissue-specific expression and function make it a difficult therapeutic option due to off-target side-effects; however, understanding the mechanisms underlying SPARC function may lead to cancer-specific downstream effector molecules that can be targeted or monitored.

Microarray analysis of our lab's *in vitro* model system of heavy metal cadmium-induced urothelial carcinoma reported SPARC as the most repressed gene across all transformed cell lines (Garrett et al., 2014). Larson et al. (2010) observed SPARC mRNA and protein levels below detectable limits in all of the transformed cell lines compared to the non-transformed UROtsa parent cell line and normal human urothelium. Fluorescence imaging found vesicular expression of SPARC in the cytoplasm of the non-transformed UROtsa parent cells; however, no SPARC expression was observed in the transformed cell lines (Larson et al., 2010). Immunohistochemical analysis compared SPARC expression in human non-cancerous and cancerous urothelial tissue. Results showed a decrease in urothelial cell SPARC expression but an increase in stromal SPARC expression from normal to cancerous urothelium as well as Cd²⁺-transformed heterotransplant tumors. There appeared to be differences in the stromal SPARC expression between tissues in regards to the inflammatory status; with inflammatory and desmoplastic (densely fibrotic) areas of low and high grade urothelial carcinomas, respectively, showing strong stromal SPARC expression (Larson et al., 2010). Therefore, it is possible that stromal SPARC is playing a role in creating or sustaining an inflammatory microenvironment to promote tumor progression.

Interestingly, exposure of UROtsa parent cells to cadmium resulted in a rapid decrease in SPARC expression clearly indicating a role, either direct or indirect, for cadmium in the repression of SPARC (Larson et al., 2010). Repression of SPARC in many epithelial tumors has been reported due to hypermethylation of the promoter (Arnold and Brekken, 2009, Chen et al., 2014, Gao et al., 2010, Socha et al., 2009). Therefore, Larson et al. (2010) treated Cd²⁺-transformed cells with either MS-275 histone deacetylase inhibitor or 5-AZC methyltransferase inhibitor but determined that SPARC repression following malignant transformation did not appear to be due to changes in common promoter methylation or histone acetylation. These results indicate an alternative regulatory mechanism resulting in SPARC repression in the heavy metal-induced urothelial carcinoma model system.

Further studies, performed to better understand the expression and function of SPARC in this model system, led to stable transfection of SPARC under a CMV promoter in two Cd²⁺-transformed cell lines (Slusser et al., 2016). Tumorigenesis experiments showed that stable transfection did not affect the ability of these cells to form colonies on soft agar, nor ability to form tumors in nude athymic mice (Slusser et al., 2016). Additional results indicated no difference in: epithelial cell morphology, intracellular location of SPARC, proliferation rates, migration, nor invasion capabilities. Interestingly, the heterotransplant tumors formed from the stably SPARC-transfected Cd²⁺-transformed cell lines completely lacked detectable SPARC expression (Slusser et al., 2016). However, heterotransplant tumors formed from the proposed cancer-initiating cell subpopulation or, UROsphere population, of the SPARC-transfected, transformed cells lines showed 10-20% focal SPARC expression compared to the SPARC-transfected,

transformed cell lines (Slusser et al., 2016). This increase in focal SPARC protein expression could indicate a potential subset of cells expressing SPARC that may contribute to tumorigenesis, tumor progression, and/or tumor metastasis.

The previous results from our lab, in conjunction with the overall desperate need for biomarkers for bladder cancer, led to this proposed research study to further analyze SPARC expression and function in an *in vitro* model of heavy metal Cd²⁺-induced urothelial carcinoma. Literature suggests tissue-specific biological roles for SPARC (Brekken and Sage, 2001). Additionally, a well-defined role for SPARC in the bladder and bladder cancer remains to be fully determined. Therefore, one hypothesis of this study is that SPARC plays a critical role in cell proliferation, migration, attachment, or spreading of urothelial cells. Our model system presents an ideal opportunity to determine a role for SPARC in non-tumorigenic SPARC⁺ UROtsa parent cells that is affected in non-SPARC expressing Cd #1 transformed cells.

Furthermore, the SPARC promoter has been shown to be hypermethylated in several cancer types (Brekken and Bradshaw, 2010). However, that does not appear to be occurring in our system. Additionally, SPARC was repressed in UROtsa parent cells following short term exposure to cadmium (Larson et al., 2010). Therefore, the goal of this study is to examine an alternative regulatory mechanism that may be contributing to SPARC repression in transformed urothelial cells, namely transcription factor binding to the SPARC promoter. The second hypothesis of this study is that cadmium significantly decreases SPARC expression by silencing the promoter early in the malignant transformation process. Finally, the significant repression of tumor cell SPARC in heterotransplant tumors generated from SPARC-transfected transformed cells (Slusser et

al., 2016), motivated further examination of SPARC and tumor initiation. The goal of this study, described in Chapter IV, is to determine SPARC expression in serially transplanted bladder heterotransplant tumors. Previous heterotransplant tumor results led to the third hypothesis that in urothelial tumors generated from the Cd²⁺-transformed cell lines, SPARC is prohibitive to tumor initiation.

CHAPTER II

SPARC AND BLADDER UROTHELIAL CARCINOMA CELL ATTACHMENT, SPREADING, AND MIGRATION

Introduction

SPARC is a matricellular glycoprotein that has both tissue specific expression and function (Nagaraju et al., 2014, Yan and Sage, 1999). It has been shown to play a tissue dependent role in contradictory biological processes (Nagaraju et al., 2014). This has led to SPARC being described as both oncogene-like and tumor suppressor-like depending on the cancer of interest (Nagaraju et al., 2014). However, its role in bladder cancer is yet to be fully elucidated. One goal of this research is to determine a role for SPARC in our model system of heavy metal induced bladder urothelial carcinoma.

This study focuses on the cell biological processes of growth, migration, attachment, and spreading; all of which are necessary for normal cell survival. However, these processes and others have also been shown to be altered in regards to tumor initiation and progression (Hanahan and Weinberg, 2000, Hanahan and Weinberg, 2011, Pickup et al., 2014). SPARC has been shown to play a role in all of these processes; therefore, it is plausible SPARC functions in one or more of them in our model system (Bradshaw and Sage, 2001, Nagaraju et al., 2014, Yan and Sage, 1999).

Cell growth and migration are both integral components of wound healing (Midwood et al., 2004). Normally, there are phases of tissue injury repair encompassing migration of immune cells and clotting factors into the wound followed by migration and

proliferation of epithelial cells and finally maturation of cells and extracellular matrix molecules to heal the wound (Midwood et al., 2004). SPARC has been described to play a role in extracellular matrix molecule deposition as well as cell-matrix de-adhesion promoting tissue injury repair and regeneration (Arnold and Brekken, 2009, Bradshaw and Sage, 2001). In a sense, a cancerous lesion is a wound in need of repair so these same processes are occurring but may be altered to promote tumor growth and progression (Dvorak, 1986, Dillekås, et al., 2019). The experiments in this study will focus on epithelial cell migration and proliferation in the presence or absence of SPARC in the first 24 hours following injury.

Two other important biological processes studied in this research are cell attachment and cell spreading. Studies have shown that these processes are separate but both are needed for adherent-dependent cell survival (Chen et al., 1997). As shown in Figure II-1, Christopher Chen and colleagues used an extracellular substrate of fibronectin. They plated a specified amount in one spot at 20 μ m in diameter, and in another location, the same amount of fibronectin was distributed over multiple spots at 3-5 μ m in diameter to mimic focal adhesion size (Chen et al., 1997). It was found that the cell that attached to the 20 μ m spot of fibronectin could not spread and died via apoptosis. However, the cell that attached onto the same amount of fibronectin spread out over multiple spots totaling 50 μ m could spread, allowing it to survive and grow (Chen et al., 1997).

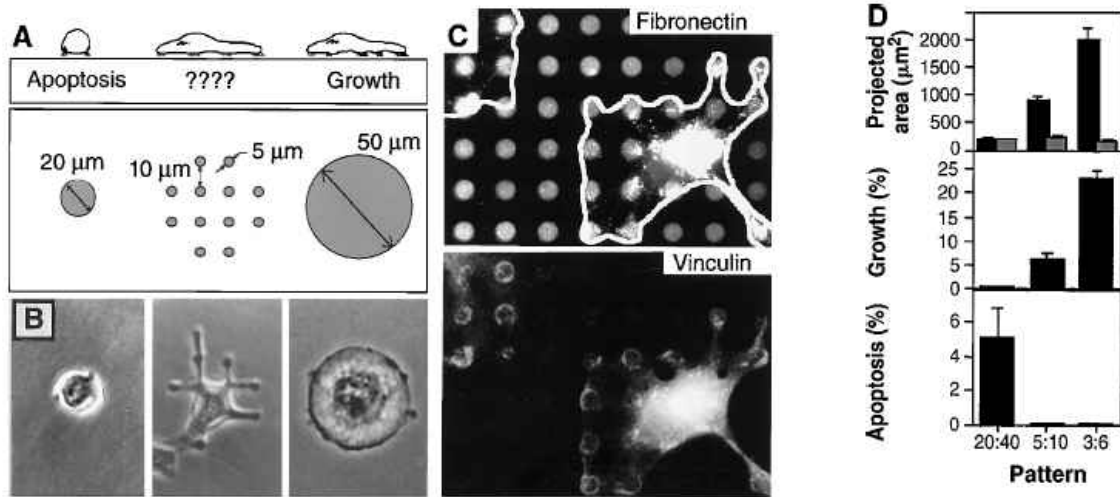


Figure II-1. Attachment and Spreading of Adherent Cells. Specified amount of fibronectin placed in single location or distributed over multiple locations illustrates both cell attachment and cell spreading are necessary for cell survival and growth. (Reprinted from Chen et al., 1997 with © permission from AAAS.)

These experiments were pivotal in determining the importance of both cell attachment and cell spreading for normal cell function and survival. There have been several studies assessing cell attachment and spreading using a variety of methods (Khalili and Ahmad, 2015). The most simple assay is the wash assay in which unattached cells are washed away; however, this method does not allow for real-time quantification so further analysis is needed (Khalili and Ahmad, 2015). This is the basic method that will be utilized to examine attachment and spreading in this study. Lane and Sage (1990) developed a method to quantitate categorized cells via observation using a rounding index (RI), with the formula $RI = (1a + 2b + 3c) / (a + b + c)$, where (a) is fully spread, (b) is spreading, and (c) is rounded. As the cells in each image become more fully spread, the RI gets closer to a value of 1. This method has been used in several subsequent studies analyzing cell spreading; however, percent attached is also commonly utilized for attachment and spreading data representation (Everitt and Sage, 1992, Motamed and

Sage, 1998, Hudson et al., 2005, Delostrinos et al., 2006, Humphries, 2009). Intriguingly, cell spreading quantitation has become more automated with computer-based classification systems using trainable classifiers to categorize cells based on morphology (Costa and Yang, 2009, Dehlinger et al., 2013, Ambühl et al., 2012, Carpenter et al., 2006, Garvey et al., 2016, Jaccard et al., 2014b). This automation reduces a level of human bias and makes analysis more consistent. Furthermore, this study is an ideal opportunity for its utilization in examining SPARC's role in urothelial cell attachment and spreading.

SPARC has been shown to have de-adhesive properties thereby decreasing cell attachment and subsequent spreading in the systems studied (Bradshaw and Sage, 2001). Interestingly, this was shown in human urothelial cells to occur via SPARC's C-terminal Ca^{2+} -binding domain (Delostrinos et al., 2006). One interaction that has been extensively studied and shown to be important for many functions is SPARC's interaction with fibrillary collagens and basement membrane collagen IV (Bradshaw, 2009). Mechanistic studies describe this as a calcium-dependent interaction involving the C-terminal domain of the SPARC protein containing two high-affinity calcium-binding EF Hands (Bradshaw, 2009). The affinity of SPARC binding to collagen can be tissue specific due to the tissue-specific glycosylation of SPARC (Bradshaw, 2009). SPARC binding sites on collagen I have been described by two different lab groups. Both groups found two similar binding sites; however, Guidici et al. (2008) found another potential site that was not described by Wang et al. (2005) (Bradshaw, 2009). Overall, both groups identified binding sites that coincide with the integrin cell adhesion receptor and/or Discoidin Domain Receptor (DDR) family binding sites which could result in altered cell

attachment and subsequent spreading. However, these processes have not been studied in the context of heavy metal induced bladder urothelial carcinoma warranting investigation in our system. Our model system of cadmium transformed urothelial carcinoma cells lacking SPARC expression presents an opportunity to explore cell attachment and spreading, as well as cell growth and migration, in regards to SPARC.

Materials and Methods

Cell Culture

SPARC⁺ UROtsa parent cells were maintained in 25cm² tissue culture flasks containing Dulbecco's Modified Eagle's Medium (DMEM) [Sigma-Aldrich, St. Louis, MO] supplemented with 5% v/v fetal calf serum (Gibco, Waltham, MA) as described in Rossi et al. (2001). Cadmium malignantly transformed cells, their respective SPARC-transfected cells, and associated destination vector-transfected control cells were also maintained in 25cm² tissue culture flasks containing DMEM supplemented with 5% v/v fetal calf serum with the addition of 1% v/v glucose. Cells were grown in a 37°C, 5% CO₂ tissue culture incubator and fed fresh media every 2 days. Confluent flasks were passaged at a 1:8 (UROtsa) and 1:10 (Cd²⁺) ratio after dislodging cells using 0.25% Trypsin-EDTA (Gibco). Cells were passaged approximately 20 times; after which, fresh vials were thawed and grown in culture.

Wound Closure Assay

Cells were plated and grown to confluency in 6-well tissue culture plates. Once confluent, wells were wounded with a plus sign mark using the pointed end of a sterile 200µL pipette tip. Wells were washed with 1xPBS and fresh growth media was added. Phase contrast images were taken at 10x magnification above and below the cross-point

at 0h, 4h, 8h, 12h, and 24h time points, using a Zeiss Axiovert 35 microscope (Carl Zeiss AG, Oberkochen, Germany) fitted with an Olympus DP72 camera (Olympus, Tokyo, Japan). Wound closure was analyzed using Olympus cellSens Standard software measuring distance between wound edges. Each well was measured in triplicate with the experiment performed in triplicate. Percent wound closure graphed using GraphPad PRISM version 5.01 (GraphPad Software, San Diego, CA).

Cell Attachment and Spreading Under Normal Tissue Culture Conditions

Cells were grown to confluency in 25cm² tissue culture flasks and passaged using 0.25% Trypsin-EDTA (Gibco). All cells were passaged using a 1:6 ratio into 25cm² tissue culture flasks. The flasks were then allowed to incubate at 37°C, 5% CO₂ in a tissue culture incubator. At 30 minutes, 60 minutes, and 120 minutes flasks were removed and imaged using phase-contrast microscopy on a Zeiss Axiovert 35 microscope (Carl Zeiss AG) at 10x magnification. Because only one flask was used for each cell line, one representative image was taken of each flask, after which the flask was placed back in the incubator. Data was graphed using Graphpad PRISM v5.01.

Fiji and PHANTAST Image Pre-Processing

Fiji is just ImageJ (Fiji) software (FIJI/ImageJ version 1.52i) freely available from the National Institutes of Health (NIH) was downloaded to aid in image pre-processing steps. A specific plugin, PHANTAST, (v0.2, www.github.com/nicjac/PHANTAST-FIJI/releases/tag/v0.2) was then downloaded to further aid in pre-processing. This plugin was developed by Jaccard et al. (2014a) to correct for the halo artifact in phase contrast microscopy images. Briefly, an algorithm was used to determine which pixels matched the cell and which matched the background using a gradient determined by multiple

Kirsch filters (Jaccard et al., 2014a). A list of potential halo locations is made and pixel by pixel each location is determined to be cell or halo/background until the list is completed (Jaccard et al., 2014a). How much each pixel analyzed is affected by or affects its nearest neighbors is determined using the sigma and epsilon values within the PHANTAST plugin which will be described later (Jaccard et al., 2014a).

Images were opened in Fiji and converted from an 8-bit image to a 32-bit image in order to run the PHANTAST plugin. Phase contrast images are greyscale resulting in a lack of contrast between the cells and the background. This required the contrast to be modified for each image to get optimal clarity. Subsequently, the PHANTAST plugin was launched and sigma and epsilon parameters were set. Sigma determines the influence of a pixel on its neighbors; therefore, increasing sigma results in more neighboring pixels that “look” like that pixel (Jaccard et al., 2014a). Epsilon determines the amount of pixels that will be recognized as cell or background. Therefore, based on the algorithm, decreasing epsilon results in an increase in the amount of pixels that will be recognized as a cell (Jaccard et al., 2014a). After the proper values are determined a binary (0 or 1) output image is created. This image shows black cells (1) on a white background (0). Following the PHANTAST segmentation, the binary image is overlaid on the original image. The result of this is an image of cells without a halo on a black background. This image is then converted back to an 8-bit image and can be analyzed using the Leica LASX software package. The overlay image helps to visualize the cell and allows for proper exclusion of non-cell debris and falsely selected background. This pre-processing was optimized for the majority of the cells in each image.

Once these steps were optimized this process was written into a macro to make this process more efficient. The macro incorporated interactive elements to further optimize these steps to achieve the best results. Briefly, all images from a single well were analyzed together using the macro. The first step is to manually modify the contrast for each image to get optimal clarity as stated previously. Subsequently a range of sigma and epsilon values were entered and each image was run through the program. Once the program finished the output image with the best border definition was chosen to be analyzed. From each well of 20-30 images, 10 images were chosen for analysis with the Leica LASX program.

Leica LASX Image Analysis

Leica LASX program version 3.0.1 (Leica Microsystems, Inc., Buffalo Grove, IL) has the ability to classify cells within an image based on morphology. Similar versions of this software have been utilized in Ristic et al. (2014) and Zorgetto et al. (2013) to assess morphology as well as count blood vessels, respectively. This software tool was important for this study, allowing for a reduction in human bias associated with cell classification. Because this program is part of a confocal microscopy system it was not designed to recognize phase contrast images. Therefore, the pre-processing through Fiji, using the PHANTAST plugin, was imperative to use the Leica LASX software. The overlay images with the black background were able to be recognized by the LASX software; therefore, this program could be used moving forward to analyze attachment and spreading images via LASX computer software.

The image was uploaded into the software and the analysis panel within the LASX program was opened. Once opened, a series of pre-filters can be utilized to

process the image as needed. One pre-filter utilized for these images was the binary pre-processing filter to size exclude small debris from selection. Another filter used was the binary image editing filter. Within this filter, cells that were touching could be manually split and cells touching the edge could be excluded. This filter also allowed for removal of larger non-cell debris as well as adjustment of any incorrect cell borders. As stated earlier, the pre-processing in Fiji was optimized for the majority of cells in each image. This resulted in manual border selection of some cells due to a lack of contrast that was unable to be corrected in the pre-processing steps. Once the pre-filter steps were finished the image was subjected to the classifier and each cell in the image was categorized based on several parameters.

The classifier feature of the Leica LASX software had to be manually trained to correctly categorize cells based on morphology. Therefore, a control image was used to train the classifier. Classes for rounded, spreading, and flattened were created. Then, several cells for each class were manually selected and the classifier was trained to categorize subsequent cells based on those cells manually selected. Initially, only two classes were created, rounded and flattened; however, the classifier could not accurately categorize cells into the two classes and needed a third to “catch” those cells in between rounded and flattened. Once optimized, the classifier measured several parameters including: surface area, length, perimeter, roundness, and shape, among others. How each parameter was weighted in the classification is proprietary information; however, once optimized, the classifier was saved and each image was classified using the same classifier. Modification of the attachment and spreading assay required modification of the classifier; but, once modified, each image was analyzed with the same classifier. The

classification resulted in a report that was exported to Excel where the number of cells in each category was calculated using the “countif” function. The percent of total cells in each category was determined by dividing the number of cells in each class by the total number of cells and multiplying that value by 100. The relative surface area was also calculated for all cells as well as for cells in each class.

Cell Attachment and Spreading Assay on a Collagen I Matrix

Cells were grown to confluency as described previously. Cells were then counted using a hemacytometer and diluted to 50,000cells/well concentration and plated in 12 well tissue culture plates. Tissue culture plates were coated with PureCol Collagen I (Advanced BioMatrix, San Diego, CA) one day prior to the experiment. 12 well plates were coated with 750 μ L PureCol Collagen I and allowed to dry for 2-4h. 1mL of Bovine Serum Albumin (BSA) blocking buffer (3% in PBS) [Alfa Aesar, Haverhill, MA] diluted to 1% was added to each collagen coated well and plates were incubated in a 37°C, 5% CO₂ tissue culture incubator overnight. Collagen coated wells were washed three times with 1xPBS prior to cell plating. Cells were plated in triplicate on both normal tissue culture wells and collagen I coated wells. Cells were placed in a 37°C, 5% CO₂ tissue culture incubator and allowed to attach for 30min, 60min, or 120min. Once removed, cells were washed quickly 3 times with 1xPBS and methanol fixed in the freezer for 3 minutes using ice-cold methanol. Cells were then quick rinsed with 1xPBS⁻ followed by three 5 minute washes with 1xPBS⁻ and one 5 minute wash with 1xPBS⁺. Cells were stored in 1x PBS⁺ at 4°C until imaged. Phase contrast images were taken of each well using a Zeiss Axiovert 35 microscope (Carl Zeiss AG) at 10x magnification. Initial cell attachment and spreading analyzed by manually counting rounded versus non-rounded

cells in 5 images. The same images were then pre-processed using Fiji and PHANTAST and analyzed using Leica LASX software (Leica Microsystems, Inc.) as described previously. Results were graphed and statistical analysis performed using GraphPad PRISM v5.01. Manual data was compared to software data to validate software analysis.

Modified Cell Attachment and Spreading Assay on a Collagen I Matrix

Cells were grown to confluency as previously described. Cells were counted using a hemacytometer, diluted to 30,000cells/well concentration, and plated in 12 well plates. Cells were plated in triplicate on both normal tissue culture wells and collagen I coated wells prepared as described previously. Cells were placed in a 37°C, 5% CO₂ tissue culture incubator and allowed to attach for 15min, 30min, 45min, and 60 min. Based on preliminary results, this experiment was carried out to 60 minutes in order to analyze the active process of cell attachment and spreading. Additionally, the cells become too confluent and too flattened for accurate analysis at later time points. Once removed, cells were methanol fixed, washed, and stored as previously described. Phase contrast images were taken of each well using a Zeiss Axiovert 35 microscope (Carl Zeiss AG) at 20x magnification. Images were pre-processed using Fiji and PHANTAST and analyzed using Leica LASX software (Leica Microsystems, Inc.) as described previously. Results were graphed and statistical analysis performed using GraphPad PRISM v5.01.

Immunofluorescent Microscopy during Cell Spreading

Cells were grown to confluency as previously described. Cells were then counted using a hemacytometer and diluted to 30,000cells/well concentration and plated in 12 well plates containing collagen I coated glass coverslips (Fisherbrand #1.5) [Fisher Scientific, Hampton, NH] prepared as described in the attachment and spreading assay on

a collagen I matrix. Cells were placed in a 37°C, 5% CO₂ tissue culture incubator for 45 minutes. Cells were washed twice with DMEM-F12-no phenol red (Gibco #11039-021) and fixed using 3.7% methanol-free formaldehyde (Polysciences, Inc., #18814-10) [Warrington, PA] for 10 minutes at room temperature. Free aldehyde groups were quenched using 0.1M NH₄Cl (Sigma-Aldrich) for 15 minutes at room temperature and cells were permeabilized using 0.1% Igepal (Sigma-Aldrich) for 10 minutes at room temperature. Coverslips were incubated with Alexa Fluor 488 Phalloidin antibody, 6.6µM (Cell Signaling #8878) [Danvers, MA] at a 1:100 dilution for 45 minutes at 37°C. Coverslips were mounted using ProLong Diamond Antifade mounting medium with DAPI (Life Technologies #P36971) [Carlsbad, CA] for nuclear staining. Cell spreading was visualized using the Leica Laser Scanning SP8 Confocal microscope (Leica Microsystems, Inc.) at 63x magnification. Maximum projection images were subjected to deconvolution using Leica LASX software. SPARC⁺ UROtsa parent cells were used as a control for cell spreading.

SPARC siRNA Transfection in the Cd #1-SPARC Transfected Cell Line

Cells were grown to confluency in 12 well plates. *TransIT*-siQUEST (Mirus #MIR2114) [Mirus Bio LLC, Madison, WI] transfection reagent was added to OptiMem (Gibco) and incubated for 15 minutes at room temperature. SPARC siRNA (Dharmacon #J-003710-07-002) [Dharmacon Inc., Lafayette, CO], Non-targeting Scrambled siRNA (Dharmacon #D-001810-01-05), or siGLO Lamin A/C control siRNA (Dharmacon #D-001620-02-05) were reconstituted in sterile 1xPBS. siRNA was diluted in OptiMem at 1:20 creating a 1µM working solution. siRNA was then added to microfuge tubes containing *TransIT*-siQUEST and OptiMem and incubated for 15 minutes at room

temperature. siRNA/transfection complexes were added in dropwise manner to respective wells containing fresh growth medium. Cells were incubated with siRNA/transfection complexes for 24 hours in a 37°C, 5% CO₂ tissue culture incubator. Cells were then harvested for RNA and protein analysis. Treatments were performed in duplicate with one well for RNA analysis and one well for protein analysis.

RNA and Protein Isolation from the Cd #1-SPARC Transfected Cell Line

Total RNA was isolated from siRNA treated cells using TRI REAGENT™ (Molecular Research Center, Inc., Cincinnati, OH). Cells were washed with cell culture PBS and 500µL TRI REAGENT was added to each well. Cell suspension was transferred to microfuge tube and incubated at room temperature for 10 minutes. 50µL 1-Bromo-3-Chloropropane (BCP) [MRC #BP151] was then added and each sample was vortexed to mix. Samples were incubated for 5 minutes at room temperature then centrifuged at 12,000g for 15 minutes at 4°C to separate sample. Aqueous phase was transferred to a fresh RNase/DNase free microfuge tube and 250µL 100% Isopropanol was added to each sample. Samples were incubated for 10 minutes at room temperature then centrifuged at 12,000g for 7 minutes at 4°C to precipitate RNA. Supernatant was removed, pellet was washed with 75% EtOH, and centrifuged at 12,000g for 7 minutes at 4°C. Again, supernatant was removed and pellet was allowed to air dry for 3-10 minutes. Pellet was reconstituted in 30µL nuclease free water (Mo Bio Laboratories, Carlsbad, CA). RNA concentration was determined using the Nanodrop One (Thermo Fisher Scientific, Waltham, MA) and a portion of each sample was diluted to 20ng/µl concentration for subsequent RT-qPCR analysis.

Total protein was isolated from siRNA treated cells using phosphate buffered saline (PBS)-based lysis buffer, comprised of: 10x PBS, 100mM magnesium chloride ($MgCl_2$), 100mM ethylene glycol tetraacetic acid (EGTA, pH 8.0), 100mM sodium pyrophosphate ($NaPpi$), 100mM sodium orthovanadate (Na_3VO_4), 1M sodium fluoride (NaF), protease inhibitor cocktail tablets (cOmplete Mini Ref# 11836153001) [Roche Diagnostics, Mannheim, Germany], 2% w/v sodium dodecyl sulfate (SDS). Cells were washed with cell culture PBS and 125 μ L PBS lysis buffer with protease inhibitors was added to each well. Cells were scraped to the bottom of each well and transferred to microfuge tube. Samples were incubated at room temperature for 5 minutes then sonicated using the 60 sonic dismembrator (Fisher Scientific) to shear the DNA. Protein concentration was determined using a BCA Assay. Albumin standards were made (Thermo Fisher Scientific) and each protein sample was diluted 5-fold. Standards and protein samples were plated in triplicate in a 96-well flat-bottom plate. Working reagent was added to each well with water and working reagent only as controls. The plate was incubated at 37°C for 30 minutes. Color change was quantified using a spectrophotometer at a 570nm wavelength. Protein concentration was further determined using Excel for subsequent use in western blot analysis.

RT-qPCR Analysis of SPARC siRNA Transfected Cd #1-SPARC Cells

SPARC mRNA expression in siRNA treated cells was determined using real-time reverse transcription polymerase chain reaction (RT-qPCR). 100ng of total RNA was used in a 20 μ L reaction volume for cDNA synthesis using the iScriptTM cDNA Synthesis Kit (#1708891) [Bio-Rad Laboratories, Hercules, CA]. Each sample was run on a thermocycler using the following protocol: priming – 5 min. at 25°C, reverse

transcription – 20 min. at 46°C, and RT inactivation – 1 min. at 95°C. cDNA samples were then used for subsequent RT-qPCR.

2µL of cDNA was amplified using 20µM SPARC specific primers (Qiagen #QT00018620) [Qiagen, Valenica, CA] and recorded using SYBR green fluorescence in a total reaction volume of 20µL. Samples were run on a CFX960 Thermocycler (Bio-Rad Laboratories) using the following cycling parameters: 5 min. at 95°C, Denaturation – 15sec. at 95°C, Annealing – 45sec. at 62°C, repeat denaturation and annealing steps x39, and the melt curve was collected. SPARC expression was determined relative to the untreated control using a standard curve generated from qualitative SPARC standards. SPARC mRNA expression was normalized to β-actin amplified using an Invitrogen primer set with the following sequences, sense: CGACAACGGCTCCGGCATGT, anti-sense: TGCCGTGCTCGATGGGGTACT. [Invitrogen, Carlsbad, CA] under the same cycling parameters. β-actin expression was determined relative to the untreated control using a standard curve generated using β-actin standards. Expression data was graphed and statistical analysis performed using GraphPad PRISM v5.01.

Western Blot Analysis of SPARC siRNA Transfected Cd #1-SPARC Cells

SPARC protein expression in siRNA treated cells was determined using Western Blot analysis. 20µg of total protein was separated on a pre-cast Any kD polyacrylamide gel (Bio-Rad #4568123). Bands were transferred from the gel onto a membrane using the TransBlot Turbo Transfer System (Bio-Rad) for 7 minutes. The membrane was blocked using 5% powdered milk in TBS-T (Tris-Buffered Saline with 0.1% Tween) blocking buffer for 1.5h at room temperature. The membrane was then incubated with mouse anti-Osteonectin antibody (Novocastra™, Cat # NCL-O-NECTIN) [Leica Biosystems Inc.,

Buffalo Grove, IL] at a 1:200 dilution in 1% milk in TBS-T overnight at 4°C. Membrane was washed three times with TBS-T and incubated with anti-mouse IgG, HRP-linked antibody (Cell-Signaling Technology, #7076S) at 1:3,000 and anti-biotin, HRP-linked antibody (Cell-Signaling Technology, #7075S) at 1:1,500 in 1% powdered milk in TBS-T for 1h at room temperature. The membrane was washed three times using TBS-T and incubated with developing solution (1:1 luminol solution:peroxide solution) (Bio-Rad) for 5min. at room temperature. The ChemiDoc MP Imaging System (Bio-Rad) was used to visualize SPARC protein expression.

The membrane used for SPARC protein expression was stripped and re-probed for β -actin by incubating in stripping buffer (Bio-Rad) for 1h at room temperature. The membrane was washed three times with TBS-T and placed in 5% BSA blocking buffer (5% w/v Bovine Serum Albumin in TBS-T) for 1.5h at room temperature. Following blocking, the blot was incubated with mouse monoclonal anti- β -actin antibody (Abcam, #ab8226) [Abcam, Cambridge, MA] at 1mg/mL using a 1:2,000 dilution in 1% BSA in TBS-T overnight at 4°C. The blot was washed three times with TBS-T and incubated with anti-mouse secondary antibody anti-mouse IgG, HRP-linked antibody (Cell-Signaling Technology, #7076S) at 1:3,000 and anti-biotin, HRP-linked antibody (Cell-Signaling Technology, #7075S) at 1:1,500 in 5% powdered milk in TBS-T for 1h at room temperature. Membrane was washed and developed as described above.

Statistics

All data was analyzed using GraphPad PRISM v5.01 software (GraphPad Software). Statistical analysis for cell attachment and spreading was performed using a one-way ANOVA and Tukey's Multiple Comparison *post hoc* testing. Statistical analysis

for mRNA expression was performed using a one-way ANOVA and Dunnett's Multiple Comparison *post hoc* test. Statistical significance was determined for all results using $p < 0.05$.

Results

Wound Closure of SPARC⁺ UROtsa Parent, Cd #1, and the Respective Cd #1-SPARC Transfected Cell Lines

SPARC⁺ UROtsa parent control cells, a cadmium transformed UROtsa cell line (Cd #1) and its respective stably transfected SPARC cell line (Cd #1-SPARC) were used to assess SPARC's role in wound closure. Previous studies analyzed wound closure in the presence of mitomycin C, to prevent cell growth, at 24 hours and 48 hours (Larson et al., 2010). This study aimed to assess wound closure at earlier time points to determine if there was a difference in wound closure between SPARC expressing and non-SPARC expressing cells up to 24 hours post-wound. Figure II-2 shows representative phase-contrast images of the wounded area in the SPARC⁺ control, Cd #1, and the Cd #1-SPARC cell lines at 0hr., 4hr., 8hr., 12hr, and 24hr. post-wound. Three locations along the wound front were analyzed in each image at each time point.

Results in figure II-3 show the percent wound closure with regard to SPARC expression. It appears there is no difference in wound closure at any time points except 24 hours post-wound. At 24 hours, both the Cd #1 and Cd #1-SPARC cell lines had a larger percent of the wound open than the SPARC⁺ control cells. It does appear there is a slight increase in wound closure of the cell lines expressing SPARC at the 8 hour and 12 hour time points; however, the results were not significant. At the 24h time point the Cd #1-SPARC shows a significant decrease in wound closure compared to the SPARC⁺ control cell line. The Cd #1 cell line continued to show a delay in wound closure

becoming significant at 24 hours. This significance may be indicative of a shift in the biological process occurring in the transformed cells. When a cell is proliferating it is not migrating and vice versa. Therefore, cell migration may still be the dominant process in the non-transformed cells while cell proliferation has become the dominant process in the cadmium transformed cells at 24 hours. Previous results show Cd #1 and Cd #1-SPARC have decreased doubling times compared to the SPARC⁺ control UROtsa cells indicating that they proliferate more quickly than the SPARC⁺ control cells (Larson, 2012).

Previous results also show variation between malignantly transformed isolates in growth, migration, and invasion (Slusser et al., 2016). Therefore, although we are assessing the same biological process of wound healing overall, the cells in this experiment were not treated to inhibit cell proliferation so both proliferation and migration are a part of this wounding assay.

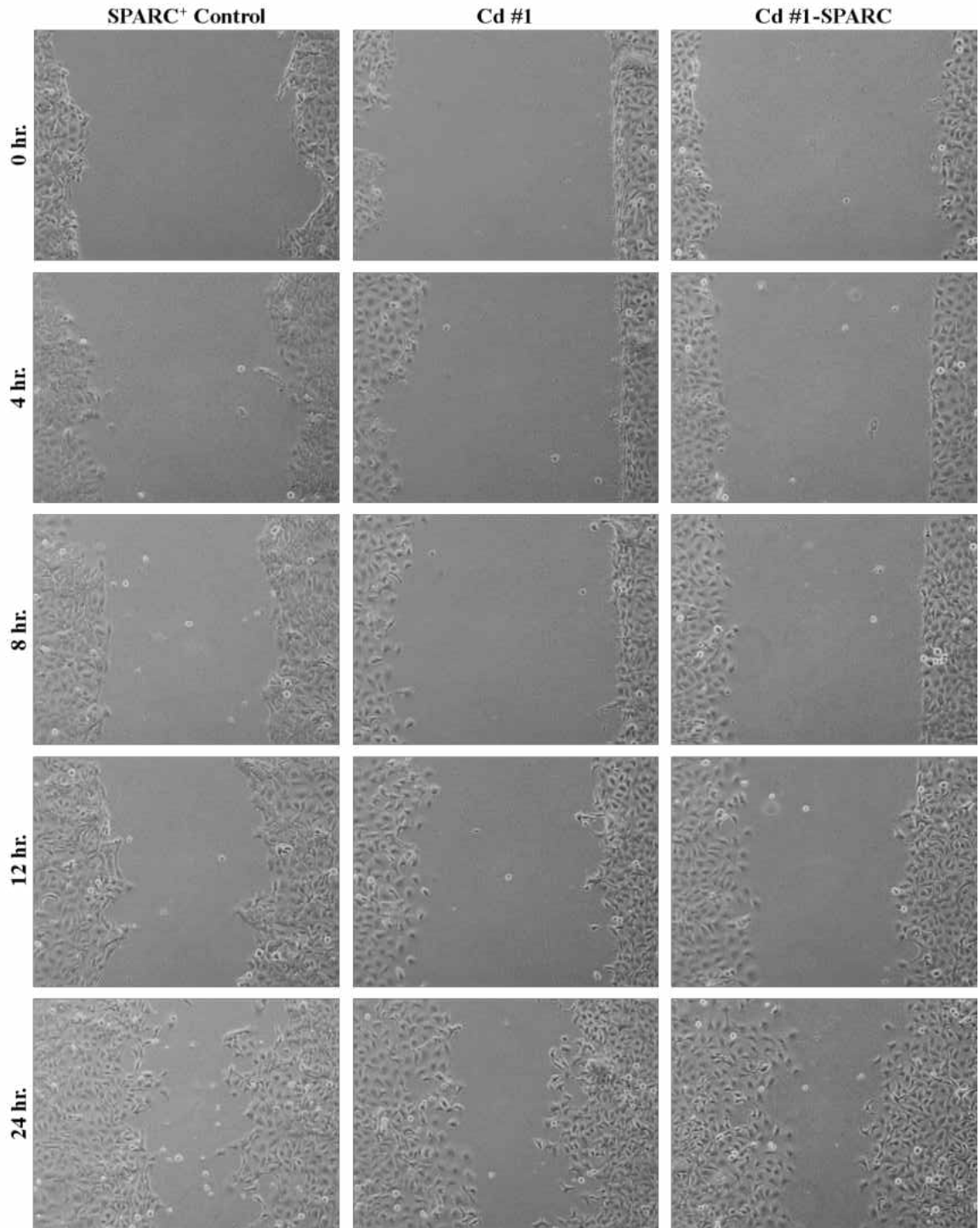


Figure II-2. Phase Contrast Images of Wound Closure. SPARC⁺ cell line, Cd #1 cell line, and Cd #1-SPARC cell lines at 0 hours, 4 hours, 8 hours, 12 hours, and 24 hours post-wound. Percent wound closure determined by measuring the distance between wound edges divided by the initial wound distance.

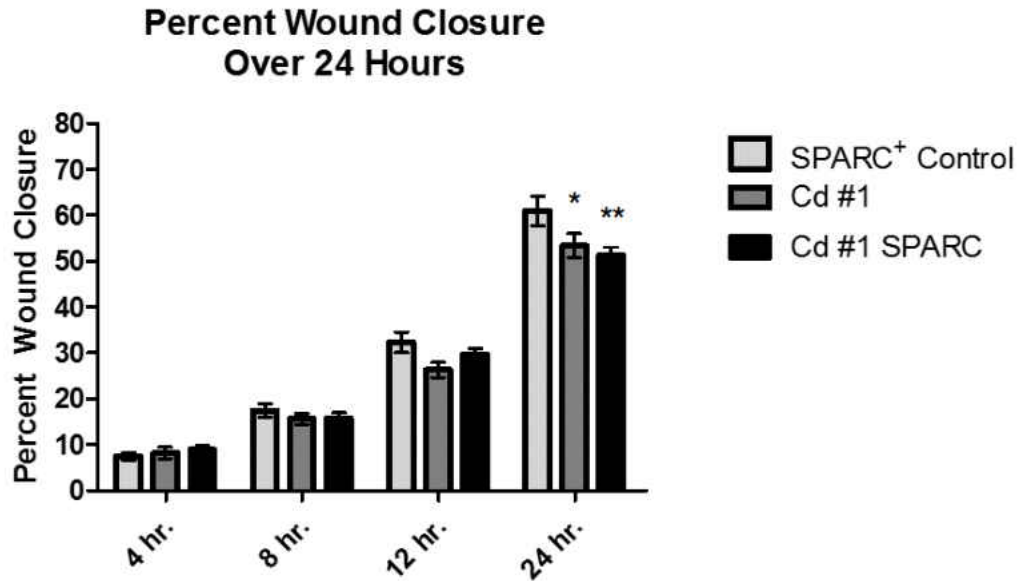


Figure II-3. Percent Wound Closure and SPARC Expression. Wound closure measured over 24 hours of SPARC⁺ control, Cd #1, and Cd #1-SPARC cell lines. Data represents the mean \pm SEM of 20 measurements. Statistical significance determined using two-way ANOVA with Bonferroni *post hoc* test. * ($p \leq 0.05$) and ** ($p \leq 0.01$).

Cell Attachment and Spreading Under Normal Tissue Culture Conditions

To assess SPARC's role in cellular attachment and spreading in our lab model system, SPARC expressing control cells (UROtsa parent), non-SPARC expressing cadmium transformed cells (Cd #1), and the respective SPARC-transfected cells (Cd #1-SPARC) were used. These cells were plated under normal cell culture conditions to initially determine if SPARC had a potential role in these cell biological processes. Figure II-4 depicts the percentage of total cells that are rounded (not spreading) at 30 minutes, 60 minutes, and 120 minutes. The SPARC expressing control UROtsa parent cells are not shown; however, Cd #1-SPARC cells show a decrease in the percentage of rounded cells compared to their respective non-transfected Cd #1 parental cell lines. Interestingly, this difference appeared to decrease with time. These preliminary results

provided confidence in moving forward to assess SPARC's role in attachment and spreading on a collagen I matrix.

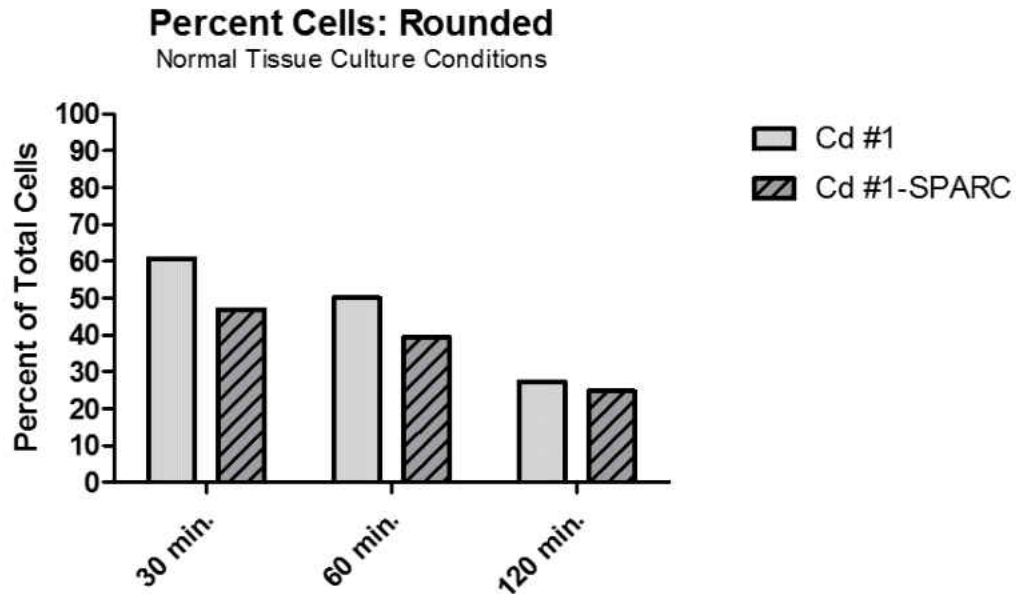


Figure II-4. Preliminary Cell Attachment and Spreading Assay under Normal Tissue Culture Conditions. Data represents the rounded percent of total cells counted in one field at 10x magnification at 30 minutes, 60 minutes, and 120 minutes. The Cd #1 cells have nearly lost all SPARC expression following heavy metal malignant transformation. The Cd #1-SPARC cells have been malignantly transformed and transfected to express SPARC under a CMV promoter.

FIJI PHANTAST Cell Attachment and Spreading Image Processing

Cellular attachment and spreading was initially analyzed via observation and manual counting of cells in each group. This process was long and tedious, introduced an element of human bias, and was generally not feasible for a larger number of conditions. Therefore, it was necessary to evaluate a software analysis process. After an extensive literature search, it was determined that Leica had developed a program, within its LASX microscope software, with a classifier that could be used to categorize cells based on morphology. However, this was initially designed to work with fluorescent images. The images from the attachment and spreading assay were grey-scale phase-contrast images

and the Leica LASX software program was not able to distinguish the cells from the background. In order to get the LASX software to classify cells from a phase-contrast image it was necessary to process the image in FIJI prior to analyzing it with the LASX software.

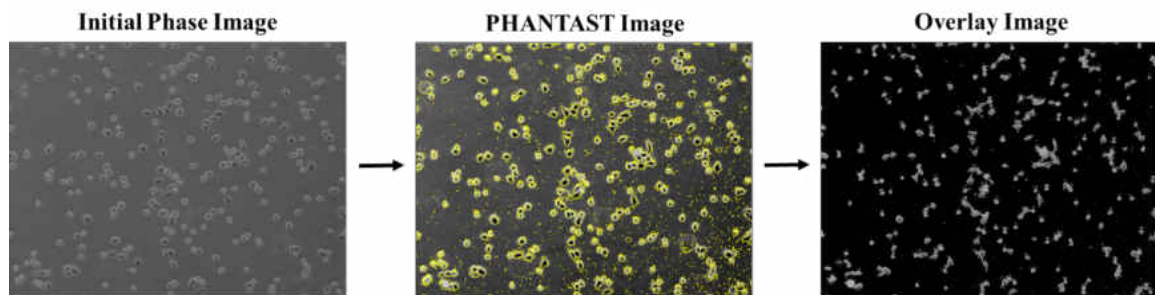


Figure II-5. Cell Attachment and Spreading Assay Image Processing. Images show the progression of processing used in FIJI. The PHANTAST plugin was used to reduce the halo-effect from phase-contrast imaging and more precisely define cell borders. The resulting overlay image can then be used in the LASX software from Leica to categorize the cells based on morphology.

Figure II-5 illustrates the image processing performed in FIJI using the PHANTAST plugin. The initial phase-contrast image is changed from an 8-bit image to a 32-bit image making it clearer. Then, this image is processed using the PHANTAST plugin. This process uses an algorithm to reduce the halo-effect seen in phase-contrast images and improve edge detection. It is necessary to have accurate edge detection when measuring surface area and categorizing cells based on morphology. The output from this processing is a black and white binary image. This is then overlaid onto the original image to create an overlay image. The overlay image shows the cells, with the edge detection determined using the PHANTAST plugin, on a black background. The overlay image is recognized by the Leica LASX software and can be analyzed. This FIJI image processing enables the use of software to analyze images, reducing human bias and increasing classification precision between images.

Leica LASX Cell Attachment and Spreading Image Analysis

Once the attachment and spreading images have been processed through FIJI they could be analyzed using Leica LASX software. The purpose of using the software was to utilize the classifier to more accurately categorize cells based on morphology. Figure II-6 shows the cells in each of three categories determined by the classifier. In order to place each cell into a category, the classifier had to be “trained” on which cells belong in which category. A control image was used to train the classifier containing several cells in each group. It is necessary to give the classifier a range of cells in each group so it can more accurately categorize every cell because each one is slightly different. Multiple factors are taken into account when determining this categorization including: area, length, perimeter, roundness, and shape, as shown in Table 1. How each factor is weighed to determine the proper category is proprietary information belonging to Leica Microsystems, Inc. Once the classifier was properly trained, the same classifier was used for every image to increase consistency in cell classification thus reducing human bias between images.

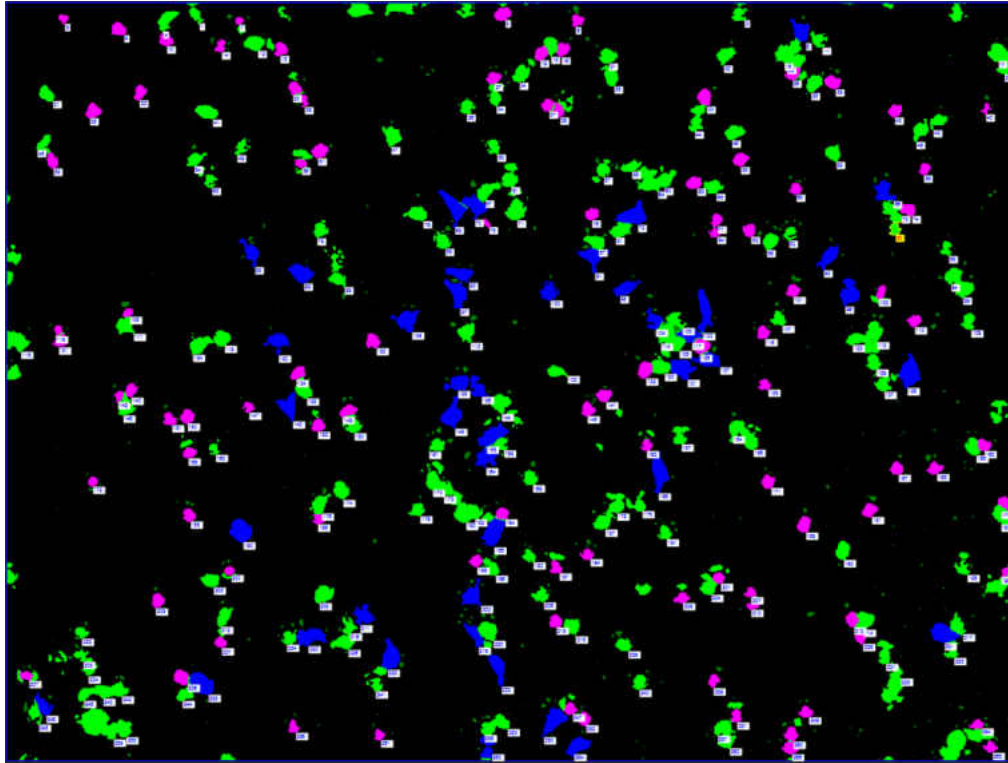


Figure II-6. LASX Classifier Image. LASX Classifier Image depicting classification of cells based on morphology. The classes are represented as: rounded (pink), spreading (green), and flattened (blue).

Table 1. LASX Classification Measurements.

LAS X Automatic Measurement Results								
Number	Accepted	Area [px ²]	Length [px]	Perimeter [px]	Roundness	Shape Factor	ClassifierUser	ClassifierAuto
1	1.000	227.000	25.080	71.422	0.559	1.788	none	Spread
2	1.000	313.000	23.854	66.899	0.879	1.138	none	Attached
3	1.000	257.000	25.080	83.096	0.468	2.138	none	Spread
4	1.000	415.000	35.468	92.771	0.606	1.650	none	Spread
5	1.000	121.000	14.765	41.699	0.874	1.144	none	Attached
6	1.000	208.000	19.723	56.945	0.806	1.241	none	Attached
7	1.000	92.000	12.530	34.391	0.978	1.023	none	Attached
8	1.000	476.000	40.311	105.339	0.539	1.855	none	Very Spread
9	1.000	277.000	21.633	62.576	0.889	1.125	none	Attached
10	1.000	268.000	21.954	63.298	0.841	1.190	none	Attached
11	1.000	290.000	26.627	99.606	0.367	2.722	none	Spread

Classification of each cell in a given image is determined by analysis of multiple measurements, including: surface area, length, perimeter, roundness, and shape. The influence of each measurement on classification is proprietary information belonging to Leica Microsystems, Inc.

During the analysis process there was a need to manually remove cell debris, or cells touching the edge of the image. It was also necessary to split cells that were touching in order for the software to recognize them as individual cells. On occasion the

PHANTAST edge detection processing incorporated some of the background into the identified cell boundary. This occurred when the initial image lacked sufficient contrast and cell borders could not be differentiated from the background at the pixel level. This was solved by manual edge detection and further exclusion of background.

A comparison of manual counts versus software counts was done to validate the use of the Leica LASX software to analyze the attachment and spreading assay images. Figure II-7 illustrates the manual classification and the software classification of SPARC⁺ UROtsa parent control cells. With the manual count, observation only allowed for classification into two categories: rounded or spreading and flattened. However, the software classifier was not able to accurately categorize cells into two categories making it necessary to split spreading and flattened into separate categories creating three total categories: rounded, spreading, and flattened. The spreading category in the software analysis is an in-between that categorizes the cells that have started spreading but have not fully flattened out. Therefore, the black bar, representing spreading and flattened cells, in the manual count is compared to the dark gray (spreading) and black (flattened) bar in the software count. These results show nearly identical cell numbers in each category between the manual count and the software count, validating that the Leica LASX software can accurately classify cells based on morphology. The classification boundary between the spreading and flattened categories may be more ambiguous than the boundary between rounded and flattened. Some cells classified as spreading may be flattened based on observation and vice versa. However, each image was analyzed with the same classifier increasing consistency between images and reducing human bias.

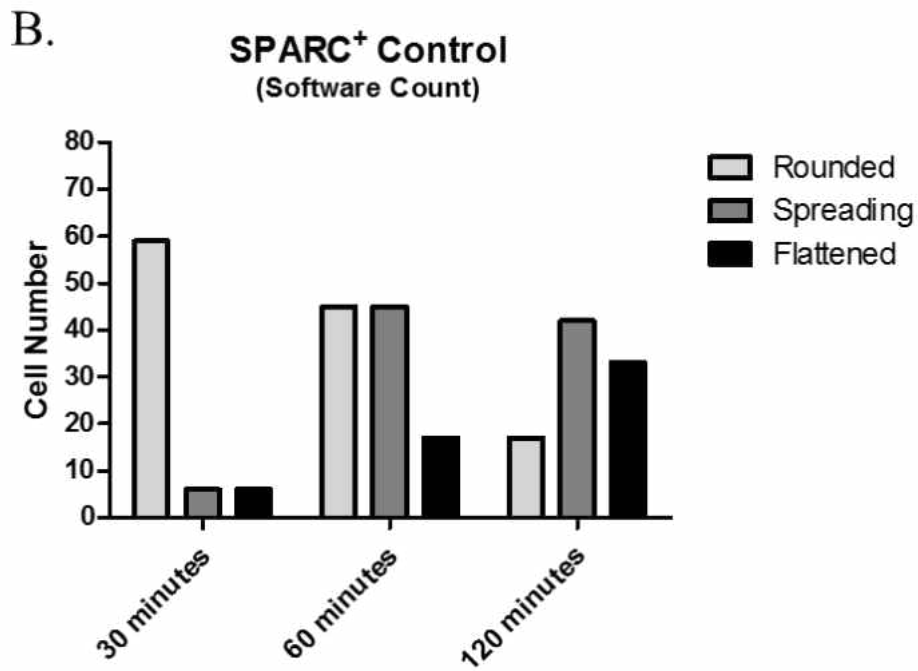
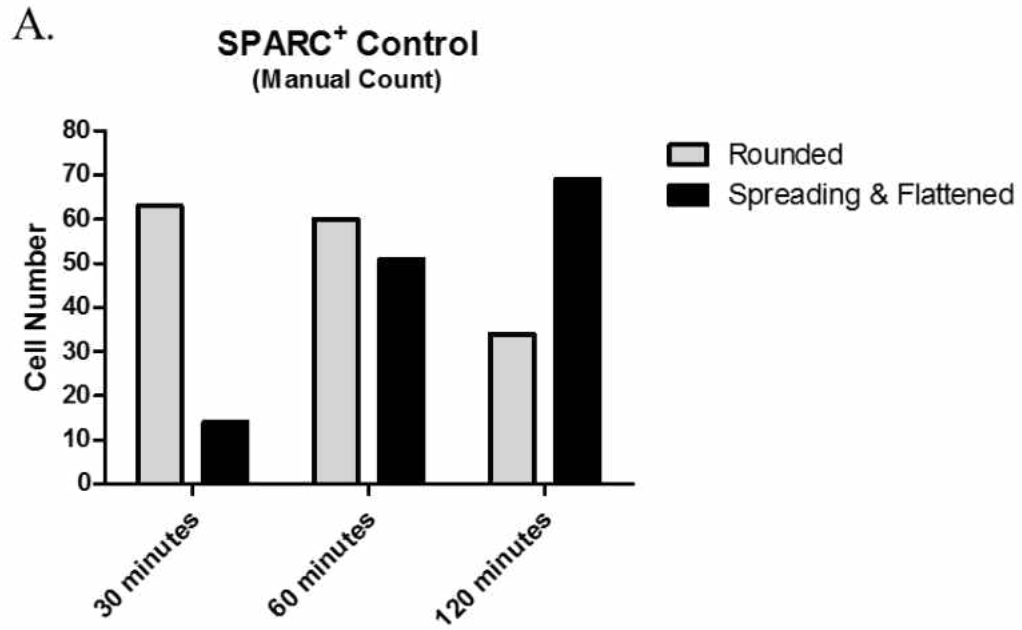
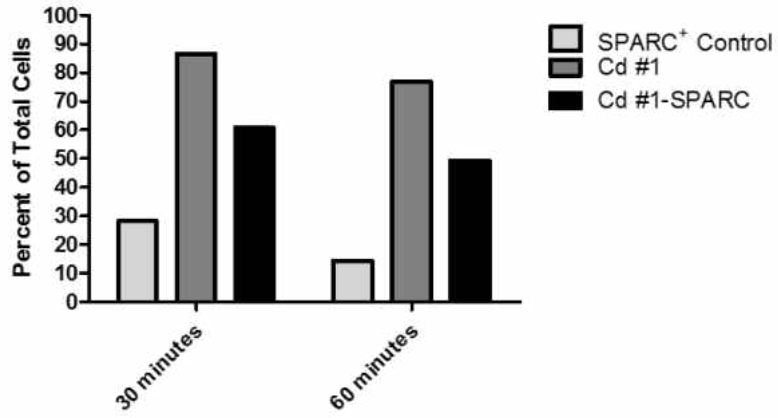


Figure II-7. Classification Comparison of SPARC⁺ UROtsa Parent Cells.
Classification of SPARC⁺ Control UROtsa parent cells counted in one field at 10x magnification comparing a (A) manual cell count and a (B) Leica LASX software cell count at 30 minutes, 60 minutes, and 120 minutes.

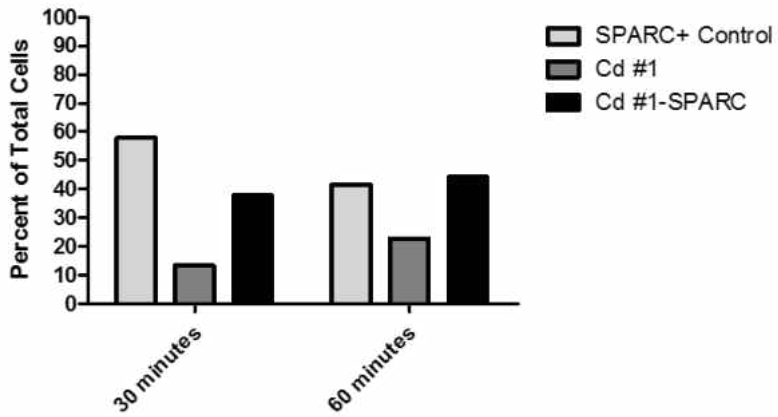
Preliminary Cell Attachment and Spreading of SPARC Expressing and Non-SPARC Expressing Urothelial Cells on a Collagen I Matrix

SPARC is known to interact with fibrillary collagens (Bradshaw and Sage, 2001). Therefore, it was important to test attachment and spreading of SPARC expressing and non-SPARC expressing bladder cells on a collagen I matrix. Figure II-8 illustrates the percent of the total cells attached in each of three categories: rounded, spreading, and flattened. Less than 30% of the SPARC⁺ control cells were still rounded at 30 minutes and that number dropped to approximately 15% at 60 minutes. Just under 60% of the SPARC⁺ control cells were spreading at 30 minutes and approximately half of the cells show a flattened phenotype at 60 minutes. In contrast, The Cd #1 cells showed nearly 90% of the cells rounded at 30 minutes with only 10% fewer rounded cells at 60 minutes. The Cd #1 cells appeared to not reach a flattened phenotype (<1%) within the experimental time frame; showing only about 20% of cells starting to spread by 60 minutes. The Cd #1-SPARC cells showed less rounded cells than Cd #1 but more rounded cells than the SPARC⁺ control at both 30 minutes (60%) and 60 minutes (50%). The Cd #1-SPARC cells did show a slightly higher percentage of cells reaching a flattened phenotype (6.75%) compared to the Cd #1 cells as well as a higher percentage of spreading cells (50-60%). Overall, these results show a delay in cell spreading in the Cd #1 cells lacking SPARC expression compared to the SPARC⁺ control cells and the Cd #1-SPARC transfected cells.

A. Cell Attachment: Rounded
(Percent of Total)



B. Cell Attachment: Spreading
(Percent of Total)



C. Cell Attachment: Flattened
(Percent of Total)

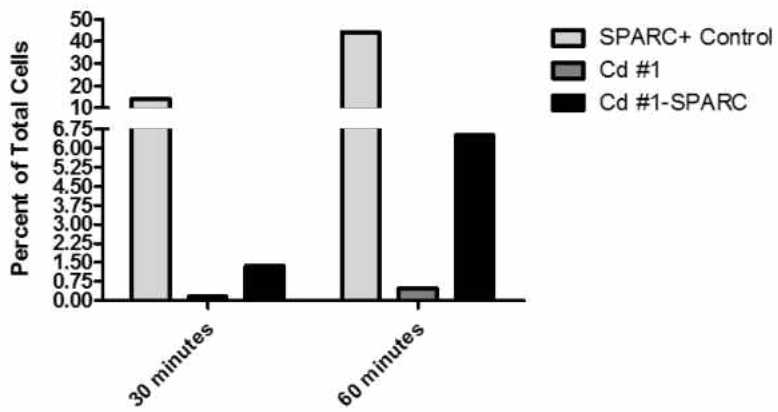


Figure II-8. Preliminary Cell Spreading Assay Quantitation on a Collagen I Matrix. Data represents the percent of total cells counted in five fields at 10x magnification in each of three classes: (A) rounded, (B) spreading, or (C) flattened at 30 and 60 minutes, analyzed using Leica LASX software.

The relative surface area (px^2) of the attached cells in Figure II-9 shows a larger surface area for the SPARC⁺ control and the Cd #1-SPARC cells than the Cd #1 non-SPARC expressing cells further indicating that SPARC⁺ cells were spreading sooner than the SPARC⁻ cells. The SPARC⁺ control cells show an increase in surface area from approximately 430px^2 at 30 minutes to just under 600px^2 at 60 minutes indicating a more flattened phenotype. Although the increase in surface area with increased time in the Cd #1-SPARC cells is not as obvious, the overall surface area (approximately 325px^2) at both time points is larger than the Cd #1 cells (approximately 250px^2). These results support the classification of the cells representing the morphology of the majority of the cell population at 30 minutes and 60 minutes.

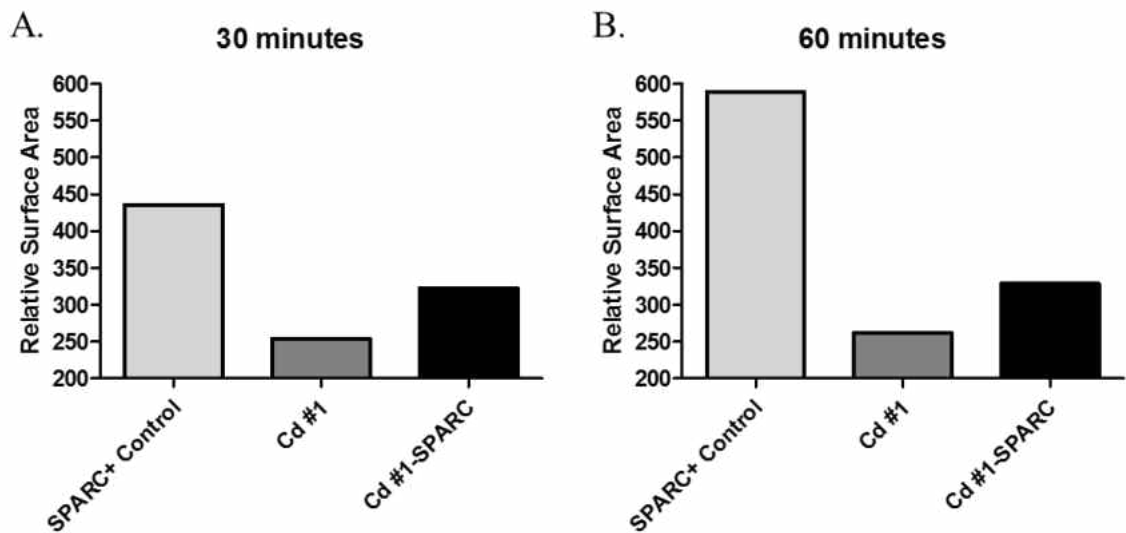


Figure II-9. Preliminary Relative Surface Area Comparison of Attached Cells. Preliminary cell attachment and spreading assay on a collagen I matrix analyzed using Leica LASX software. Each graph depicts the relative surface area of all attached cells in 5 fields at 10x magnification at (A) 30 minutes, and (B) 60 minutes.

The total number of cells attached in figure II-10 potentially illustrates an interaction between SPARC and collagen I that is inhibitory to cell attachment. Results showed 3 to 3.5 times more non-SPARC expressing Cd #1 cells attached than the SPARC⁺ control cells or the Cd #1-SPARC cells. Although there are less total cells attached in the SPARC expressing cell lines these cells appeared to spread sooner than the non-SPARC expressing cells. Taken together these results indicate that SPARC plays a potential role in both cell attachment and cell spreading. Furthermore, the results were conclusive enough to warrant further assessment and experimental optimization to elucidate a cell biological role for SPARC in our model system.

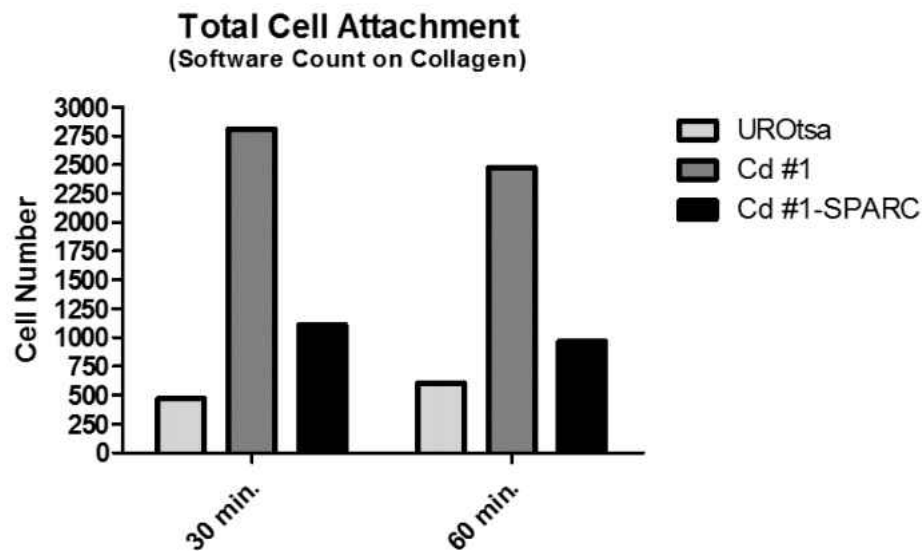


Figure II-10. Preliminary Total Cell Attachment on a Collagen I Matrix. Preliminary attachment and spreading assay total cell count of SPARC⁺ Control UROtsa parent, Cd #1, and Cd #1-SPARC cells on a collagen I matrix. Graph shows the total number of cells counted in 5 fields at 10x magnification at 30 and 60 minute time points.

Cell Attachment and Spreading of SPARC Expressing and Non-SPARC Expressing Urothelial Cells on a Collagen I Matrix

Once experimental conditions were optimized the cell attachment and spreading assay was repeated on a collagen matrix using additional time points. As seen in Figure

II-11, the cell spreading results from this experiment were similar to those from the preliminary experiment. At 30 and 45 minutes post-plating, non-SPARC expressing Cd #1 cells show greater than 80% and 50% of the population, respectively, still rounded. In contrast, the SPARC⁺ control cells and Cd #1-SPARC cells show less than 30% of their cell populations rounded at the same time points. The SPARC expressing cell lines show a more flattened phenotype at 30 and 45 minutes post-plating compared to the non-SPARC expressing Cd #1 cells. 15-20% of SPARC⁺ control cells show a flattened morphology at 30 minutes with this percentage increasing to more than 40% at 45 minutes. The Cd #1-SPARC cells show an even greater percentage of flattened cells with 35-40% of the population flattened at 30 minutes and 45-50% of cells flattened at 45 minutes. The non-SPARC expressing Cd #1 cells show a delay in reaching a flattened phenotype in the first 60 minutes post-plating. At 30 minutes less than 2% of the cells have flattened and this percentage only increases to 5% at 45 minutes. Cellular spreading at 60 minutes shows the same trend as earlier time points; however, there is no statistical difference in the amount of spreading. Overall, similar to the preliminary results, non-SPARC expressing cells show a delay in cell spreading compared to SPARC expressing cells.

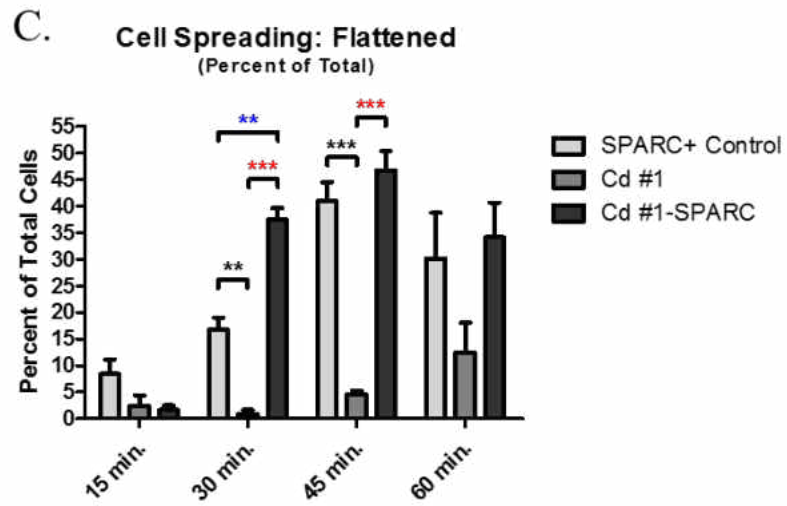
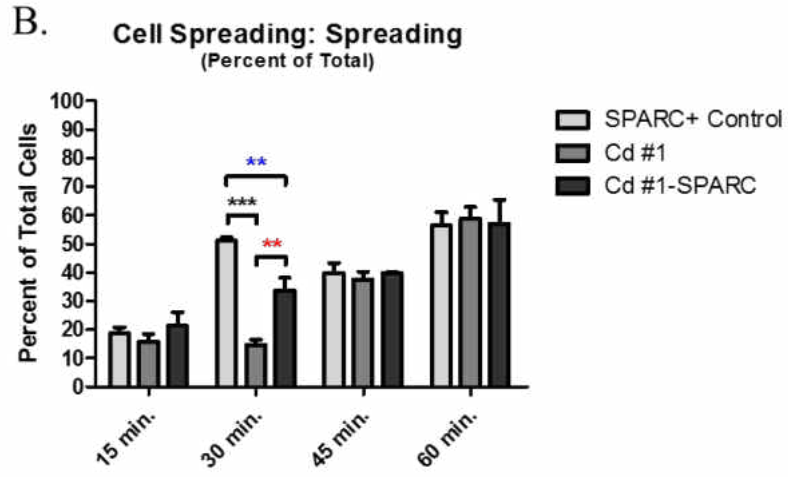
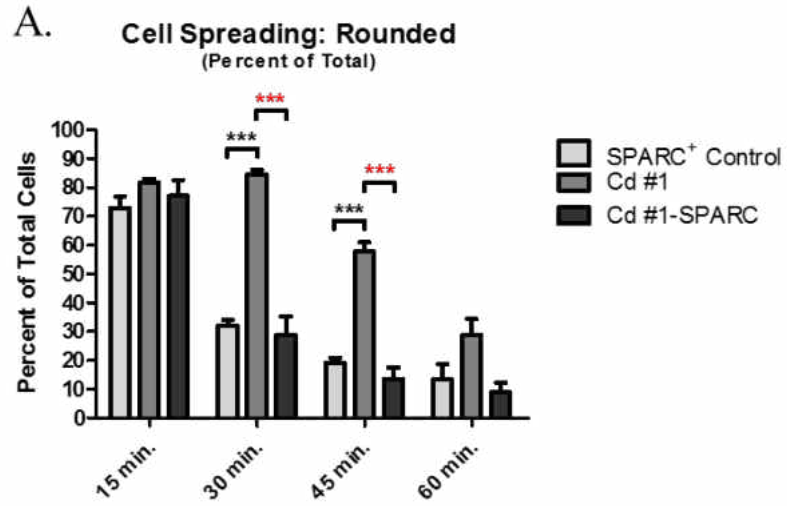


Figure II-11. Quantitation of Cell Spreading on a Collagen I Matrix. Data shows the percent of total cells in each of three classes: (A) rounded, (B) spreading, or (C) flattened. Experiment was performed in triplicate with each time point representing the mean \pm SEM of 10 fields analyzed using Leica LASX software. Statistical significance determined using a one-way ANOVA with Dunnett's Multiple Comparison *post hoc* test. **($p \leq 0.01$), ***($p \leq 0.001$).

The relative surface area results shown in Figure II-12 support the classification results shown in the previous figure. All cell lines show an overall increase in relative surface area (px^2) as time increases. However, the SPARC expressing cells show a larger surface area at 30, 45, and 60 minutes post-plating. This difference is significant when compared to the Cd #1 cells at 45 minutes. Interestingly, the Cd #1-SPARC cells show a significantly larger relative surface area at 30 minutes compared to the Cd #1 cells. The SPARC⁺ control cells do show a larger relative surface area at 30 minutes although the difference is not significant. Additionally, Cd #1 cells do not reach a surface area larger than 1500px^2 in the experimental time frame, when compared to SPARC⁺ control cells and Cd #1-SPARC cells showing surface areas larger than 1500px^2 at the final three time points. Therefore, Cd #1 cells remain rounded for a longer period of time than SPARC⁺ control cells and Cd #1-SPARC cells which attach and start spreading quickly.

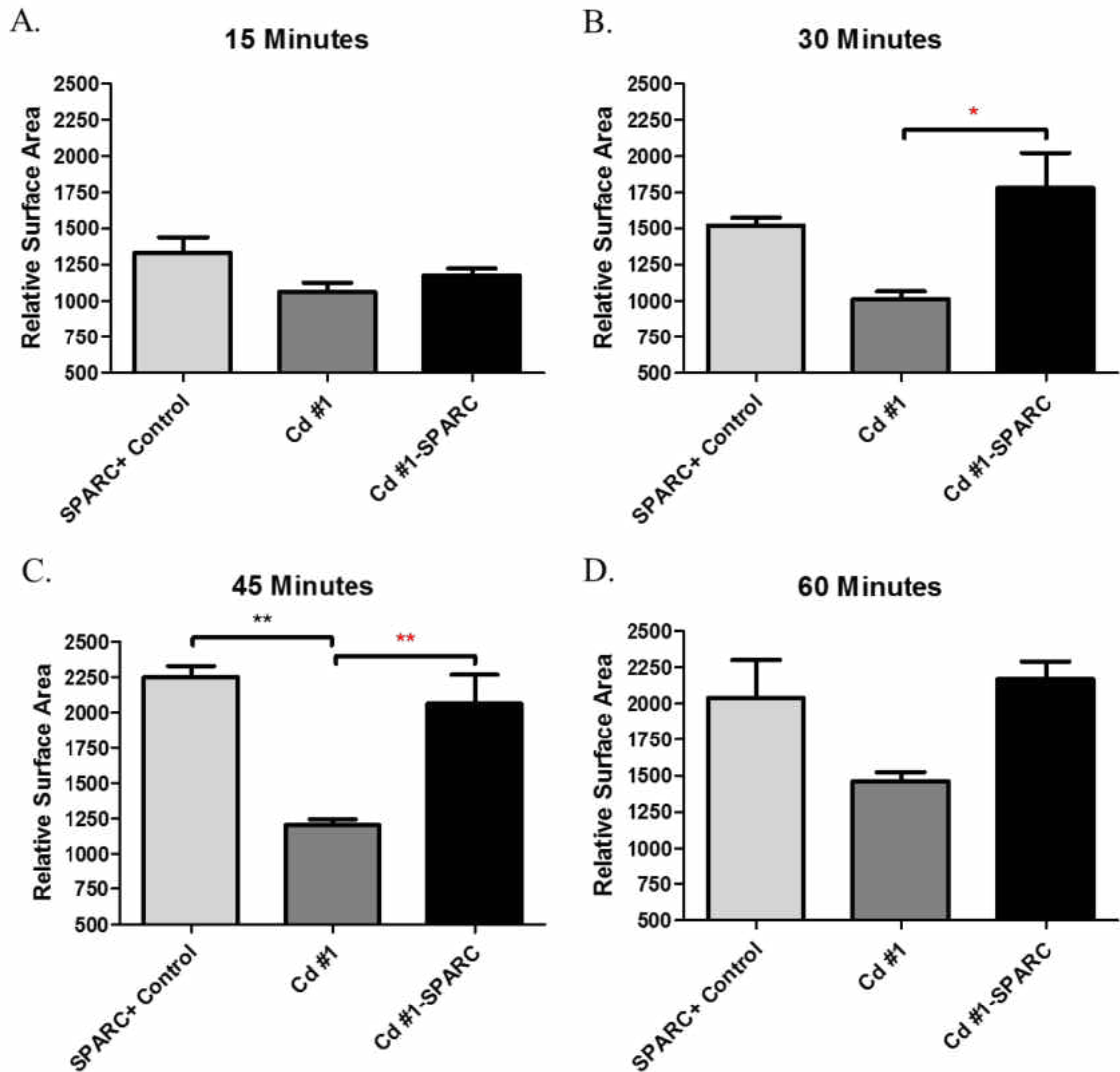


Figure II-12. Relative Surface Area Comparison of Attached Cells. Cell attachment and spreading assay analyzed using Leica LASX software. Graphs show the relative surface area of all cells attached for each cell line at (A) 15 minutes, (B) 30 minutes, (C) 45 minutes, and (D) 60 minutes. Experiment was performed in triplicate with each graph depicting the mean \pm SEM. Statistical analysis was determined using Dunnett's Multiple Comparison *post hoc* test. *($p \leq 0.05$), **($p \leq 0.01$).

The total number of cells attached, spreading, and flattened in Figure II-13 illustrates no difference in the number of cells attached at any time points between cell lines. Generally, the number of cells attached increases as time increases. This is somewhat expected as both SPARC expressing and non-SPARC expressing cell lines

form a monolayer at confluency (Rossi et al., 2001, Somji et al., 2010, Slusser et al., 2016). Unfortunately, this is different than the preliminary results, depicted in Figure II-10, which showed decreased cell attachment of SPARC expressing cells. Optimization of attachment and spreading assay conditions, namely the decreased number of cells plated, may have abrogated SPARC's effect on cell attachment, resulting in a similar number of cells attached across all cell lines.

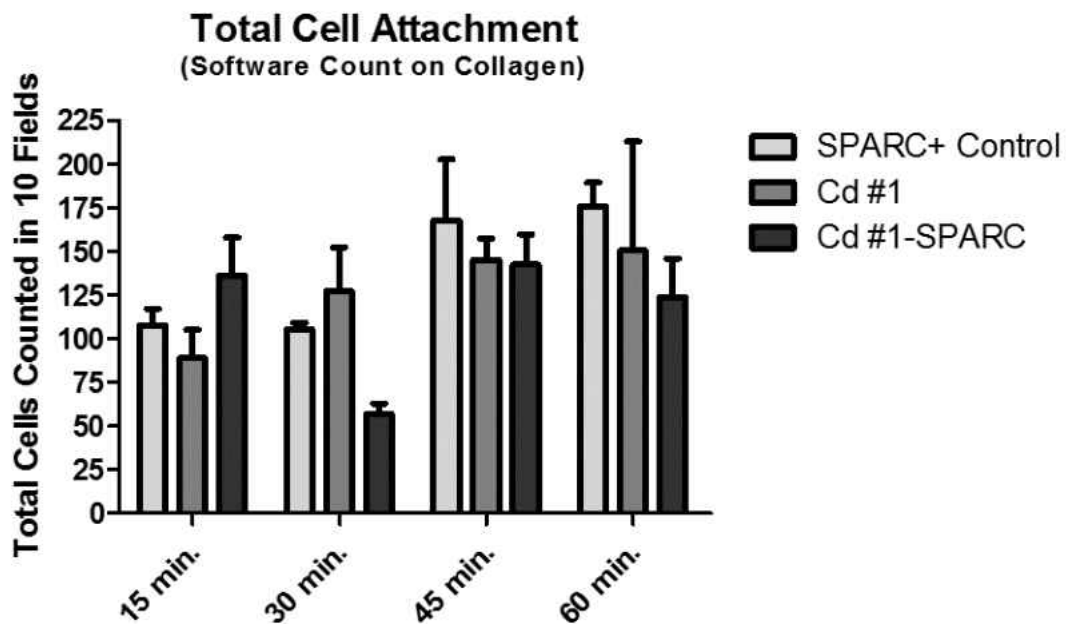


Figure II-13. Total Cell Attachment on a Collagen I Matrix. Attachment and spreading assay total cell count of UROtsa parent, Cd #1, and Cd #1-SPARC cells on a collagen I matrix. Graph shows the total number of cells counted in 10 fields at 20x magnification for each of four 15 minute time points. Each bar represents triplicate wells. Statistical significance determined using a one-way ANOVA with Dunnett's Multiple Comparison *post hoc* test.

Immunofluorescent Microscopy of F-actin during Cell Spreading

Representative images in figure II-14 show F-actin localization of cell spreading at 45 minutes. The SPARC⁺ control cells show strong stress fiber formation illustrating flattened cells with well-organized cytoskeletal structure in long stress fibers. The Cd #1

cells, in contrast, show very little stress fiber formation and cell populations are still rounded or potentially very early in the spreading process. When comparing these two cell populations to the Cd #1-SPARC cells, stress fiber formation is evident mostly at the cell periphery, indicating that they fall between the SPARC⁺ control cells and the Cd #1 cells. These cells are late in the spreading process or early in the flattening process and progressing toward a mature phenotype. These results show that SPARC is important for cell spreading and potentially actin organization, ultimately aiding in cell survival.

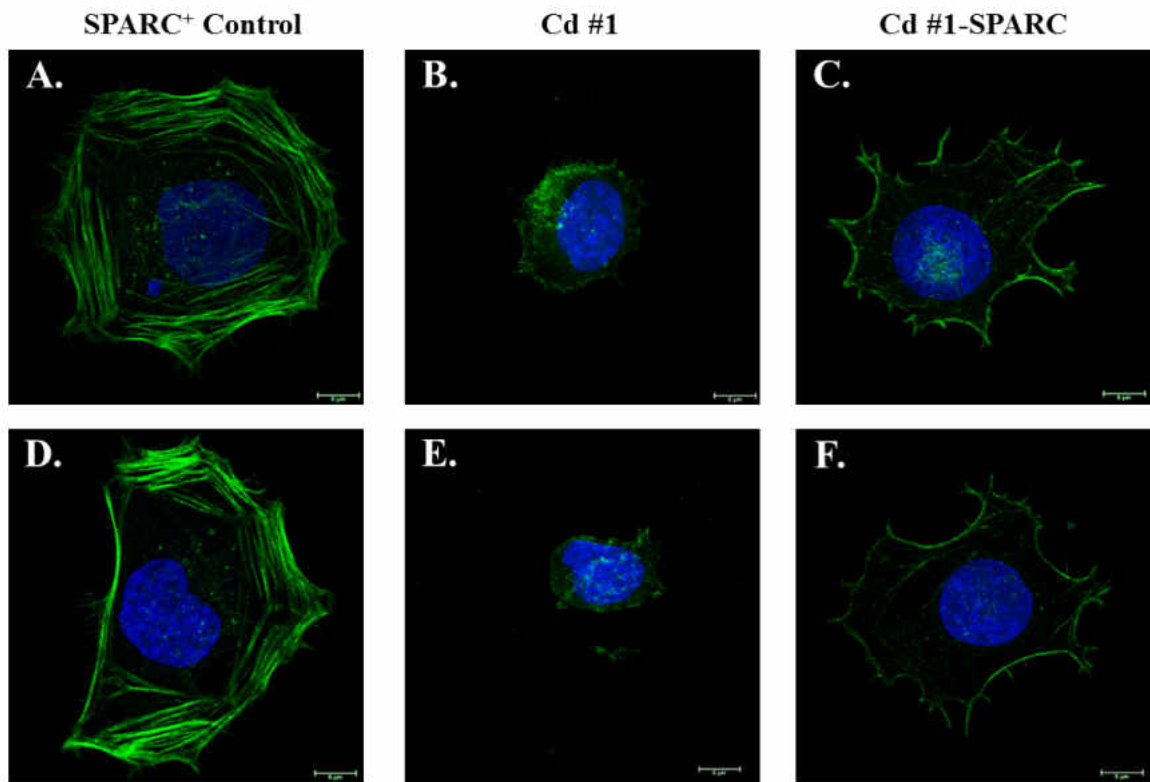
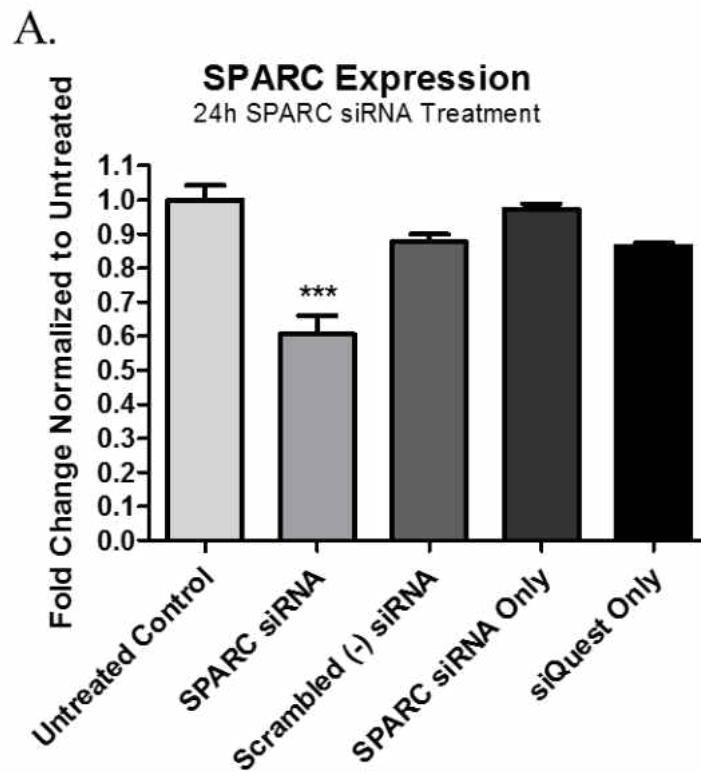


Figure II-14. F-Actin Localization during Cell Spreading on a Collagen I Matrix. Representative immunofluorescent microscopy images of cell spreading. Images show actin cytoskeletal organization using Phalloidin antibody with DAPI as a nuclear stain. (A and D) SPARC⁺ control cells, (B and E) Cd #1 cells, (C and F) Cd #1-SPARC cells.

SPARC siRNA Knockdown in Cd #1-SPARC Transfected Cell Line

Previous results indicate a potential role for SPARC in urothelial cell spreading. Therefore, to further validate this, SPARC was knocked down via siRNA transfection

with the ultimate goal to test cell attachment and spreading when SPARC is repressed in cells previously forced to express SPARC. Figure II-15 shows SPARC mRNA and protein expression following 24 hour transfection with SPARC specific siRNA. mRNA results, in Figure II-15A, show a greater than 40% knockdown in SPARC expression with the control transfections not showing any significant change in expression. Protein expression was then determined to ensure that the knockdown in mRNA also resulted in decreased protein expression within the experimental time frame. Western blot analysis, in Figure II-15B, shows knockdown of SPARC expression in the siRNA treated cells with no change in expression in the control transfections. These results indicated successful knockdown of SPARC in Cd #1-SPARC cells, at both the mRNA and protein levels, at 24 hours post-transfection.



B.

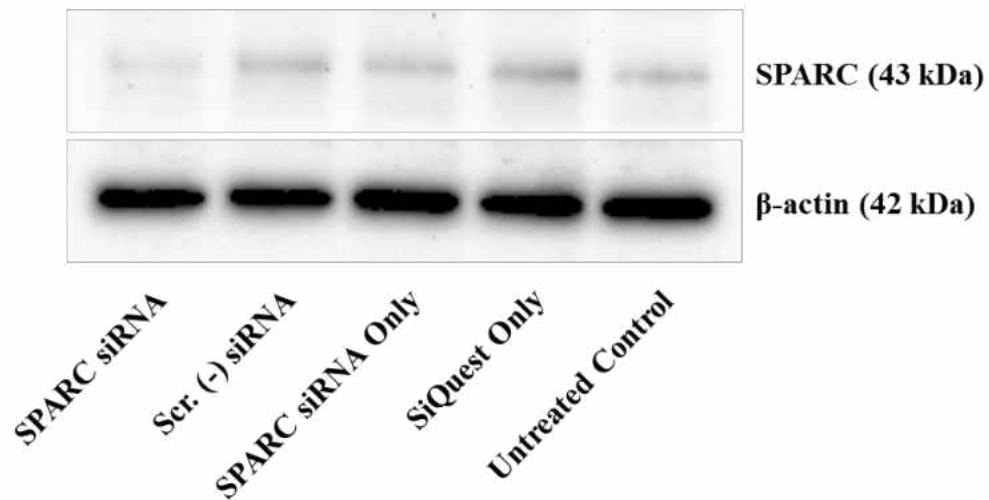
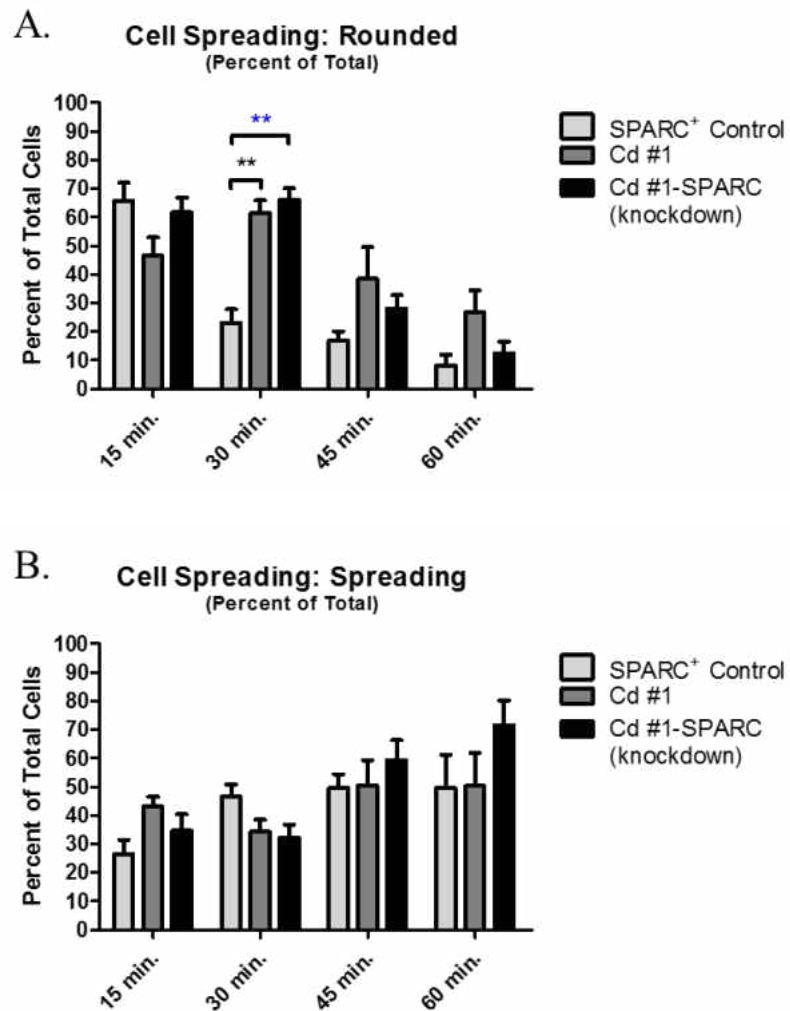


Figure II-15. siRNA Knockdown of SPARC in Cd #1-SPARC Cells. SPARC mRNA and protein expression in Cd #1-SPARC cells treated with SPARC siRNA for 24 hours. (A) RT-qPCR results normalized to Untreated Control with data represented as mean \pm SEM. Statistical significance determined using a one-way ANOVA with Dunnett's Multiple Comparison *post hoc* test. *** denotes significance ($p \leq 0.001$). (B) Western blot analysis showing SPARC and its corresponding β -actin expression.

Cell Attachment and Spreading Following SPARC siRNA Knockdown in Cd #1-SPARC Cells.

Cell attachment and spreading was tested following siRNA knockdown of SPARC in Cd #1-SPARC cells. Previous results showed delayed cell spreading in non-SPARC expressing Cd #1 cells compared to SPARC⁺ control cells and Cd #1-SPARC cells. Results in Figure II-16 show that the increased cell spreading of Cd #1-SPARC cells, depicted as Cd #1-SPARC (knockdown), is reversed when these cells are transfected with SPARC siRNA. After 24 hours of transfection with SPARC-specific siRNA and 30 minutes post-plating, Cd #1 and Cd #1-SPARC (knockdown) cells show 60-70% of the cell population rounded compared to the SPARC⁺ control cells showing less than 30% of the cell population rounded. 30% of the SPARC⁺ control cells have

reached a flattened phenotype at 30 minutes compared to the Cd #1 and Cd #1-SPARC (knockdown) cells showing less than 5% of cells reaching a flattened phenotype. Although the results at 45 minutes and 60 minutes are not significant, the SPARC⁺ control cells show a greater percentage of flattened cells compared to Cd #1 and Cd #1-SPARC (knockdown) cells. Overall, there is a delay in cell spreading of Cd #1 cells and Cd #1-SPARC (knockdown) cells following siRNA knockdown of SPARC.



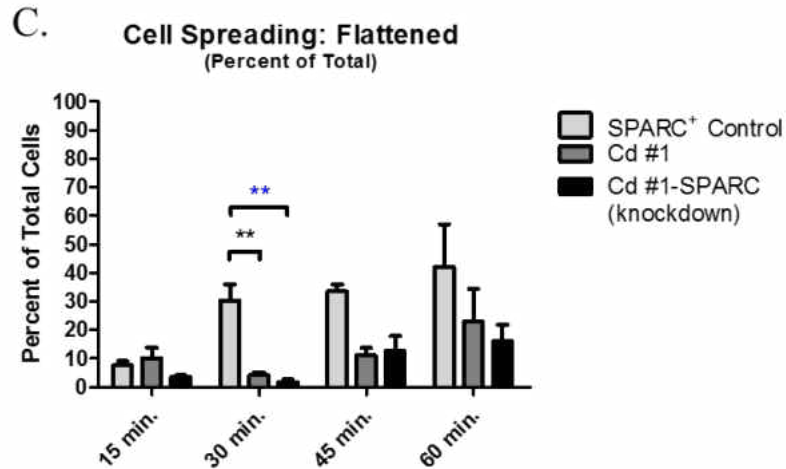


Figure II-16. Quantitation of Cell Spreading Following SPARC siRNA Knockdown. Data shows the percent of total cells in each of three classes: (A) rounded, (B) spreading, or (C) flattened. Experiment was performed in triplicate with each time point representing the mean \pm SEM of 10 fields analyzed using Leica LASX software. Statistical significance determined using a one-way ANOVA with Dunnett's Multiple Comparison *post hoc* test. ******($p \leq 0.01$).

As with previous results, relative surface area (px^2) shown in Figure II-17 shows a general overall increase in surface area as time increases. Cd #1 and Cd #1-SPARC (knockdown) cells do not reach a relative surface area larger than 1900px^2 by 60 minutes. In comparison, SPARC⁺ control cells reach a relative surface area of 1900px^2 at 30 minutes and ultimately reach a relative surface area of 2250px^2 at 60 minutes. Interestingly, the difference in relative surface area observed at 30 minutes is significant for both Cd #1 and Cd #1-SPARC (knockdown) cells. Additionally, the difference in relative surface area remains significant for the Cd #1 cells at 45 minutes; however, the difference between the SPARC⁺ control cells and the Cd #1-SPARC (knockdown) cells, although observable, is no longer significant. Overall, these results support the classification results, in Figure II-16, that knockdown of SPARC in Cd #1-SPARC (knockdown) cells delays cell spreading similar to that of Cd #1 cells.

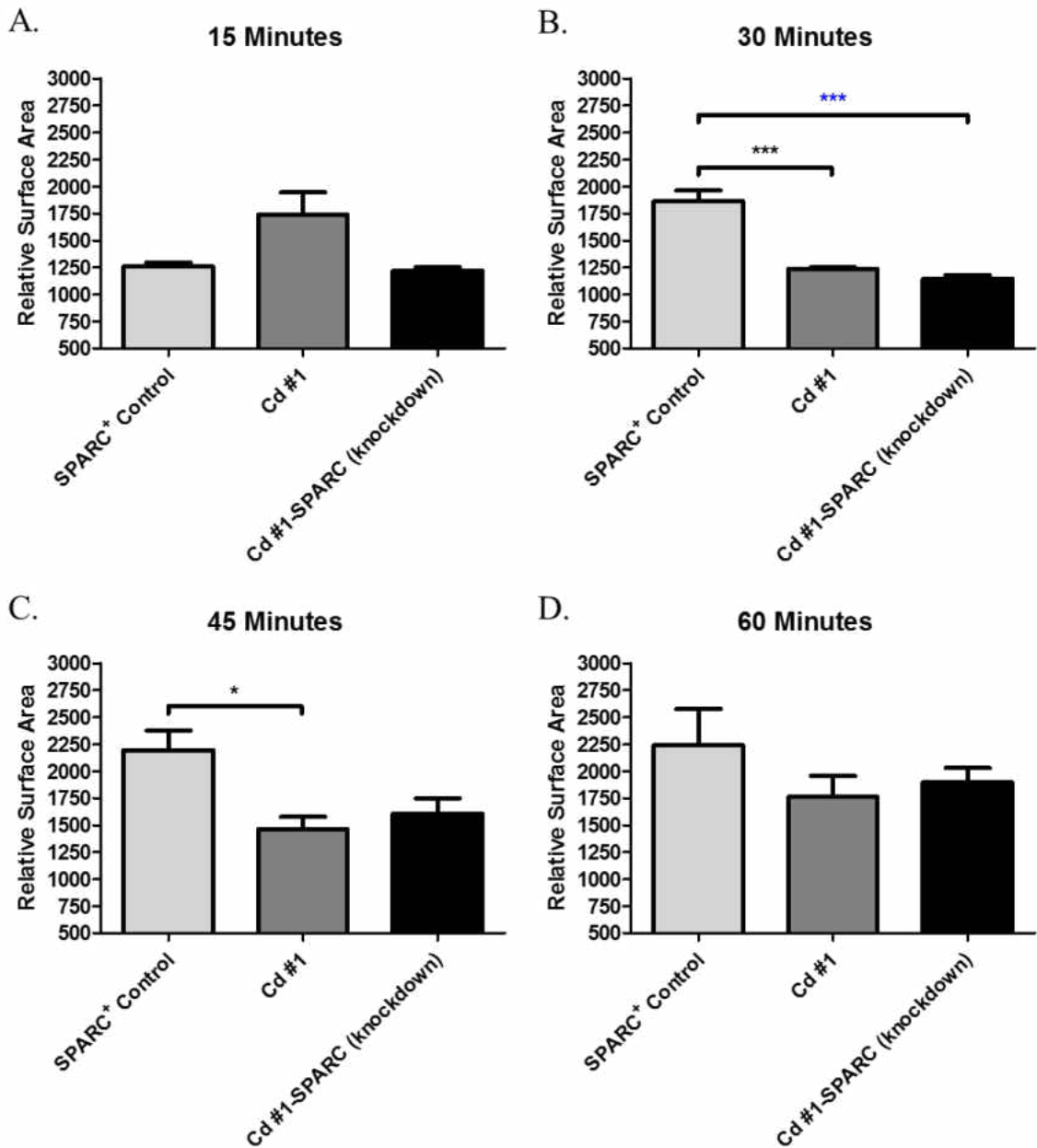


Figure II-17. Relative Surface Area Comparison of Attached Cells Following SPARC siRNA Knockdown. Cell attachment and spreading assay analyzed using Leica LASX software. Graphs show the relative surface area of all cells attached for each cell line at (A) 15 minutes, (B) 30 minutes, (C) 45 minutes, and (D) 60 minutes. Experiment was performed in triplicate with each graph depicting the mean \pm SEM. Statistical analysis was determined using Dunnett's Multiple Comparison *post hoc* test. *($p \leq 0.05$), ***($p \leq 0.001$).

The total number of attached cells (Figure II-18) was calculated for this experiment and, again, there was no difference in the total number of cells attached between cell lines at any time point. As seen in the previous experiment, there is an overall increase in the number of cells attached as time increases. Therefore, it does not appear that SPARC is significantly influencing urothelial cell attachment to collagen I.

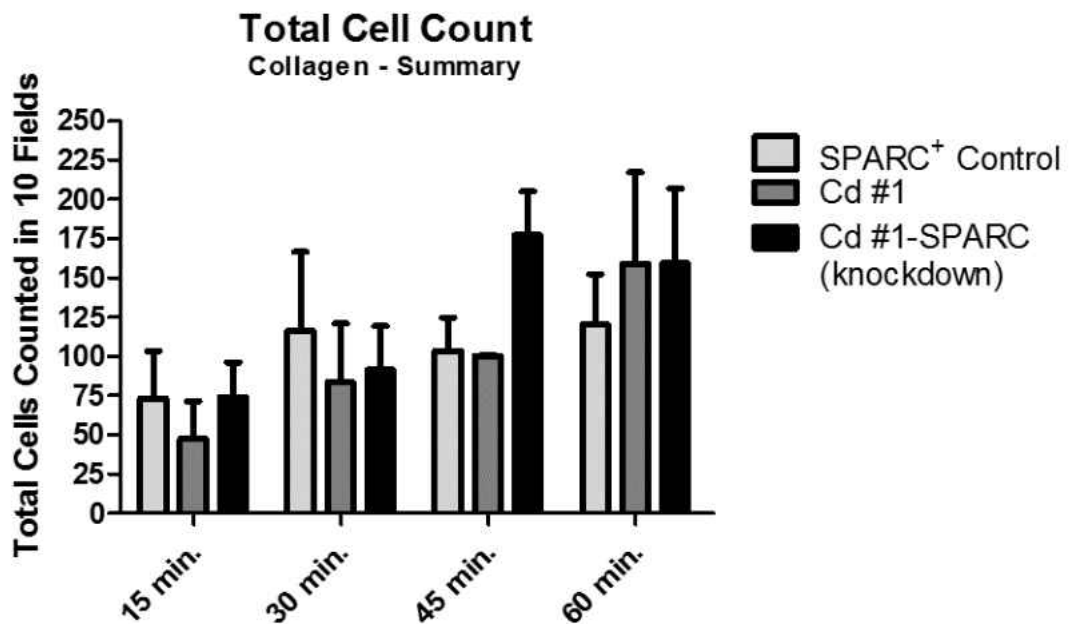


Figure II-18. Total Cell Attachment on a Collagen I Matrix Following SPARC siRNA Knockdown. Attachment and spreading assay total cell count of SPARC⁺ Control UROtsa parent cells, Cd #1, and Cd #1-SPARC (knockdown) cells on a collagen I matrix. Graph represents the total number of cells counted in 10 fields at 20x magnification for each of four 15 minute time points. Experiment was done in triplicate with data represented as the mean \pm SEM. Statistical significance determined using a one-way ANOVA with Dunnett's Multiple Comparison *post hoc* test.

Discussion

Previous lab results have analyzed various cell biological roles for SPARC including cell growth, migration, and invasion. Here, a variation of the wound closure experiment was used to analyze migration and proliferation of non-SPARC expressing and SPARC expressing bladder cells. Interestingly, based on results from this study and

previous studies, SPARC does not appear to play a significant role in wound closure in our model system. Alternatively, SPARC may play a role in wound closure that can be overtaken by a similar protein such as Hevin, from the same family, when SPARC is absent; resulting in no obvious difference in wound closure. SPARC and other family members have been described to play a role in normal wound closure processes, including the inflammatory phase as well as the proliferation and migration phase (Kyriakides and Bornstein, 2003). Because these results do not indicate a role for SPARC in wound closure in urothelial cells, it is possible there is an alternative role for SPARC that is more important to cell survival in this system.

SPARC's known interaction with collagen I, the most abundant collagen in the extracellular matrix space, and overall unknown functional role in bladder cancer prompted assessment of cellular attachment and spreading. Preliminary results showed a decrease in SPARC expressing cell attachment indicating a potential role for SPARC. SPARC has been shown to bind to collagen in a calcium-dependent manner blocking integrin-mediated cell binding to collagen (Bradshaw et al., 2009). Although subsequent experiments showed no difference in cell attachment to a collagen I matrix, it is possible that reducing the number of cells plated from 50,000 cells/well to 30,000 cells/well was sparse enough to abrogate paracrine effects of SPARC on cell attachment. Interestingly, results consistently showed a delay in cell spreading in cells lacking SPARC expression. Sufficient knockdown of SPARC in the malignant cell line transfected with SPARC was necessary to provide further evidence for SPARC's role in cell spreading. Overall, there was no difference in cell attachment; however, the results of cell spreading indicate a potential autocrine role for SPARC in our model system. Based on these results, once

SPARC expressing cells attach, secreted SPARC may act to increase cell spreading allowing this cell to receive survival signals quicker.

Manual analysis of cell attachment and spreading was a tedious process and imparted an aspect of human bias that needed to be addressed. Several studies have utilized observation to classify cells based on morphology (Everitt and Sage, 1992, Motamed and Sage, 1998, Hudson et al., 2005, Delostrinos et al., 2006). The large experimental set up in this study necessitated use of an automated, computer-based method to classify cells. Fiji, with the PHANTAST plugin, developed by Jaccard et al. (2014), allowed gray-scale phase contrast images to be analyzed and categorized using the classifier from the Leica LASX program. Interestingly, several programs have been developed to analyze cell attachment and spreading; however, the user-friendly interface of the Leica LASX program was important, considering the amount of images needed to be classified. Although there was an increase in the “pre-processing” needed to analyze the attachment and spreading results, these tools taken together made the end result more efficient and more consistent by reducing human bias. To the author’s knowledge, this work represents the first time these two software programs have been used in conjunction for cell attachment and spreading analysis of phase contrast images.

The described role for SPARC promoting cell spreading in our model system of cadmium induced bladder cancer is contradictory to the literature. SPARC has been shown to play tissue-specific roles in cell biological processes, including inducing cell rounding in other systems via focal adhesion turnover (Lane and Sage, 1994). Since this role for SPARC has not been previously described, the mechanism behind SPARC’s role in promoting urothelial cell spreading remains unknown. It is possible that SPARC’s

interaction with the cell surface did not interfere with the receptors for attachment, but rather promoted activation of those receptors utilized for cell spreading. Interestingly, the $\alpha_2\beta_1$ integrin receptor is known to bind to collagen I fibrils and promote cell spreading (Jokinen et al., 2004). Therefore, SPARC could be preferentially inhibiting binding of alternative integrins to collagen leaving the $\alpha_2\beta_1$ integrin receptor available for enhanced binding and subsequent cell spreading. However, currently there are no known epithelial cell surface receptors for SPARC so it is also possible that SPARC's role is indirect and its effect is elicited through regulation of growth factors or other cell signaling molecules. Analysis of relevant cell signaling pathways could provide further insight into the mechanism behind SPARC's role in promoting cell spreading. These results suggest a role for SPARC in promoting cell spreading that may inhibit tumor formation, requiring it to be repressed.

CHAPTER III

TRANSCRIPTION FACTOR BINDING AND SPARC REPRESSION IN CD-TRANSFORMED UROTHELIAL CARCINOMA CELLS

Introduction

SPARC, has been shown to be differentially regulated in many types of cancers (Nagaraju et al., 2014). This has led to it being described as oncogene-like and tumor suppressor-like depending on the cancer (Nagaraju et al., 2014). There have been organ-specific and cancer-specific publications proposing mechanisms for SPARC gene regulation, including: promoter hypermethylation, microRNA inhibition, and alternative transcription factor binding (Liu et al., 2018, Ahir et al., 2019, Munk et al., 2019). However, there is little known about the regulation of SPARC in bladder and bladder cancer.

Previous microarray analysis of the arsenic and cadmium transformed UROtsa cells showed SPARC as the gene with the largest change in expression across all of the transformed lines (Garrett et al., 2014). SPARC was significantly repressed to below detectable limits following arsenic or cadmium exposure (Larson et al., 2010, Garrett et al., 2014). These results warranted investigation into the mechanism by which SPARC was being repressed. One hypothesis was that this repression was the result of one or more epigenetic modifications. Two modifications previously studied were histone acetylation and methylation. Experiments were performed to inhibit methylation and acetylation in the arsenic and cadmium transformed cells using methyltransferase

inhibitor 5-Aza-2'-deoxycytidine (5-AZC) and/or a histone deacetylase inhibitor MS-275 in an attempt to rescue SPARC expression (Larson et al., 2010). Results from this experiment showed that inhibiting DNA methylation, or histone acetylation, did not result in an increase in SPARC expression (Larson et al., 2010). Based on these results, it was concluded that DNA methylation and/or histone acetylation was most likely not responsible for SPARC gene repression in our system. Additionally, several miRNAs were investigated for differential expression in the transformed cell lines; however, no clear results were found. These results lead the current study to focus on an alternative explanation for SPARC gene repression by analyzing transcription factor binding to the SPARC promoter.

The SPARC promoter region has been described and characterized by several groups and determined to be highly conserved between human, mouse, and bovine species (Hafner et al., 1994, McVey et al., 1988, Young et al., 1989). Vial et al. (2000) summarizes important similarities in the SPARC promoter between these species. All three contain a GGA-rich motif that is necessary for transcriptional activation. There are two described GGA boxes that are separated by a small spacer region that has been associated with gene repression (Hafner et al., 1994). Interestingly, Hafner et al. (1994) found that the GGA boxes did not contribute to human cell-specific expression of SPARC, in contrast to this being described for GGA sequences in the bovine SPARC promoter. Additionally, there is no TATA box or CAAT box for RNA polymerase II docking and transcription initiation (McVey et al., 1988). The GGA boxes are located between 50 and 130bp upstream of the transcriptional start site located within the short first exon (McVey et al., 1988, Young et al., 1989). In a TATA-less promoter region, Sp1

and/or Sp3 bind and recruit the necessary transcription machinery, including the TATA-box binding protein (TBP) using tethering co-factors (Vizcaíno et al., 2015).

Interestingly, Sp1, specifically, has been described as necessary for activation of TATA-less genes (Vizcaíno et al., 2015). Therefore, with SPARC lacking a TATA box, Sp1 and Sp3 present as intriguing transcription factors to focus on with this study.

Specificity Protein 1 (Sp1) and Sp3 are two transcription factors that have been described to bind to the SPARC gene promoter and activate gene expression (Chamboredon et al., 2003, Briggs et al., 2002, Xu et al., 2010). They contain three highly conserved C-terminal zinc-finger motifs and bind to the same GC-rich consensus sequence; however, DNA-binding properties and regulatory functions differ between the two (Vizcaíno et al., 2015). Sp1 has been described to have two isoforms, differing only slightly in the N-terminal domain. In contrast, Sp3 has been shown to have four isoforms due to multiple translational start sites (Li and Davie, 2010). The two long isoforms only differ slightly, again, in the N-terminal domain and resemble the structure of Sp1; however, the short isoforms are missing one of the activating domains near the N-terminus of the full-length protein and is thought to be responsible for Sp3 gene repression (Li and Davie, 2010). Sp1 and Sp3 transcription factors are ubiquitously expressed and can positively or negatively regulate thousands of gene targets, including autoregulating itself (Vizcaíno et al., 2015). Interestingly, Sp1 and Sp3 may preferentially bind to specific binding sites on the same promoter (Li and Davie, 2010). Which transcription factor is bound to which site could potentially influence gene expression via recruitment of active or repressive transcription complexes (Li and Davie, 2010). Downstream target genes include those for many important cellular processes, cell cycle

regulation, development, and hence, those important for the “hallmarks of cancer” (Li and Davie, 2010, Vizcaíno et al., 2015). Additionally, these transcription factors have been shown to be susceptible to oxidative stress resulting in their repression; as well as, post-translational modifications affecting DNA binding, subcellular localization, and ability to recruit chromatin remodeling complexes (Jutooru et al., 2010, Larabee et al., 2005, Vizcaíno et al., 2015).

SOX5 is an alternative transcription factor implicated in regulating SPARC expression (Huang et al., 2008). SOX5 is one of over 20 members belonging to the sex-determining region on the Y chromosome-related high mobility group box (SOX) transcription factor family (Grimm et al., 2019). SOX5 is in group D with SOX6 and SOX13 showing a relatively extensive and conserved N-terminal domain as well as a coiled-coil domain. The coiled-coil along with a leucine zipper and glutamine-rich domain enable formation of dimers that can enhance DNA binding (Grimm et al., 2019). This family of proteins is structurally quite diverse; however, they are defined by the highly conserved High Mobility Group (HMG) domain containing the DNA binding motif (Grimm et al., 2019). Also within this domain are nuclear localization signals and a leucine-rich nuclear export signal for efficient transport into and out of the nucleus (Grimm et al., 2019). This domain was found to recognize a (A/T)(A/T)CAA(A/T) consensus sequence on the DNA; but, SOX transcription factors do not show a high binding affinity (Grimm et al., 2019, Harley et al., 1994). However, Wegner (2010) addresses the short length of the consensus sequence and extensively reviews proposed mechanistic details regarding differences in DNA binding between specific SOX family

groups. Ultimately, it was concluded that more than the consensus sequence is needed to fully describe SOX transcription factor binding to DNA (Wegner, 2010).

SOX transcription factors are critical for development and cell fate; hence, their expression is tightly regulated (Grimm et al., 2019, Lefebvre et al., 2007). They show tissue and time-specific expression and can be regulated by post-translational modifications as well as recruitment of necessary protein partners (Grimm et al., 2019). Tightly regulated proteins can be ideal targets for cancer initiation and progression, especially those important for development and cellular reprogramming. Two recent studies linked SOX5 to epithelial to mesenchymal transition (EMT) via regulation of Twist1 in breast cancer and hepatocellular carcinoma progression (Pei et al., 2014, Wang et al., 2015). Interestingly, one study linked SOX5 to nasopharyngeal carcinoma progression via downregulation of SPARC (Huang et al., 2008). Additionally, Huang et al. (2008) found no change in SPARC expression with treatment of 5-AZC; similar to previous studies performed by Larson et al. (2010) in our model system of bladder urothelial carcinoma. Analysis of the SPARC sequence from UCSC genome browser, identified a putative SOX5 consensus sequence within the SPARC promoter approximately 650bp upstream of the transcriptional start site. SOX5 has been implicated in a few cancer types with both tumor suppressor and oncogene characteristics; however, not much is known about SOX members, SOX5 specifically, in bladder cancer.

Cadmium has been described to indirectly increase ROS production, ultimately increasing oxidative stress (Rani et al., 2014). Cadmium has also been shown to replace zinc in zinc-finger transcription factors (Larabee et al., 2004); making Sp1 and Sp3 transcription factors viable targets to study their binding to the SPARC promoter and

potential regulation of gene expression in our model system. However, the link between cadmium and SOX5 is not as clear as that with Sp1 and Sp3. Although there is currently no literature linking cadmium to SOX5, cadmium may be indirectly promoting its binding to the SPARC promoter. Lefebvre et al., (1998) showed that SOX5 homo- or heterodimerization with SOX6, through conserved coiled coil motifs, enhanced transcription factor binding of two or more neighboring recognition sites. Interestingly, there are three putative SOX5 recognition sites in the SPARC promoter (Kent et al., 2002). This, in conjunction with, Huang et al. (2010) reporting SOX5 repression of SPARC, make SOX5 a reasonable transcription factor to study in our model system.

Preliminary studies performed by Vijayalekshmi Nair in our laboratory (unpublished data) assessed Sp1 and Sp3 expression in our model system along with the effect of acute cadmium exposure on Sp1 and Sp3 expression. Expression results showed a slight decrease in mRNA expression in the cadmium-transformed cell lines compared to the non-transformed UROtsa parent cells. However, protein expression was variable among the cadmium-transformed cell lines showing increased expression, decreased expression, and no change in expression. Next, 24h exposure to 0.5, 1, 2, or 4 μ M cadmium to UROtsa parent cells resulted in a dose-dependent decrease in Sp1, Sp3, and SPARC protein expression in this cell line. Therefore, cadmium may be influencing expression of transcription factors necessary for SPARC expression in the control, SPARC-expressing parental cell line. These preliminary results, in conjunction with the strong permanent repression of SPARC led to our hypothesis that cadmium may be significantly decreasing SPARC expression by silencing the promoter early in the malignant transformation process. Alternative transcription factor binding may be

contributing to the mechanism used by cadmium to silence the promoter in our *in vitro* model system of cadmium-induced bladder urothelial carcinoma.

Materials and Methods

Cell Culture

SPARC⁺ UROtsa parent and Cd #1 cells were maintained in 25cm² tissue culture flasks and cultured as previously described in Chapter II Materials and Methods section. Cells were expanded into 75cm² tissue culture flasks when experimental protocols dictated. Once expanded, cells were fed fresh growth media every 3 days and cultured as previously described.

RNA and Protein Isolation from SPARC⁺ UROtsa Parent and Cd #1 Cell Line

Total RNA and protein were isolated from cells as previously described in Chapter II Materials and Methods section, using TRI REAGENT[™] (MRC), and PBS lysis buffer with protease inhibitors, respectively. RNA concentration was determined using the Nanodrop One (Thermo Scientific) and a portion of each sample was diluted to 20ng/μl concentration for subsequent RT-qPCR analysis. Protein concentration was determined via BCA colorimetric assay, as previously described, for subsequent use in Western Blot analysis.

RT-qPCR Analysis of Sp1, Sp3 and SOX5 Transcription Factors in SPARC⁺ UROtsa Parent and Cd #1 Cell Line

Sp1, Sp3, and SOX5 mRNA expression in UROtsa Parent and Cd #1 cells was determined using real-time reverse transcription polymerase chain reaction (RT-qPCR). cDNA synthesis was performed as previously described in Chapter II Materials and Methods section.

2 μ L of cDNA was amplified using 20 μ M Sp1, Sp3, or SOX5 specific primers (Qiagen #QT01870449, #QT00094892, and #QT00084784 respectively) and recorded using SYBR green fluorescence in a total reaction volume of 20 μ L. Samples were run on a CFX960 Thermocycler (Bio Rad) using the following cycling parameters for Sp1 and Sp3: 5 min. at 95°C, denaturation – 15sec. at 95°C, annealing – 45sec. at 62°C, repeat denaturation and annealing steps x39, and collection of the melt curve. SOX5 cycling parameters were similar but used a slightly lower annealing temperature at 60°C. Sp1 and Sp3 expression was determined using a relative standard curve generated from 1:2 dilutions of the SPARC⁺ UROtsa Parent cells. SOX5 expression was determined using a relative standard curve generated from 1:2 dilutions of Cd #1 cells. Sp1, Sp3, and SOX5 mRNA expression was normalized to β -actin amplified using an Invitrogen primer set with the following sequences, sense: CGACAACGGCTCCGGCATGT, anti-sense: TGCCGTGCTCGATGGGGTACT, under the same cycling parameters as Sp1 and Sp3. β -actin expression was determined using a relative standard curve generated from 1:2 dilutions of UROtsa Parent cells. Expression data was graphed and statistical analysis performed using Graphpad PRISM v5.01 (Graphpad Software).

Western Blot Analysis of Sp1, Sp3 and SOX5 Transcription Factors in SPARC⁺ UROtsa Parent and Cd #1 Cell Lines

Sp1, Sp3, and SOX5 protein expression in UROtsa Parent and Cd #1 cells was determined using Western Blot analysis as previously described in Chapter II Materials and Methods section. Membranes were incubated with rabbit anti-human Sp1 antibody (Cell Signaling #9389) using a 1:1,000 dilution, mouse anti-human Sp3 antibody (Santa Cruz Biotechnology, Inc. #sc-28305X) [Dallas, TX] at 2.0 μ g/mL using a 1:500 dilution, or rabbit anti-human SOX5 antibody (Abcam #ab94396) at 1.0mg/mL concentration

using a 1:1,000 dilution in 5% powdered milk in TBS-T overnight at 4°C. Membranes were washed three times with TBS-T and Sp1 and SOX5 membranes were incubated with anti-rabbit IgG HRP-linked antibody (Cell Signaling #7074) at 1:3,000 and anti-biotin HRP-linked antibody (Cell Signaling #7075) at 1:1,500 in 1% powdered milk in TBS-T for 1.25h at room temperature. SOX5 membrane was incubated with anti-mouse IgG HRP-linked antibody (Cell Signaling #7076) at 1:3,000 and anti-biotin HRP-linked antibody (Cell Signaling #7075) at 1:1,500 in 1% powdered milk in TBS-T for 1.25h at room temperature. Membranes were washed and protein visualized as previously described in Chapter II Materials and Methods section. The membranes used for Sp1, Sp3, and SOX5 protein expression were then stripped and re-probed for β -actin as previously described in Chapter II Materials and Methods section.

PCR Primer Design Using NCBI Genome Browser and Oligo7 for Transcription Factor Binding to SPARC Promoter

The SPARC gene sequence plus 1,000 base pairs upstream was extracted from the NCBI UCSC Genome Browser (Kent et al., 2002) into a word document. A literature search revealed putative binding sites within the SPARC promoter for Sp1, Sp3, and SOX5 transcription factors (Chamboredon et al., 2003, Huang et al., 2008, Xu et al., 2010). The SPARC sequence extracted from UCSC Genome Browser was searched for these binding sites to validate using Oligo7 to design primers for Chromatin Immunoprecipitation experiments.

The sequence upstream of the SPARC gene containing the putative transcription factor binding sites was uploaded into Oligo7. Once there, primers were designed to amplify those specific regions using PCR. Briefly, 19-25 base pair segments of the sequence upstream and downstream of the putative binding sites were analyzed for

potential primers. Once segments were selected, several measurements were determined to estimate the success of the primer. The measurements included: melting temperature, product size, CG content, and priming efficiency. Based on these measurements, ten primer pairs were designed for the putative Sp1 and Sp3 transcription factor binding sites and ten primer pairs were designed for the putative SOX5 transcription factor binding site within the SPARC promoter. Primers were obtained from Invitrogen with sequences outlined below in Table 2.

Table 2. Sp1/Sp3 and SOX5 Primer Sequences.

Sp1/Sp3 Primer Pairs		SOX5 Primer Pairs	
Primer Name	Sequence (5'-3')	Primer Name	Sequence (5'-3')
SP1-1: sense	GTGAGTCGGTTAGGCAGCA	SOX5-1: sense	GCCTAAGATAAGGGGTTGCTGT
SP1-1: anti-sense	GGGGTTAGAGACAGGCAACA	SOX5-1: anti-sense	AGACATCTAGCTGGTGGACCT
SP1-2: sense	GCCTCACTTGCCCTCTGAAC	SOX5-2: sense	TGCCTAAGATAAGGGGTTGCTG
SP1-2: anti-sense	AGCTCTGGGCTGGGTCTAT	SOX5-2: anti-sense	CCACTGTACAGACAAGACAAGC
SP1-3: sense	GGCACTCTGTGAGTCGGTTTA	SOX5-3: sense	GCCTAAGATAAGGGGTTGCTG
SP1-3: anti-sense	AGGGGTTAGAGACAGGCAAC	SOX5-3: anti-sense	TAGACATCTAGCTGGTGGACCT
SP1-4: sense	AGCCCCGGAACAGATGAGG	SOX5-4: sense	AAGGGGTTGCTGTGAAGATT
SP1-4: anti-sense	CGGGAATGTGGAGGGGTTAG	SOX5-4: anti-sense	CACTCAAACCTCCACTTGTACC
SP1-5: sense	CCTCACTTGCCCTCTGAACAA	SOX5-5: sense	TGCCTAAGATAAGGGGTTGC
SP1-5: anti-sense	CAGGCAACAGGAAACCACTCA	SOX5-5: anti-sense	TCCCACTCAAACCTCCACTTG
SP1-6: sense	CTCTGTGAGTCGGTTAGGCA	SOX5-6: sense	CCTAAGATAAGGGGTTGCTGTG
SP1-6: anti-sense	ACAGGCAACAGGAAACCACTC	SOX5-6: anti-sense	GGGATTAGACATCTAGCTGGTGG
SP1-7: sense	ACTCTGTGAGTCGGTTAGGC	SOX5-7: sense	AGATAAGGGGTTGCTGTGAAGA
SP1-7: anti-sense	GACAGGCAACAGGAAACCACT	SOX5-7: anti-sense	TCCCACTCAAACCTCCACTTGTA
SP1-8: sense	TCTGTGAGTCGGTTAGGCA	SOX5-8: sense	CCTAAGATAAGGGGTTGCTGTGA
SP1-8: anti-sense	GGGAATGTGGAGGGGTTAGA	SOX5-8: anti-sense	CCACTCAAACCTCCACTTGTACC
SP1-9: sense	GGCACTCTGTGAGTCGGTT	SOX5-9: sense	CAATGCCTAAGATAAGGGGTTGC
SP1-9: anti-sense	GGTTTAGAGACAGGCAACAGGA	SOX5-9: anti-sense	TTAGACATCTAGCTGGTGGACCT
SP1-10: sense	TGGCACTCTGTGAGTCGGTT	SOX5-10: sense	ATGCCTAAGATAAGGGGTTGC
SP1-10: anti-sense	GGGAATGTGGAGGGGTTAGAG	SOX5-10: anti-sense	CCCACTCAAACCTCCACTTGTA

Genomic DNA Isolation from SPARC⁺ UROtsa Parent Cell Line

Genomic DNA was isolated from the UROtsa Parent cell line to verify PCR product amplification using the primers designed for the Chromatin Immunoprecipitation experiments. DNA was isolated and purified according to the manufacturer's protocol using the DNeasy Blood and Tissue Kit (Qiagen #69504). Briefly, a harvested UROtsa Parent cell pellet was resuspended in PBS and Proteinase K and buffer were added. The sample was vortexed and incubated at 56°C for 10 minutes. Then ethanol was added and the solution was pipeted into a DNeasy mini spin column to precipitate out the DNA. The column/DNA was then washed and centrifuged at $\geq 8,000$ rpm. This was followed by a second wash and centrifuge at $\geq 14,000$ rpm to dry the membrane. The column was then removed and placed in a clean RNase/DNase free tube and buffer was added to the membrane. This was then centrifuged at $\geq 8,000$ rpm to elute the DNA. The DNA was then quantified using the Nanodrop One (Thermo Scientific). Once the concentration was determined the sample was utilized for conventional PCR analysis.

Conventional PCR and Gel Electrophoresis of Genomic DNA from SPARC⁺ UROtsa Parent Cell Line

Conventional PCR was run to analyze the success of the primers designed for Sp1, Sp3, and SOX5 transcription factor putative binding sites within the SPARC promoter. Briefly, a 45 μ L mastermix was made for each primer set using: 4.5 μ L/reaction PCR Buffer II (10% of total reaction volume), 3.6 μ L/reaction Magnesium Chloride (8% of total reaction volume), 0.9 μ L/reaction upper primer (2% of total reaction volume), 0.9 μ L/reaction lower primer (2% of total reaction volume), 0.45 μ L/reaction TAQ Polymerase (1% of total reaction volume), 18.45 μ L/reaction PCR H₂O (41% of total reaction volume), 7.2 μ L/reaction dNTP mixture (16% of total reaction volume), and

9 μ L/reaction genomic DNA (20% of total reaction volume). The mastermix constituents were part of the GeneAmp PCR Reagent Kit with AmpliTaq[®] DNA Polymerase (Applied Biosystems #N801-0055) [Foster City, CA] The samples were then run on a GeneAmp PCR System 9700 (Applied Biosystems) using the following cycling parameters: 5 min. at 94 $^{\circ}$ C; denaturation – 30sec. at 94 $^{\circ}$ C; annealing – 30sec. at 55 $^{\circ}$ C; extension – 30sec. at 72 $^{\circ}$ C; repeat denaturation, annealing, and extension steps x39, followed by a final extension at 72 $^{\circ}$ C for 7m, and a hold at 4 $^{\circ}$ C until samples were properly stored. The cycling parameters for the SOX5 primers were the same except an annealing temperature of 52 $^{\circ}$ C was used. 10 μ L of sample was removed from each tube and added to a fresh 0.5 μ L cDNA microfuge tube every 5 cycles starting at 25 cycles to optimize the amount of cycles needed to amplify product.

Once products were amplified, gel electrophoresis was used to visualize the products. 500mL of 1xTAE was made from a 50x TAE stock solution. 2% small or medium agarose gels were made by adding 0.8g agarose (Fisher Scientific) to 40mL 1xTAE or 1.3g agarose to 65mL 1xTAE, respectively, in an Erlenmeyer flask. This was then covered using a paper towel and microwaved until solution was clear. Once clear, the solution was cooled slightly until able to be handled. Then, 1 μ L or 1.62 μ L, based on the gel size, of 10 μ g/ μ L ethidium bromide (EtBr) was added to the agarose solution and it was poured into a taped gel cassette. While the gel was solidifying the samples were prepared to be loaded. 9 μ L sample was added to 2.25 μ L loading dye and mixed.

Once the gel was solidified the tape was removed and the comb was removed revealing the wells. The gel was placed into the electrophoresis chamber and covered with 1xTAE buffer. 5 μ L of the high/lo ladder (Bionexus #BN2050) [Oakland, CA] was

loaded into the first and last well and 10 μ L of each sample were loaded into respective wells between the ladder. The cover was placed on the electrophoresis unit and the electrodes were connected to the power source. The DNA in the wells that had been amplified was separated on the gel from anode (negative) to cathode (positive) for 1-1.5h at 100-110 volts.

Once the gel finished, it was removed from the electrophoresis chamber and stained with an EtBr solution (80 μ L H₂O:2 μ L EtBr for small gel and 160 μ L H₂O:4 μ L EtBr for a medium gel) on the orbital shaker at room temperature for 30 minutes. The gel was then quick washed three times with H₂O followed by three 5-10 minute washes with H₂O. The gel was then taken and imaged on the ChemiDoc MP Imaging System (Bio Rad).

Chromatin Immunoprecipitation Assay for Sp1, Sp3, and SOX5 Transcription Factors In SPARC⁺ UROtsa Parent and Cd #1 Cell Lines

Chromatin Immunoprecipitation was performed using the ChIP-IT Express Enzymatic Magnetic Chromatin Immunoprecipitation Kit and Enzymatic Shearing Kit (Active Motif #53009 and #53035, respectively) [Carlsbad, CA] and as described in Somji et al. (2011). UROtsa Parent and Cd #1 cells were expanded and grown in 75cm² tissue culture flasks. Once cells were a confluent monolayer they were fixed using 1% formaldehyde (Sigma #F8775) for 10 minutes. The cells were washed with 1xPBS and treated with glycine stop solution to stop the fixation. The cells were then washed again and the monolayer was scraped off the flask using PBS containing 2mM PMSF. The cell/scraping solution was transferred into a 15mL conical tube and centrifuged at 2,500rpm for 10 minutes at 4°C. The supernatant was removed and the cell pellet was stored at -80°C.

The thawing cell pellet was resuspended in lysis buffer containing PMSF and Protease Inhibitor Cocktail (PIC) and incubated on ice for 30 minutes. Then, the cell/lysis buffer solution was transferred to the dounce homogenizer (Active Motif #40401) and homogenized on ice for 10 strokes to aid in nuclei release from cells. Homogenate was transferred to a RNase/DNase free tube and centrifuged at 5,000rpm for 10 minutes at 4°C to pellet the nuclei. The supernatant was removed and the pellet was resuspended in digestion buffer supplemented with PMSF and PIC and incubated for 5 minutes at 37°C. Enzymatic shearing cocktail was added to warmed nuclei and incubated for 5 minutes for UROtsa Parent nuclei and 7.5 minutes for Cd #1 nuclei. This difference in incubation times is due to the compactness of the epithelial monolayer formed by the malignant Cd #1 cells and has been previously optimized (Somji et al., 2011). The enzymatic shearing was stopped by adding ice-cold EDTA and tubes were chilled on ice for 10 minutes. The sheared chromatin was then centrifuged at 4°C for 10 minutes at maximum speed. The sheared chromatin supernatant was then transferred to RNase/DNase free tubes.

An aliquot of UROtsa Parent and Cd #1 sheared chromatin was then cleaned to assess the shearing efficiency and obtain a DNA concentration. 5M NaCl was added to each sample followed by a 4h incubation at 65°C to reverse the protein-DNA cross-linking. RNase A was then added and samples were incubated at 37°C for 15 minutes to degrade RNA. Protein was degraded by adding Proteinase K and incubating samples at 42°C for 1.5h. Ultrapure™ Phenol:Chloroform:Isoamyl Alcohol (Invitrogen #15593-031) was added and samples were vortexed. They were then centrifuged for 5 minutes at maximum speed and the aqueous phase transferred to a fresh RNase/DNase microfuge tube. Finally, 3M sodium acetate pH 5.5 (Ambion®, Waltham, MA) and 100% EtOH

(Sigma-Aldrich) were added and the samples were vortexed and placed in the -20°C freezer overnight.

Samples were then centrifuged at 4°C for 10 minutes at maximum speed and the supernatant discarded. The DNA pellet was washed with ice-cold 70% EtOH and centrifuged at 4°C for 5 minutes at maximum speed. The supernatant was discarded and the pellet was air dried and resuspended in 1xTE. DNA concentration was determined using the NanoDrop One (Thermo Scientific). Once the concentration was determined, samples were run on a 1% agarose gel, prepared as previously described, loading 5µL and 10µL of each sample and visualized on the ChemiDoc MP Imaging System (Bio Rad) showing 200bp-1500bp fragments of chromatin. The concentration determined here was used to add equal amounts of chromatin to each immunoprecipitation reaction.

Once the shearing efficiency and DNA concentration were determined, immunoprecipitation was performed. 10µL of input DNA from each sample was set aside, not immunoprecipitated, and stored. ChIP reactions were set up for UROtsa Parent and Cd #1 cells using 4 different antibodies: Sp1, Sp3, SOX5, and Negative IgG control resulting in eight total reactions. 50µg/µL Bovine Serum Albumin (BSA) was added to each reaction to coat the magnetic beads and reduce any non-specific binding. 7µg of sheared chromatin was incubated with: BSA, Protein-G magnetic beads, buffer, protease inhibitor cocktail (PIC), H₂O, and 3µg of Sp1, Sp3, SOX5, or Negative IgG control antibody. Samples were incubated on an end-to-end rotator for 4h at 4°C. The samples were briefly spun and then placed on a magnetic stand to pellet the beads. The supernatant was discarded and the beads were washed three times with ChIP Buffer 1 and

2. Each time they were washed, the samples were placed back in the magnetic stand to pellet the beads and discard the supernatant.

The washed beads were then resuspended in elution buffer and incubated on an end-to-end rotator for 15 minutes at room temperature. Samples were briefly spun and reverse cross-linking buffer was added. The samples were then, again, placed in the magnetic stand and the beads were pelleted. The supernatant containing the chromatin was then transferred to a fresh RNase/DNase free tube. The input DNA was then processed with the ChIP samples. 5M NaCl and buffer were added to the input DNA bringing the volume to equal that of the ChIP samples. All samples, input and ChIP, were then incubated at 95°C for 15 minutes in the GeneAmp PCR System 9700 (Applied Biosystems). Samples were brought back to room temperature and Proteinase K was added to degrade any remaining protein. The samples were then incubated at 37°C for 1h. Again, samples were returned to room temperature and Proteinase K Stop Solution was added. All samples could then be used for conventional PCR and gel electrophoresis analysis; or, samples could be further purified for use in RT-qPCR analysis.

Conventional PCR and Gel Electrophoresis of Sp1, Sp3 and SOX5 ChIP DNA in SPARC⁺ UROtsa Parent and Cd #1 Cell Lines

Conventional PCR was run to analyze the amplification of DNA associated with Sp1, Sp3, and SOX5 transcription factor putative binding sites within the SPARC promoter. Briefly, a 20µL/reaction mastermix was made for each primer set as described previously, comprised of: PCR Buffer II (10% of total reaction volume), Magnesium Chloride (8% of total reaction volume), upper primer (2% of total reaction volume), lower primer (2% of total reaction volume), TAQ Polymerase (1% of total reaction volume), PCR H₂O (41% of total reaction volume), dNTP mixture (16% of total reaction

volume), and CHIP DNA (20% of total reaction volume). The CHIP samples were then run on a GeneAmp PCR System 9700 (Applied Biosystems) using Sp1/Sp3-10 or SOX5-5 primer sets (Invitrogen) with sequences outlined in Table 2. This was performed using the cycling parameters described previously.

Once products were amplified, gel electrophoresis was used to visualize the products as previously described in this section. Integrated Optical Densitometry (I.O.D.) analysis was performed using ImageLab version 4.1 (Bio Rad). Data was graphed and statistical analysis performed using Graphpad PRISM v5.01 (GraphPad Software).

Sp1, Sp3, and SOX5 siRNA Transfection of SPARC⁺ UROtsa Parent and Cd #1 Cell Lines

UROtsa Parent and Cd #1 cells were plated and grown to confluency in 12 well tissue culture plates. Two wells of each plate contained coverslips for confocal visualization of fluorescently labeled positive control siRNA. These wells were seeded with more cells than the other wells of the plate due to slightly delayed growth on glass coverslips compared to tissue culture plastic. Once confluent, duplicate wells were treated with one of five siRNAs: siGLO Lamin A/C control (Dharmacon #D-001620-02-05) a fluorescently labeled positive control, Non-targeting Scrambled (Dharmacon #D-001810-01-05), Human Sp1 (Dharmacon #J-026959-05-0002), Human Sp3 (Dharmacon #J-023096-07-0002), or Human SOX5 (Dharmacon #J-008203-05-0002), for 24h or 48h.

siRNAs were added to specified wells as described previously in Chapter II Materials and Methods section. The plate was gently swirled to mix and placed in the 37°C tissue culture incubator for 24h or 48h. The siGLO Lamin A/C and Non-targeting Scrambled siRNA were used as controls along with: siQuest only, Sp1 siRNA only, and untreated wells.

SiGLO Lamin A/C treated coverslips were then washed twice with DMEM-F12-
no phenol red (Gibco) and incubated in 3.7% methanol-free formaldehyde (Polysciences,
Inc., #18814-10) for 10 minutes at room temperature. Coverslips were washed twice with
PBS⁻ and once with PBS⁺ containing calcium and magnesium salts. Free aldehyde groups
were quenched using 0.1M NH₄Cl (Sigma) in PBS for 15 minutes at room temperature
and again washed. Coverslips were then mounted on microscope slides using ProLong
DIAMOND DAPI medium (Life Technologies, #P36971) for nuclear staining.
Transfection efficiency was visualized and shown to be successful under the transfection
parameters used (data not shown).

RNA Isolation of Sp1, Sp3, and SOX5 siRNA Transfected SPARC⁺ UROtsa Parent and Cd #1 Cell Lines

Total RNA was isolated from siRNA treated cells using TRI REAGENTTM
(MRC) as previously described in Chapter II Materials and Methods section. RNA
concentration was determined on the Nanodrop One (Thermo Scientific) and a portion of
each sample was diluted to 20ng/μl concentration for subsequent RT-qPCR analysis.

RT-qPCR Analysis of Sp1, Sp3, and SOX5 Transcription Factors in siRNA Treated SPARC⁺ UROtsa Parent and Cd #1 Cell Lines

Sp1, Sp3, and SOX5 mRNA expression in siRNA treated UROtsa Parent and Cd
#1 cells was determined using real-time reverse transcription polymerase chain reaction
(RT-qPCR) as previously described in this section. Expression data was graphed and
statistical analysis performed using Graphpad PRISM v5.01 (GraphPad Software).

RT-qPCR Analysis of SPARC mRNA Expression in siRNA Treated SPARC⁺ UROtsa Parent and Cd #1 Cell Lines

SPARC mRNA expression in siRNA treated cells was determined using real-time
reverse transcription polymerase chain reaction (RT-qPCR) as previously described in

Chapter II Materials and Methods section, using 20 μ M human SPARC specific primers (Qiagen #QT00018620). Expression data was graphed and statistical analysis performed using Graphpad PRISM v5.01 (GraphPad Software).

Statistics

All data was analyzed using Graphpad PRISM v5.01 software (GraphPad Software). ChIP statistical analysis was performed using a 1-way ANOVA and Bonferroni's Multiple Comparison *post hoc* testing. Statistical analysis for mRNA expression was performed using a 1-way ANOVA and Dunnett's Multiple Comparison *post hoc* testing. Statistical significance determined for all results using $p < 0.05$.

Results

Sp1 mRNA and Protein Expression in SPARC⁺ UROtsa Parent and Cd #1 Cell Lines

UROtsa parent and Cd #1 cells were analyzed for Sp1 expression. This is a transcription factor that has been implicated in binding to the SPARC promoter and has shown susceptibility to cadmium exposure (Chamboredon et al., 2003, Larabee et al., 2004). Cadmium has been shown to use mimicry and take the place of essential metals such as zinc (Zalups et al., 2003). In this case, it is plausible that cadmium is replacing zinc in the zinc-finger transcription factor and changing its shape; ultimately, rendering it inactive and unable to bind to the promoter region to activate gene expression. Although cadmium may be replacing zinc, Figure III-1 shows mRNA (A) and protein (B) expression of Sp1 is not significantly different between the Cd #1 cells and the SPARC⁺ UROtsa parent cells. Therefore, it does not appear that cadmium is repressing Sp1 expression following long-term exposure and malignant transformation. Protein

expression of Sp1 appears to be slightly higher in the Cd #1 cells compared to the SPARC⁺ UROtsa parent cells, which is consistent with previous preliminary studies.

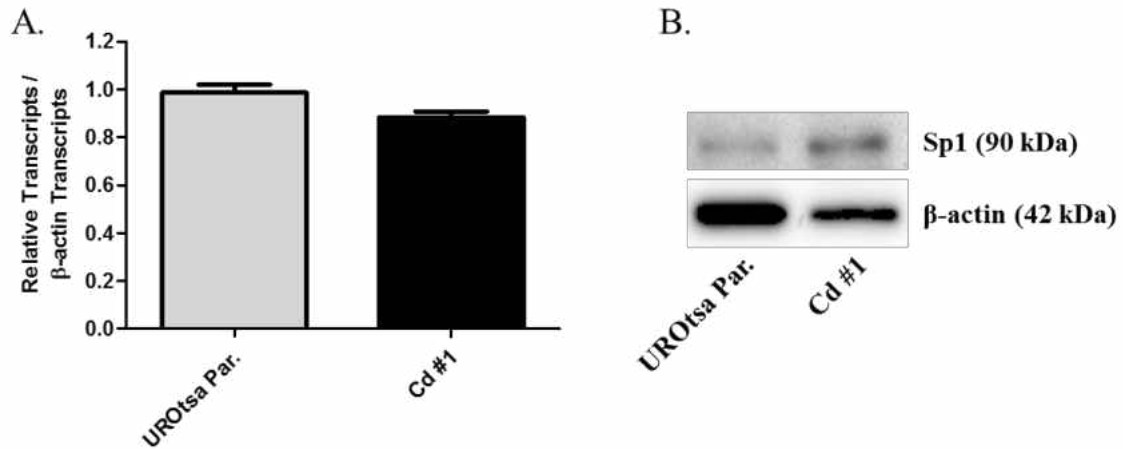


Figure III-1. Sp1 mRNA and Protein Expression in SPARC⁺ UROtsa Cells and Non-SPARC Expressing Cd #1 Cells. (A) Relative mRNA expression was determined using RT-qPCR, with a human Sp1 specific primer, and normalized to β -actin. Experiment was run in triplicate with statistical analysis determined using an unpaired student's t-test. (B) Western blot analysis showing total cellular Sp1 protein expression with the corresponding β -actin control.

Sp3 mRNA and Protein Expression in SPARC⁺ UROtsa Parent and Cd #1 Cell Lines

UROtsa parent and Cd #1 cells were analyzed for Sp3 expression. Sp3 transcription factor is in the same family as Sp1, and therefore has a conserved zinc-finger motif subject to cadmium replacement. Figure III-2 shows no statistical difference in Sp3 mRNA (A) and protein (B) expression between SPARC⁺ UROtsa parent cells and Cd #1 cells. Again, it appears there is a slight increase in protein expression, which is consistent with previous preliminary results. Cadmium exposure does not seem to significantly alter expression of Sp3 zinc-finger transcription factor.

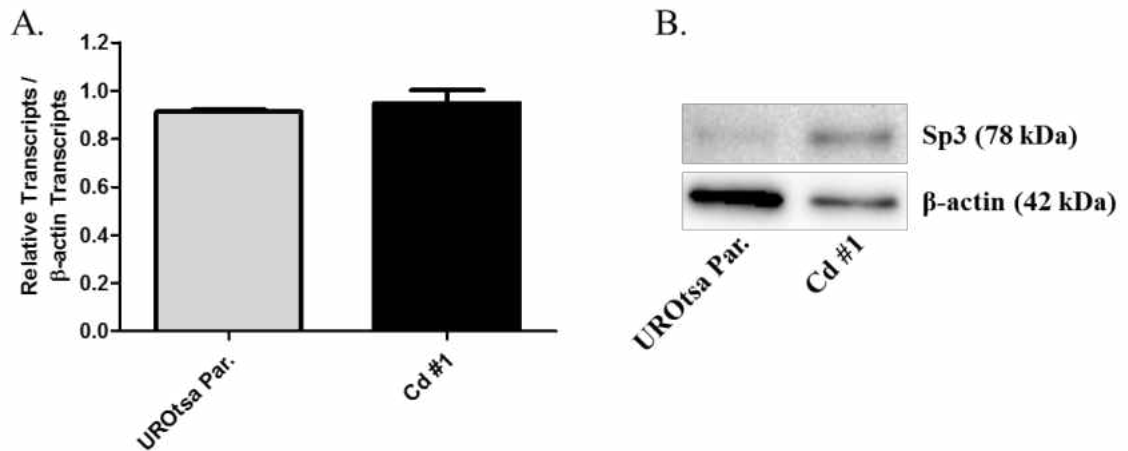


Figure III-2. Sp3 mRNA and Protein Expression in SPARC⁺ UROtsa Cells and Non-SPARC Expressing Cd #1 Cells. (A) Relative mRNA expression was determined using RT-qPCR, with a human Sp1 specific primer, and normalized to β -actin. Experiment was run in triplicate with statistical analysis determined using an unpaired student's t-test. (B) Western blot analysis showing total cellular Sp3 protein expression with the corresponding β -actin control.

SOX5 mRNA and Protein Expression in SPARC⁺ UROtsa Parent and Cd #1 Cell Lines

UROtsa parent and Cd #1 cells were also analyzed for SOX5 transcription factor. This is an alternative transcription factor that has been implicated in binding to the SPARC promoter contributing to its repression in nasopharyngeal cancer (Huang et al., 2008). Although not significant, mRNA (A) and protein (B) expression analysis show an increase in SOX5 expression in the Cd #1 cells compared to the SPARC⁺ UROtsa parent cells. The western blot analysis does not appear to show a band for the UROtsa parent cells and only a faint band for the Cd #1 cells. The mRNA expression levels, although present, were fairly low for both UROtsa parent and Cd #1 cells.

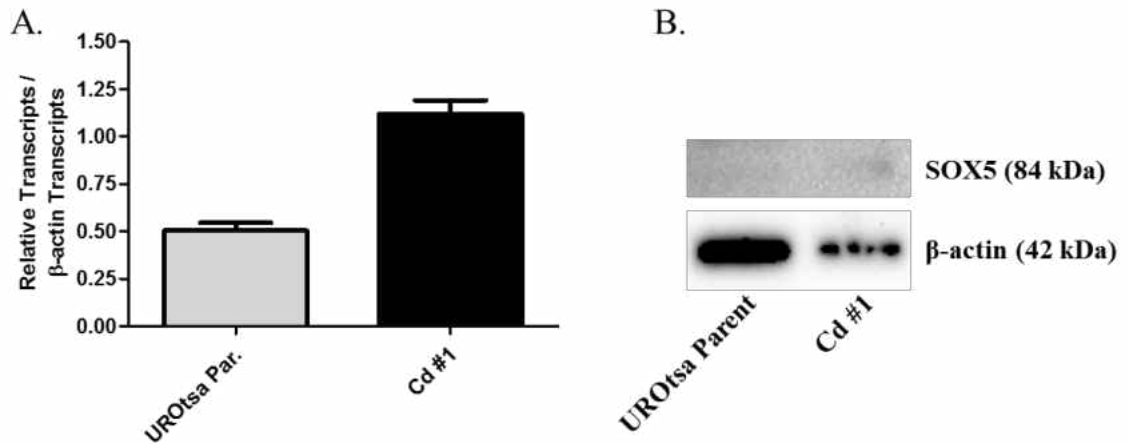


Figure III-3. SOX5 mRNA and Protein Expression in SPARC⁺ UROtsa Cells and Non-SPARC Expressing Cd #1 Cells. (A) Relative mRNA expression was determined using RT-qPCR and normalized to β -actin. Experiment was run in triplicate with statistical analysis determined using an unpaired student's t-test. (B) Western blot analysis showing total cellular SOX5 protein expression with the corresponding β -actin control.

ChIP Analysis of Sp1 and/or Sp3 Transcription Factor Binding to the SPARC Gene Promoter in UROtsa Parent and Cd #1 Cell Lines

Once it was determined that both Sp1 and Sp3 were expressed in the SPARC⁺ UROtsa parent control cells and the Cd #1 cells and that there was not significant difference in expression; the functional role for SPARC was investigated. DNA binding is a primary role for transcription factors. If cadmium is mimicking zinc and changing the shape of Sp1 and/or Sp3 it is possible this change is rendering the protein inactive. Therefore, there will be no DNA binding or abnormal DNA binding resulting in gene repression. ChIP results were normalized to sheared, non-precipitated input DNA and presented as percent input. Conventional PCR was run utilizing primer sets specifically designed for the putative binding sites within the SPARC promoter. Once designed, primers were tested on genomic DNA isolated from UROtsa parent cells (data not shown) and chosen based on specificity. Figure III-4 illustrate that Sp1 and Sp3 appear to be binding to the SPARC promoter region in the SPARC⁺ UROtsa parent cells. Results

also show little, if any, binding of Sp1 and Sp3 to the SPARC promoter in the Cd #1 cells. Sp3 binding does not appear to be significantly higher than the input in the UROtsa parent; however, it is significantly higher than Sp3 binding in the Cd #1 cells. These results indicate that Sp1 and/or Sp3 are necessary transcription factors for SPARC expression. Without Sp1 and/or Sp3 binding to the SPARC promoter, gene transcription will not occur resulting in little, if any, SPARC expression in cadmium-transformed UROtsa cells. It is possible the long-term exposure to cadmium resulted in a permanent change in transcription factor binding contributing to the continued repression of SPARC.

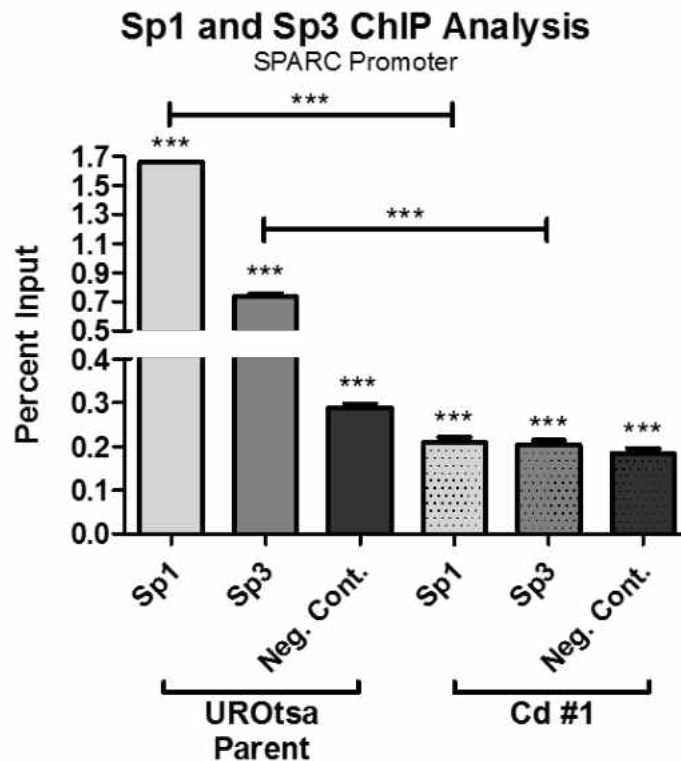


Figure III-4. Chromatin ImmunoPrecipitation Analysis of Sp1/Sp3 Binding at the SPARC Promoter. Sp1 and Sp3 transcription factor binding represented as percent input. Negative control immunoprecipitated with non-specific negative IgG antibody. Statistical analysis determined using a One-Way ANOVA with Bonferroni *post hoc* test. ***($p \leq 0.001$).

ChIP Analysis of SOX5 Transcription Factor Binding to the SPARC Gene Promoter in UROtsa Parent and Cd #1 Cell Lines

It was determined that SOX5 was expressed in both UROtsa parent and Cd #1 cells and was slightly higher in the Cd #1 cells. These results supported our hypothesis of alternative transcription factor binding to the SPARC promoter resulting in its repression in cadmium-transformed cells. Therefore, it was plausible to investigate SOX5 binding to the SPARC promoter, here. As described earlier, conventional PCR was run utilizing validated primer sets, specifically designed for the putative binding site within the SPARC promoter. Results in Figure III-5, are presented as percent input and indicate significant enrichment of SOX5 at the SPARC promoter region in Cd #1 cells compared to SPARC⁺ UROtsa parent cells which show limited binding of SOX5. Earlier results indicated that both UROtsa parent and Cd #1 cells express SOX5; however, these results indicate that SOX5 is preferentially binding to the SPARC promoter in the Cd #1 cells.

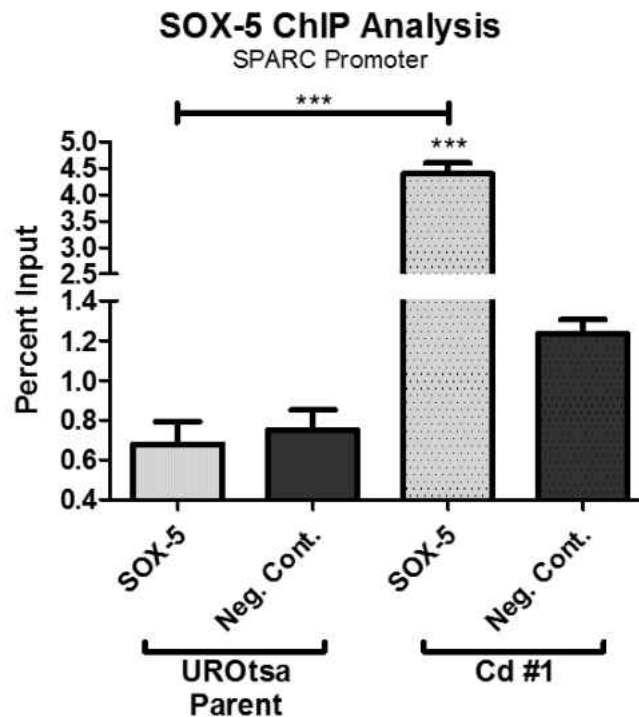


Figure III-5. Chromatin Immunoprecipitation Analysis of SOX5 Binding at the SPARC Promoter. SOX5 transcription factor binding represented as percent input. Negative control immunoprecipitated with non-specific negative IgG antibody. Statistical analysis determined using a One-Way ANOVA with Bonferroni *post hoc* test. ***($p \leq 0.001$).

Sp1, Sp3, and SOX5 mRNA Expression in siRNA Treated SPARC⁺ UROtsa Parent and Cd #1 Cell Lines

The next experiment was to knockdown expression of these three transcription factors and determine mRNA expression levels of SPARC. This was done using siRNA transfection for 24 and 48 hours in SPARC⁺ UROtsa parent cells and Cd #1 cells. The results from this experiment were somewhat ambiguous and difficult to interpret. Overall, there appears to be successful knockdown of the three transcription factors in both UROtsa parent cells and Cd #1 cells with the exception of Sp3 in the Cd #1 cells at 48 hours. Figure III-6 illustrates similar Sp1 knockdown of < 0.6 that of the untreated control, between UROtsa parent (A and B) and Cd #1 (C and D) cells at both time points. Sp1 showed further knockdown in the both cell lines from 24 hours to 48 hours; however, the continued knockdown in UROtsa parent was slightly more than in Cd #1 cells. Sp3 did not show as significant of knockdown in the Cd #1 cells (C and D) compared to the UROtsa parent cells (A and B) at either time point in Figure III-7. In fact, at 48 hours it appears there is little, if any, knockdown of Sp3 in the Cd #1 cells compared to > 0.8 fold knockdown in the UROtsa parent cells. This transcription factor may be necessary for specific gene expression and therefore is most likely resistant to knockdown to prevent cell death. SOX5, as with Sp1, showed similar knockdown at 24 hours in both UROtsa parent (A) and Cd #1 (C) cells, as seen in Figure III-8. There was also significant knockdown of SOX5 in the Cd #1 cells at 48 hours (Figure III-8, D). However, SOX5 expression in the UROtsa parent cells at 48h (Figure III-8, B) is variable potentially due

to the low expression levels prior to knockdown. It also appears there is alteration of Sp1 and SOX5 transcription factor expression in various controls. However, Sp3 did not show any change in expression in the control samples. This could be indicative of stress from the transfection and further suggest that Sp1 and SOX5 expression and subsequent function may be particularly susceptible to stress.

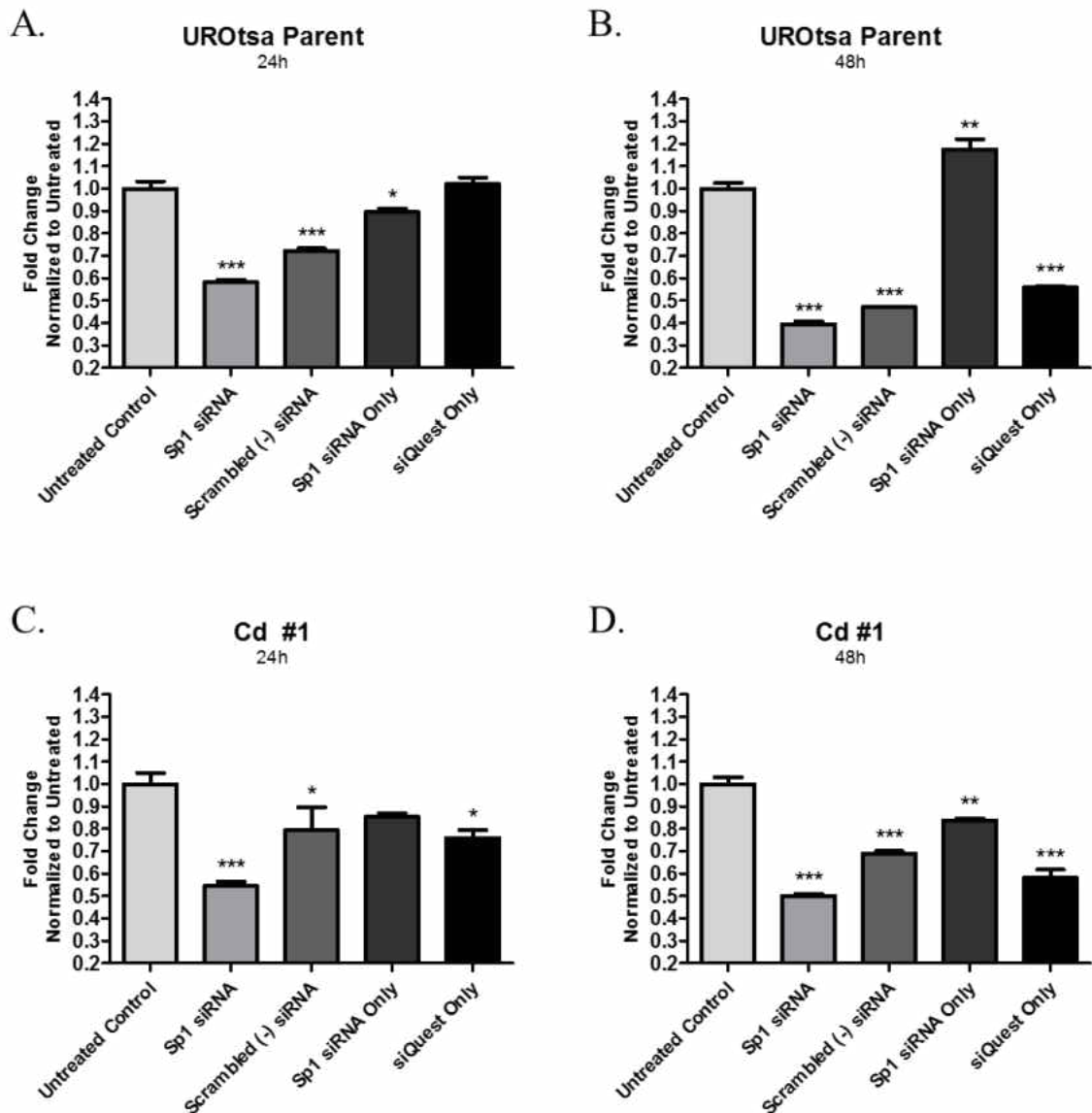


Figure III-6. Sp1 mRNA Expression in SPARC⁺ UROtsa Cells and Non-SPARC Expressing Cd #1 Cells Following siRNA Knockdown of Sp1. (A) 24 hour and (B) 48 hour siRNA treatment in UROtsa parent cells. (C) 24 hour and (D) 48 hour siRNA

treatment in Cd #1 cells. Untreated samples used as control as well as scrambled siRNA, Sp1 siRNA only, and siQuest transfection reagent only. All data represented as mean \pm SEM of triplicates normalized to the untreated control. Statistical significance determined with one-way ANOVA and Dunnett's Multiple Comparison *post hoc* test. *($p \leq 0.05$), **($p \leq 0.01$), and ***($p \leq 0.001$).

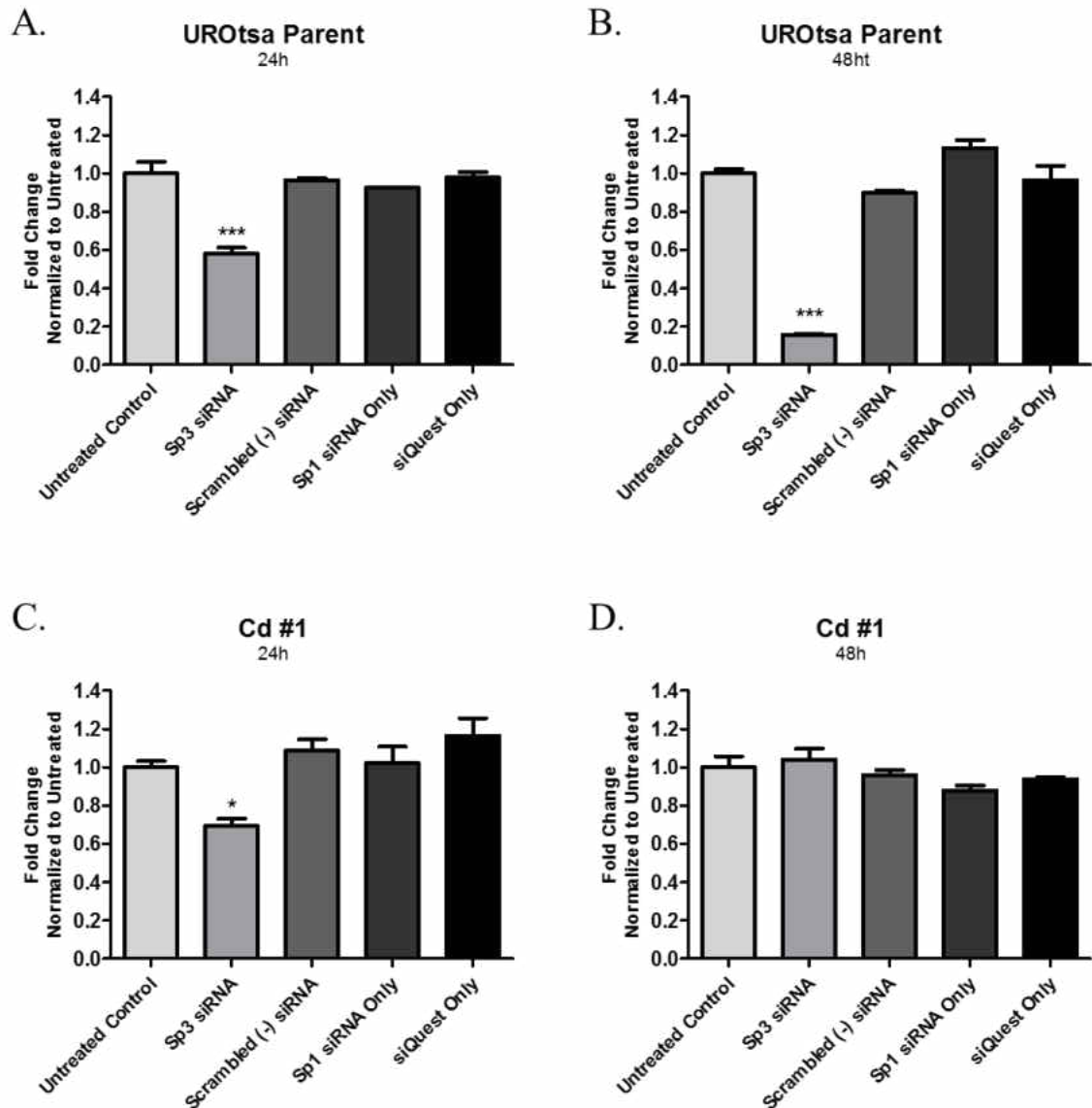


Figure III-7. Sp3 mRNA Expression in SPARC⁺ UROtsa Cells and Non-SPARC Expressing Cd #1 Cells Following siRNA Knockdown of Sp3. (A) 24 hour and (B) 48 hour siRNA treatment in UROtsa parent cells. (C) 24 hour and (D) 48 hour siRNA treatment in Cd #1 cells. Untreated samples used as control as well as scrambled siRNA, Sp1 siRNA only, and siQuest transfection reagent only. All data represented as mean \pm SEM of triplicates normalized to the untreated control. Statistical significance determined with one-way ANOVA and Dunnett's Multiple Comparison *post hoc* test. *($p \leq 0.05$), and ***($p \leq 0.001$).

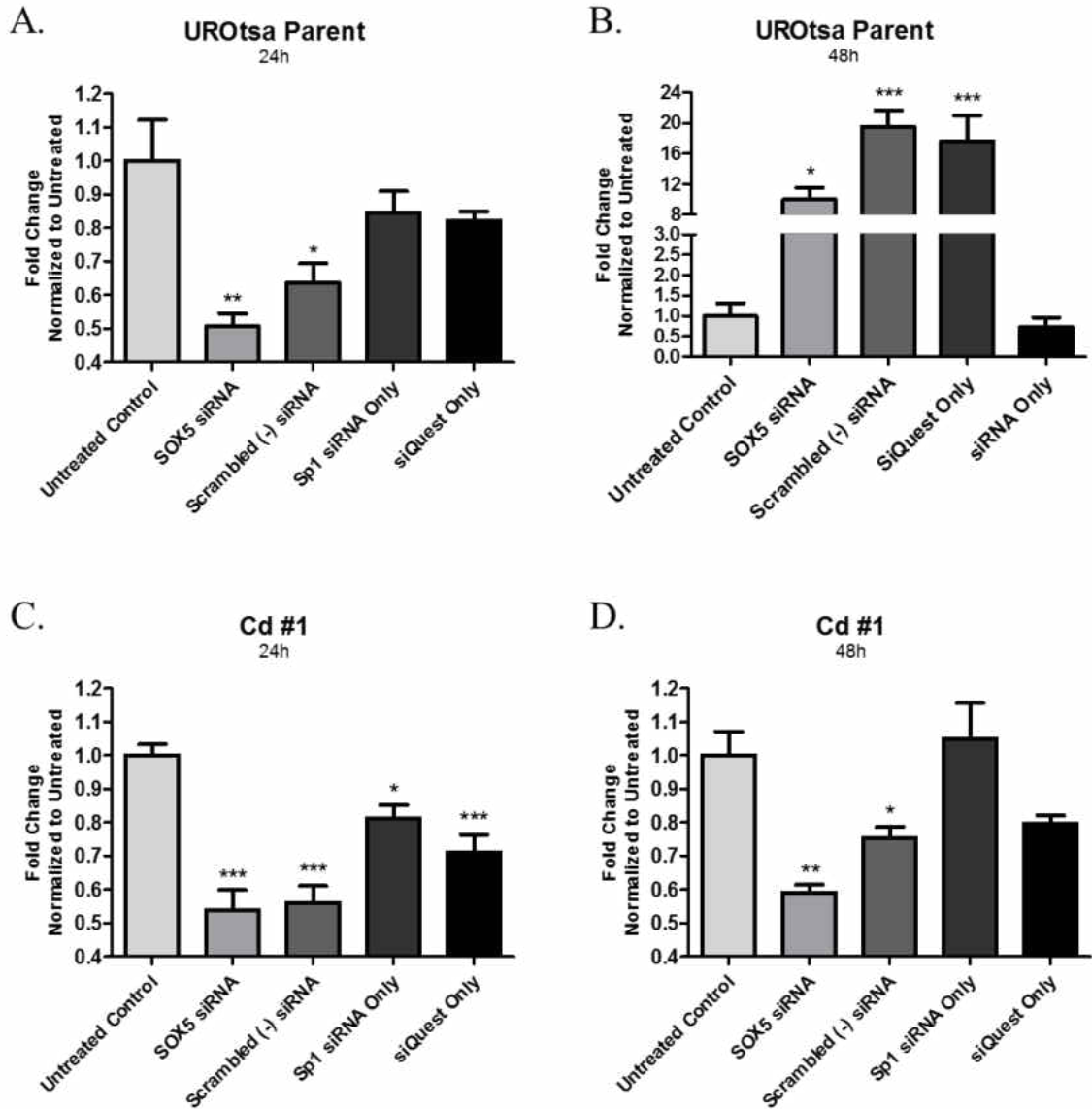


Figure III-8. SOX5 mRNA Expression in SPARC⁺ UROtsa Cells and Non-SPARC Expressing Cd #1 Cells Following siRNA Knockdown of SOX5. (A) 24 hour and (B) 48 hour siRNA treatment in UROtsa parent cells. (C) 24 hour and (D) 48 hour siRNA treatment in Cd #1 cells. Untreated samples used as control as well as scrambled siRNA, Sp1 siRNA only, and siQuest transfection reagent only. All data represented as mean \pm SEM of triplicates normalized to the untreated control. Statistical significance determined with one-way ANOVA and Dunnett's Multiple Comparison *post hoc* test. *($p \leq 0.05$), **($p \leq 0.01$), and ***($p \leq 0.001$).

SPARC mRNA Expression in siRNA Treated SPARC⁺ UROtsa Parent and Cd #1 Cell Lines

After siRNA knockdown of Sp1, Sp3 or SOX5 transcription factors in SPARC⁺ UROtsa cells and Cd #1 cells, it was necessary to determine if SPARC expression was affected. Figure III-9 illustrates SPARC mRNA expression in all siRNA treated samples as well as the control samples for both UROtsa parent (A and B) and Cd #1 (C and D) cells. Results showed that in the UROtsa parent cells, there is a significant decrease in SPARC expression when Sp3 is knocked down for 48 hours. However, this was not the case for Sp3 at 24 hours. The knockdown of the other transcription factors, Sp1 and SOX5, did not show any significant difference in SPARC expression in the UROtsa parent cell line at either time point. It was consistently noted that the untreated control and the Sp1 siRNA only samples appeared more confluent at 24 hours and 48 hours than the samples treated with the transfection reagent, based on phase-contrast microscopy observation (data not shown). The Cd #1 cells already repress SPARC expression below detectable limits so the goal with this experiment was to determine if knockdown of SOX5, specifically, resulted in an increase in SPARC expression. Results show that there is, in fact, a significant increase in SPARC expression at 48 hours with knockdown of SOX5 transcription factor. Sp1 and Sp3 knockdown resulted in a slight increase in SPARC expression but it was not significant. Concerns with these experiments include the Sp1 siRNA only control consistently showing a slight increase in SPARC expression; as well as, increased variabilities with detecting SPARC levels in cells that have little to no SPARC expression initially. These results do, however, further indicate that alteration of transcription factor binding, Sp1/Sp3 to SOX5, could potentially contribute to the

permanent repression of SPARC in our model system of cadmium-induced bladder urothelial carcinoma.

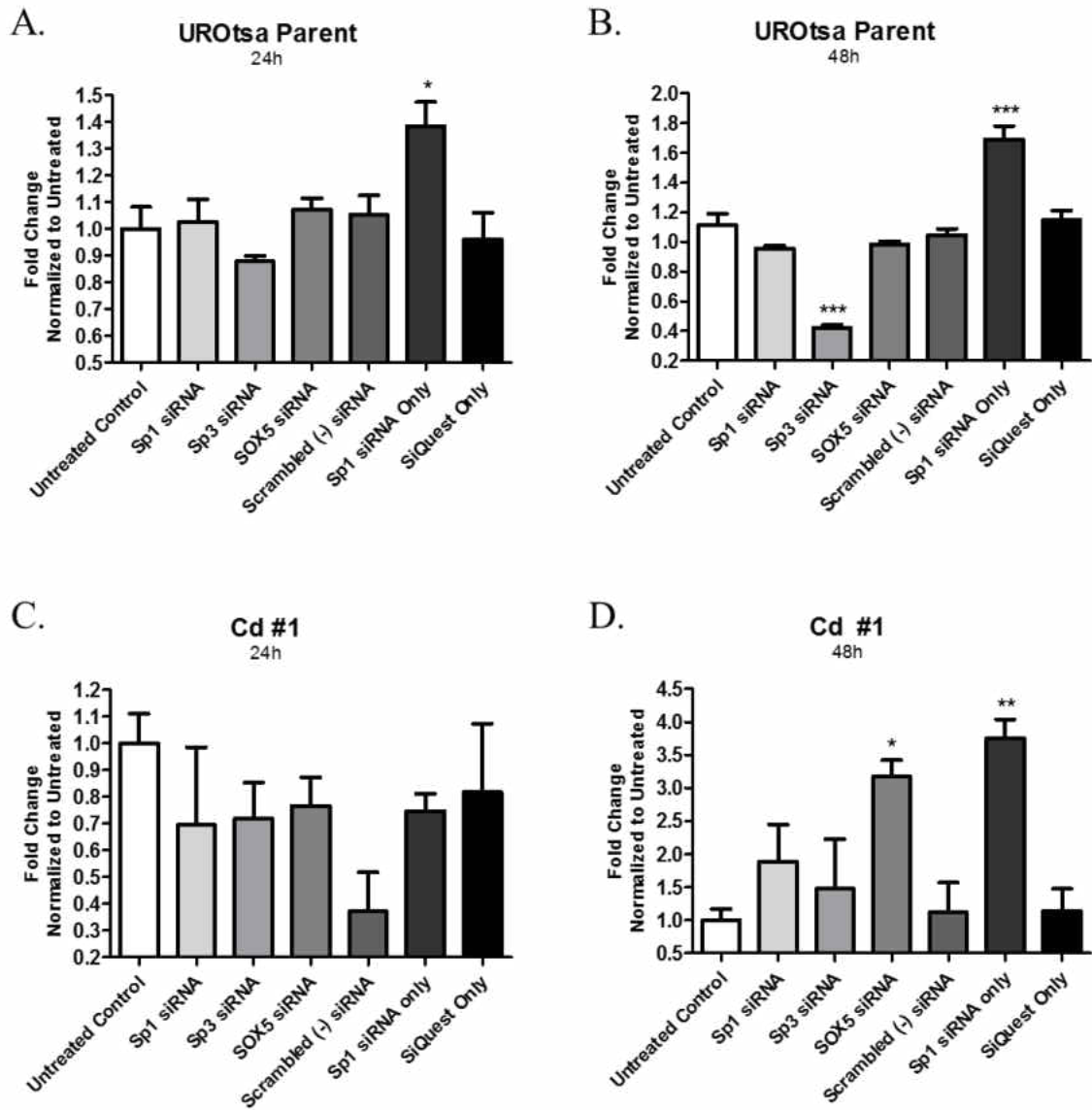


Figure III-9. SPARC mRNA Expression in SPARC⁺ UROtsa Cells and Non-SPARC Expressing Cd #1 Cells Following siRNA Knockdown of Sp1, Sp3, or SOX5. (A) 24 hour and (B) 48 hour siRNA treatment in UROtsa parent cells. (C) 24 hour and (D) 48 hour siRNA treatment in Cd #1 cells. Untreated samples used as control as well as scrambled siRNA, Sp1 siRNA only, and siQuest transfection reagent only. All data represented as mean \pm SEM of triplicates normalized to the untreated control. Statistical significance determined with one-way ANOVA and Dunnett's Multiple Comparison *post hoc* test. *($p \leq 0.05$), **($p \leq 0.01$), and ***($p \leq 0.001$).

Discussion

The strong repression of SPARC observed in our system warranted investigation into the potential mechanism utilized by cadmium to inhibit SPARC expression after transformation by long term, low dose cadmium exposure. Previous studies assessed aberrant DNA methylation and histone acetylation by treating cells with 5-AZC and MS-275, respectively; where, results from these studies did not show any change in SPARC expression, indicating that these common methods of transcriptional repression were not contributing to decreased SPARC levels (Larson et al., 2010). Studies performed in other laboratories described hypermethylation as a mechanism for repression of SPARC in several cancer types, including: gastric, prostate, ovarian, and T-cell non-hodgkins lymphoma; in which, treatment with 5-AZC restored SPARC expression and function (Chen et al., 2014, Liu, et al., 2018, Socha, et al., 2009, Yan et al., 2018). However, this did not appear to be the case with our cadmium-induced bladder urothelial carcinoma system and required further investigation into gene repression via alternative mechanisms, primarily related to transcription factor binding to the SPARC promoter.

Mechanisms proposed for SPARC regulation focused on transcription factor binding to the promoter. Studies performed by Huang et al. (2008) investigated SPARC regulation in nasopharyngeal carcinoma. Interestingly, they also could not restore SPARC expression and function by treating with 5-AZC; however, short-hairpin RNA (shRNA) knockdown of SOX5 transcription factor resulted in restoration of tumor-suppressor actions attributed to SPARC (Huang et al., 2008). In addition, two other transcription factors, Sp1 and/or Sp3, have been shown to bind to the SPARC promoter and elicit gene activation (Chamboredon et al., 2003). Additionally, cadmium cannot

directly bind to DNA; however, it has been shown to replace zinc in zinc-finger transcription factors, such as Sp1 and Sp3, thereby rendering them inactive (Kothinti et al., 2010a, 2010b).

Results from this study show that following malignant transformation with cadmium, Sp1 and Sp3 are expressed at a level similar to that of the non-transformed UROtsa parent cells; indicating, cadmium does not appear to be drastically altering Sp1 and Sp3 expression. Interestingly, SOX5 appears to be slightly up-regulated in Cd #1 cells compared to the non-transformed UROtsa parent cells, although both cell lines expressed SOX5 at low levels. The verification of similar transcription factor expression in both cell lines indicates cadmium transformation may be hindering proper functioning of the transcription factors and hence affecting transcription of downstream target genes during the malignant transformation process.

Although cadmium cannot directly bind to DNA, it can elicit DNA damage through a variety of mechanisms, including ROS production (Rani et al., 2014). It has been shown that prolonged DNA damage can result in carcinogenesis and a state of redox imbalance (Dayem et al., 2010, Ogasawara and Zhang, 2009). Therefore, it is possible that long-term cadmium exposure is causing indirect, prolonged DNA damage resulting in aberrant transcription of SPARC. Alternatively, cadmium can directly affect gene transcription by replacing zinc in zinc-finger transcription factors changing their shape. This can affect steric hindrance of DNA binding sites within transcription factors and lead to a reduction in DNA binding and ultimately, gene repression (Kothinti et al., 2010a, 2010b). Results from this study indicated decreased binding of Sp1 and Sp3 to the SPARC promoter in Cd #1 cells. Cadmium may not be significantly affecting expression

of Sp1 and Sp3 in our model system; however, it could be replacing zinc and negatively affecting its functionality.

Therefore, it is possible that Sp1 binding is inhibited by cadmium incorporation into the zinc-finger DNA-binding domain resulting in a lack of chromatin remodeling complex recruitment and ultimately transcriptional repression. This leaves open the opportunity for potential alternative transcription factor binding to accessible chromatin, further impacting gene transcription. Interestingly, results indicated increased binding of SOX5 to the SPARC promoter in Cd #1 transformed cells. Cadmium's association with SOX5 transcription factor is not as strong as that with Sp1/Sp3. In fact, currently, there is no literature to suggest that cadmium has a direct interaction with SOX5. It is not a zinc-finger transcription factor so cadmium's impact on SOX5 DNA-binding is likely indirect; such as, changes in chromatin accessibility. Nonetheless, there was a slight increase in expression of SOX5 in Cd #1 cells along with an increase in SOX5 binding to the SPARC promoter; potentially indicating an additional role for cadmium-induced changes in gene expression through permanent altered redox homeostasis associated with long-term stress.

Transcriptional regulation is a complex process, and understandably so. To better understand Sp1, Sp3, and SOX5 impact on SPARC gene expression, siRNA knockdown experiments were performed. All three transcription factors were knocked down by 35% or more by 24 hours. However, results on the impact of SPARC expression were ambiguous and somewhat difficult to interpret. Although there was successful knockdown of the transcription factors, there was also varied changes in transcription factor expression in the control samples. This was also apparent with β -actin expression

in the siRNA transfected cells, as well as the control samples exposed to the transfection reagent alone and occasionally siRNA alone as well (data not shown). These results indicate potential susceptibility to stress from the siRNA transfection reagents. Although ambiguity is somewhat present, SPARC expression did show a significant decrease in the SPARC⁺ UROtsa parent cells following 48 hour Sp3 siRNA exposure. This indicates that Sp3 is a potential necessary transcription factor for SPARC expression in our system. This is in accord with some studies suggesting Sp3 importance for induced gene activation (Li and Davie, 2010). Results also showed a significant increase in SPARC expression in Cd #1 cells following 48 hour SOX5 siRNA exposure, suggesting that SOX5 is potentially acting as a repressive transcription factor for SPARC, as well. Overall, it appears that alternative transcription factor binding to the SPARC promoter is contributing to its repression in our *in vitro* model system of cadmium-induced bladder transitional cell carcinoma. The permanence of this change may be due to advantageous changes in gene expression, further implicating SPARC as a tumor suppressor-like protein in this system.

CHAPTER IV
SPARC AND TUMOR INITIATION IN SERIALY TRANSPLANTED
BLADDER UROTHELIAL TUMORS

Introduction

SPARC has been shown to play a variety of roles in cancer; however, its expression and whether changes in expression promote or inhibit tumor initiation and progression is tissue- and cancer-dependent. Unfortunately, mechanistic roles are not well understood, and are complicated by the complex, tissue-specific roles for SPARC. Studies have shown that epithelial cancers show a reduction in SPARC expression, while other cancer types have increased SPARC expression; yet, others show a mix of SPARC expression, with an increase in expression associated with tumor aggressiveness (Brekken and Bradshaw, 2010, Said and Theodorescu, 2013, Podhajcer et al., 2008). Interestingly, stromal SPARC expression is similarly variable between cancers (Vaz et al., 2015). Therefore, important consideration must be given to the complex interaction between the tumor and host microenvironment.

Utilization of a SPARC-null mouse model has been instrumental in attempting to decipher the impact of stromal SPARC on tumor progression; but, it has also led to conflicting results. SPARC-null mice display abnormalities in stroma composition and strength; therefore, it is thought that stromal SPARC exerts some of its effects through extracellular matrix modulation to promote tumor growth (Bradshaw et al., 2003, Brekken and Bradshaw, 2010). Brekken et al. (2003) found that Lewis Lung Carcinoma

cells subcutaneously injected into SPARC- null mice produced larger tumors than those injected into the SPARC-expressing control mice. However, another study showed that mouse-derived breast cancer cells had impeded tumor growth in SPARC-null mice, resulting in smaller tumors compared to the SPARC-expressing control (Sangaletti et al., 2003). They concluded that host leukocytes, lacking SPARC expression, did not adequately contribute to the stromal organization and support for proper tumor growth. These controversial studies indicate that not only is stromal SPARC expression important, but also the source of the tumor tissue is important to consider SPARC's role in the dynamic tumor progression process.

Overexpression of SPARC has been shown in several cancers, including, melanoma and gliomas. It appears that overexpression of SPARC in these cancers is associated with increased invasion. Interestingly, Ledda et al. (1997) found that decreased SPARC within melanoma tumor cells resulted in decreased tumorigenic growth. A separate study found that tumorigenesis and invasiveness in nude mice is dependent upon tumor cell SPARC expression and matrix metalloproteinase activity rather than stromal SPARC expression; further supporting a tumor promoting role for SPARC in melanoma cells (Prada et al., 2007). Gliomas have conflicting reports, with some studies showing increased SPARC expression promoting tumor progression and being associated with more invasive tumors; however, another report found that increased expression of both SPARC and doublecortin in glioma cell lines resulted in: abrogated SPARC-mediated cell invasion, increased apoptosis induced by irradiation, along with cell cycle turnover interference (Schultz et al., 2002, Shi et al., 2007, Xu et al., 2013). A different study by Capper et al. (2010) described high expression of SPARC in astrocytomas that decreased

with tumor progression; concluding, that the observed decrease in cell proliferation was associated with increased SPARC expression.

There are also several cancers that show repression of SPARC within tumor cells, including pancreatic cancer and ovarian cancer. In these cancers it appears SPARC is inhibitory to tumor formation and progression. Studies of SPARC repression in these systems has revealed hypermethylation of the promoter region that was responsible for decreased SPARC expression; that was subsequently reversed following treatment with 5-Aza-2'-deoxycytidine (Gao et al., 2010, Sato et al., 2003, Socha et al., 2009). It has been shown that the majority of pancreatic cell lines repress SPARC; however, there are some pancreatic cell lines that show an overexpression of SPARC. Furthermore, there is variability in SPARC expression within some forms of human pancreatic tumors (Sato et al., 2003, Prenzel et al., 2006). Interestingly, the stromal fibroblasts that surround the tumor often show strong expression of SPARC (Vaz et al., 2015). One study found that SPARC expressed by the pancreatic stellate cells increased invasion of pancreatic cancer cells via a paracrine action (Mantoni et al., 2008). It was also found that increased SPARC expression in surrounding fibroblast cells correlated with poor patient survival (Infante et al., 2007). Additionally, it has been consistently found that orthotopic pancreatic tumors in SPARC-null mice result in increased metastasis compared to SPARC-expressing controls (Arnold et al., 2008, Puolakkainen et al., 2004). This study found that the observed increase in metastasis was probably occurring via MMP-9 effects on extracellular matrix deposition.

Ovarian cancer also shows repression of SPARC within cancer cells; which, inversely correlates with the degree of malignancy (Mok et al., 1996). Similar to

pancreatic cancer, SPARC expression is high in the supporting stromal cells of advanced stage ovarian cancer (Said et al., 2007). Interestingly, it appears that stromal SPARC attempts to neutralize the microenvironment by decreasing inflammation and subsequent tumor growth (Said et al., 2007). Furthermore, SPARC-null mice showed increased peritoneal metastasis along with increased macrophage recruitment and subsequent decreased activity of ascitic fluid (Said et al., 2007). Additionally, it was shown that increased SPARC expression within the ovarian cancer cells resulted in disrupted tumor-stromal interplay, decreased macrophage recruitment and increased expression of inflammatory markers (Said et al., 2008). Interestingly, both pancreatic and ovarian cancers show poorer patient survival with increased stromal SPARC expression (Vaz et al., 2015). Therefore, it appears that SPARC within the tumor cells is acting in a tumor suppressor-like role, while stromal SPARC appears to act in promoting tumor progression.

Bladder cancer is another cancer type that shows an overall repression of SPARC within bladder cancer cells (Larson et al., 2010). Studies have determined an inverse correlation between SPARC expression and patient prognosis (Said, 2016, Yamanaka et al., 2001). It was also determined that decreased SPARC within bladder cancer cells resulted in increased cell proliferation (Said, 2016). This was likely due to cell cycle dysregulation at the G1/S checkpoint via increased cyclins A1, D1, and E2 with a concomitant decrease in expression of cell cycle inhibitors such as p21 and p27 (Shariat et al., 2006, Galmozzi et al., 2006). Said et al. (2013) used a carcinogen-induced bladder cancer model and found that SPARC expression within cancer lesions decreased ROS generation, along with DNA, protein, and lipid oxidative damage; which, was opposite in

lesions from SPARC-null mice. They also found that decreased SPARC in cancer cells resulted in strong invasion, increased metastasis, as well as early-onset metastasis. Interestingly, Yamanaka et al. (2001) determined that increased SPARC correlated with increased MMP-2 expression. However, this group did not appear to distinguish between tumor cell-derived SPARC and stromal SPARC expression. Although it appears that SPARC is a tumor suppressor-like molecule in bladder cancer cells, the supporting stromal tissue shows a high degree of SPARC expression that needs to be considered (Said et al., 2013). Overall, there is limited research addressing SPARC and bladder cancer. Therefore, further research into SPARC expression, its origin of expression, and its function in bladder cancer is critical information that could lead to potential future therapeutics.

Previous studies in this lab investigated SPARC expression in heterotransplant tumors generated from heavy metal Cd²⁺-transformed UROtsa bladder cells along with human transitional cell carcinoma tumors. Larson et al. (2010) found that SPARC expression was significantly repressed within heterotransplant tumors and low-grade human transitional cell carcinoma tumors. However, human high grade invasive carcinoma tumor samples showed strong staining for SPARC protein expression in the supporting stroma (Larson et al., 2010). The significant repression of SPARC in both the cell lines and heterotransplant tumors prompted investigation into SPARC overexpression via stable transfection in Cd²⁺-transformed malignant cell lines. Interestingly, immunohistochemical results showed significant repression of SPARC within heterotransplant tumor cells, despite the strongly forced expression in the injected cells; with, Cd #1-SPARC transfected heterotransplant tumors showing very low levels of

focal SPARC expression in approximately 10% of the total tumor mass (Slusser et al., 2016). Further experimentation led to the isolation of the proposed cancer-initiating cell population (Urospheres) and subsequent heterotransplant tumor formation. These tumors resulted in 5-20% focal expression of SPARC within tumor cells generated from the SPARC-transfected Urosphere population (Slusser et al., 2016). Additionally, heterotransplant tumors generated from one of the two non-SPARC transfected cadmium cell lines showed 10-20% focal expression of SPARC within tumor cells (Slusser et al., 2016). These results led to our hypothesis that SPARC is inhibitory to bladder tumor initiation and progression. Therefore, this study will examine SPARC expression in serially transplanted bladder heterotransplant tumors.

Materials and Methods

Cell Culture

Cells were maintained as previously described in Chapter II Materials and Methods. The isolation and growth of the proposed cancer initiating cell subpopulation (Urospheres) was performed as described in Slusser et al. (2016). Briefly, cells were expanded to 75cm² tissue culture flasks and grown until confluent. Cells were passaged and seeded at a 1x10⁶ cell density in 75cm² Ultra-low attachment flasks (Corning, Inc., Corning, NY). Cells were grown in serum-free media containing a 1:1 mixture of DMEM (Sigma-Aldrich) and Ham's F-12 (Sigma-Aldrich) growth medium. The media was supplemented with: 5ng/mL selenium, 5µg/mL insulin, 5µg/mL transferrin, 36ng/mL hydrocortisone, 4pg/mL triiodothyronine, and 10ng/mL epidermal growth factor. Spheres were grown for approximately 7 days and then harvested via centrifugation for transplantation into nude athymic mice or for RNA or protein isolation.

RNA and Protein Isolation From SPARC⁺ UROtsa Parent, Cd #1, and Cd #1-SPARC Cell Lines

Total RNA and protein were isolated as previously described in Chapter II Materials and Methods section. Concentrations were determined using a Nanodrop One (Thermo Fisher Scientific). Samples were then utilized for subsequent RT-qPCR and Western Blot analysis.

RT-qPCR Analysis of SPARC mRNA Expression in SPARC⁺ UROtsa Parent, Cd #1, and Cd #1-SPARC Cell Lines

SPARC mRNA expression from UROtsa Parent, Cd #1, and Cd #1-SPARC cells was determined using RT-qPCR as previously described in Chapter II Materials and Methods section. SPARC mRNA expression was verified using 20 μ M SPARC specific primers (Qiagen #QT00018620) prior to progressing into *in vivo* serial heterotransplant experiments. Data was graphed and statistical analysis performed using GraphPad PRISM v5.01 (GraphPad Software).

Secreted SPARC Protein Purification from Media of SPARC⁺ UROtsa Parent, Cd #1, and Cd #1-SPARC Cell Lines

Secreted SPARC protein was purified from the media of cells grown in culture, with reference to Sage (2003) and using a protocol refined by Slusser et al. (2016). Briefly, UROtsa parent, Cd #1, and Cd #1-SPARC cells were grown to confluency in serum-containing media in 75cm² tissue culture flasks. Once confluent, media was replaced with serum-free medium and cells were placed in a 37°C, 5% CO₂ tissue culture incubator for 24 or 48 hours. Media was collected and centrifuged at 2000 rpm for 5 minutes at 4°C. During this time, cells were harvested for subsequent RNA and protein isolation. The media was then filtered through a 0.2 μ m syringe filter into a fresh, cooled 50mL tube and placed on ice. Tubes were placed on an end-over-end rotator and 50%

w/v solid ultrapure ammonium sulfate (Sigma #A2939-500G) was added to each sample over several hours [5g [NH₄]SO₄/10mL media] to efficiently precipitate protein while maintaining a neutral pH, then incubated on an end-to-end rotator in the 4°C fridge overnight. Media was then transferred to high velocity centrifuge tubes and centrifuged using a Sorval centrifuge with the SS-34 rotor at 40,000xg for 30 minutes at 4°C.

Samples were placed on ice and supernatant removed. The pellet was resuspended in PBS lysis buffer with protease inhibitors for subsequent Western Blot analysis. Because SPARC protein was precipitated from the media, no sonication to shear DNA was necessary prior to determining protein concentration via BCA assay.

Western Blot analysis was performed similarly to that described in Chapter II Materials and Methods section using mouse anti-Osteonectin primary antibody (Novocastra™, Cat # NCL-O-NECTIN) followed by anti-mouse IgG, HRP-linked antibody (Cell-Signaling Technology, #7076S) at 1:3,000 and anti-biotin, HRP-linked antibody (Cell-Signaling Technology, #7075S) at 1:1,500. The blot for this experiment could not be stripped and re-probed for β-actin because the protein was not from the cellular fraction but rather the media supernatant; therefore, β-actin was not present.

Visualization of SPARC Expression in SPARC⁺ UROtsa Parent, Cd #1, and Cd #1-SPARC Cell Lines via Immunofluorescent Microscopy

Cells were grown to confluency on glass coverslips in 24 well tissue culture plates (Corning, Inc.). Cells were washed twice with DMEM-F12-no phenol red (Gibco #11039-021) and fixed using 3.7% Formaldehyde (Polysciences, Inc. #18814-10) for 10 minutes at room temperature. Free aldehyde groups were quenched using 0.1M NH₄Cl (Sigma-Aldrich) for 15 minutes at room temperature and cells were permeabilized using 0.1% Igepal (Sigma-Aldrich) for 10 minutes at room temperature. Coverslips were

incubated with a 1:20 dilution of mouse monoclonal anti-Osteonectin antibody (Novocastra™, Cat # NCL-O-NECTIN) [Leica Biosystems Inc.] for 45 minutes at 37°C. Coverslips were washed and incubated with AlexaFluor594 goat-anti-mouse secondary antibody (2mg/ml) [Life Technologies #A11005] for 45 minutes at 37°C. Coverslips were, again, washed and mounted using ProLong Diamond Antifade mounting medium with DAPI (Life Technologies #P36971) for nuclear counterstaining. Cellular SPARC expression was visualized using the Leica Laser Scanning SPE Confocal microscope at 63x magnification. Secondary antibody only samples were used as a control.

Serial Heterotransplant Tumors in Nude Mice

Three mice for each of 4 groups: (1) Cd #1 cells and (2) Cd #1 Urospheres, and (3) Cd #1-SPARC cells and (4) Cd #1-SPARC Urospheres were used for tumor formation studies. Tumor transplantation was performed as described in Sens et al. (2004). Briefly, approximately 1×10^6 cells, suspended in PBS, were subcutaneously injected into the dorsal thoracic midline of nude athymic mice. Tumor formation, growth, and overall mouse health were assessed weekly. Mice were cared for through tumor formation and growth, unless conditions dictated euthanasia, under an Institutional Animal Care and Use Committee (IACUC) approved protocol as well as in accordance with the National Research Council's Guide for the Care and Use of Laboratory Animals. Once tumors were large enough, approximately 1cm or larger, the mice were sacrificed and the tumor was harvested. Approximately 1/3 of the tumor was utilized for Hematoxylin and Eosin staining (H&E) along with immunohistochemical analysis of SPARC expression. Another 1/3 of the tumor was snap frozen for RNA isolation. Finally, 1/3 of the tumor was used for serial transplantation into a subsequent mouse. The tumor

tissue used for serial transplantation was mechanically homogenized using scalpel blades in a sterile petri dish. The tumor was resuspended in approximately 500 μ L of PBS and homogenized until able to pass through a 20 gauge needle. 200 μ L tumor suspension was then subcutaneously injected into a subsequent mouse. The serial transplantation process was repeated a second time for a total of three rounds of tumor inoculation and formation events.

Immunohistochemical Localization of SPARC Protein Expression in Serial Heterotransplant Tumors

Immunohistochemical analysis was performed on serial heterotransplant samples to assess SPARC expression. Additionally, human high grade invasive bladder carcinoma was used as a control. Briefly, tumor tissue was formalin fixed and paraffin embedded. Then, tissue blocks were serially sectioned at 4-5 μ m, and placed on microscope slides. Slides were then stained using the Leica Bond Max Automated Stainer (Leica Microsystems, Inc.) with the Bond Polymer Refine Detection kit (Leica Biosystems #DS9800). Generally, slides were heated at 60°C for 15-20 minutes, dewaxed using xylene, rehydrated using decreasing concentrations of alcohol and then subjected to antigen retrieval. Slides were washed with wash buffer and incubated with a peroxidase block. Slides were then stained using a 1:20 dilution of mouse monoclonal anti-Osteonectin primary antibody (Novocastra™, Cat # NCL-O-NECTIN) [Leica Biosystems, Inc.] for 30 minutes. Again, slides were washed with wash buffer and staining was detected using a horseradish peroxidase DAB solution. Slides were then counterstained with H&E and visualized and imaged using light microscopy.

Immunohistochemical Localization of α -Smooth Muscle Actin Protein Expression in Serial Heterotransplant Tumors

Immunohistochemical analysis was performed on serial heterotransplant samples, with the addition of human high grade invasive bladder carcinoma as a control, to assess α -smooth muscle actin expression; identifying an activated stroma. Briefly, tumor tissue was formalin fixed and paraffin embedded. Then, tissue blocks were serially sectioned at 4-5 μ m, and placed on microscope slides. Slides were heated at 60°C for 15-20 minutes, dewaxed using xylene, rehydrated using decreasing concentrations of alcohol, and then subjected to antigen retrieval using 1x DakoCytomation Target Retrieval Solution Citrate buffer (Dako #S2369). Slides were incubated with 1x Tris Buffered Saline with Tween 20 (TBS-T) [Dako #S3306], washed with wash buffer (Dako #S3006), and incubated with peroxidase block (Dako, #K4011). Slides were then stained with rabbit polyclonal anti- α -smooth muscle actin antibody (0.2mg/ml) [Abcam #ab5694] for 30 minutes. Slides were washed with wash buffer, and stained using Labelled Polymer-HRP Anti-Rabbit (Dako #K4011) for 30 minutes. Slides were washed and staining was detected using a DAB Substrate Chromogen System (Dako #K3466). Slides were then counterstained with H&E and visualized using light microscopy.

RNA Isolation from Serial Heterotransplant Tumors

RNA was isolated from serial heterotransplant tumor tissue using the TissueLyser LT (Qiagen). Tumor tissue was weighed and cut into three 30mg portions of tissue. Each portion was placed in a pre-cooled 2mL bullet tube containing one 5mm diameter stainless steel bead (Qiagen #69989). 500 μ L TRI Reagent (MRC) was added to each sample and homogenized using: 45Hz for 3 minutes, 35Hz for 2 minutes, and 35Hz for 2 minutes as recommended in the manufacturer's protocol. Homogenized tissue was then

transferred to a fresh microfuge tube containing 500 μ L TRI Reagent and RNA isolation continued as described previously in Chapter II Materials and Methods section. RNA pellet was resuspended in 100 μ L nuclease free water (MO BIO Laboratories, Inc.) due to pellet size. RNA concentration was determined, using the NanoDrop One (Thermo Scientific), for all three portions of tumor tissue separately; then, a fraction of each portion was combined, and the concentration determined, to get an even distribution of each tumor to sample for PCR analysis.

RT-qPCR Analysis of hSPARC and mSPARC mRNA Expression in Serial Heterotransplant Tumors

Human SPARC and mouse SPARC mRNA expression from serial heterotransplant tumor samples were determined using real-time reverse transcription polymerase chain reaction (RT-qPCR), as previously described in Chapter II Materials and Methods section. cDNA was amplified using 20 μ M human SPARC specific primers (Qiagen #QT00018620) or 20 μ M mouse SPARC specific primers (Qiagen #QT00161721) and recorded using SYBR green fluorescence. Human SPARC expression was determined relative to the UROtsa parent cell line control and mouse SPARC was determined relative to mouse brain control. Expression data was graphed and statistical analysis performed using Graphpad PRISM v5.01 (GraphPad Software).

Recombinant hSPARC or mSPARC Treatment of Cd #1-SPARC Cell Line

Cd #1-SPARC cell line was exposed to recombinant human SPARC (rhSPARC) [R&D Systems #941-SP-050] or recombinant mouse SPARC (rmSPARC) [R&D Systems #942-SP-050] to determine an effect on endogenous SPARC expression. Cells were plated in a 12-well tissue culture plate (Corning, Inc.) and grown to confluency. Preliminary experiments tested dose efficacy using: 2.0 μ g, 0.2 μ g, 0.02 μ g, or 0.002 μ g

rhSPARC added to respective wells with an untreated well as a control. Cells were incubated in a tissue culture incubator at 37°C, 5% CO₂ for 24 hours then harvested for RNA isolation and PCR analysis to determine endogenous SPARC expression. In a subsequent time-course study, Cd #1-SPARC cells were exposed to 2.0µg rhSPARC for 12h, 24h, 36h, 48h, and 72h using 0h as a control. Each time point also had an untreated well to control for changes in confluency over time.

Once the correct dosing and optimal time line were determined, Cd #1-SPARC cells were exposed to rhSPARC or rmSPARC. Cells were again plated in a 12-well tissue culture plate and grown to confluency. 2.0µg, 0.2µg, 0.02µg, or 0.002µg rhSPARC was added to respective wells with an untreated well as a control. Additionally, 20.0µg, 2.0µg, 0.2µg, 0.02µg, or 0.002µg rmSPARC was added to respective wells with an untreated well as a control. An additional higher dose was added for rmSPARC exposure to account for crossing species. Cells were incubated with rhSPARC or rmSPARC for 36 hours, based on the previous time-course study, at 37°C, 5% CO₂ in a tissue culture incubator. Cells were then harvested for RNA isolation and RT-qPCR analysis.

RNA Isolation of Cd #1-SPARC Cell Line Following Recombinant SPARC Treatment

Total RNA was isolated from human or mouse recombinant SPARC treated cells using TRI REAGENT™ (MRC) as described in Chapter II Materials and Methods section. RNA concentration was determined on the Nanodrop One (Thermo Scientific) and a portion of each sample was diluted to 20ng/µl concentration. Samples were then utilized for subsequent RT-qPCR analysis to assess SPARC mRNA expression.

RT-qPCR Analysis of SPARC Expression in Cd #1-SPARC Cell Line Following Recombinant SPARC Treatment

SPARC mRNA expression in human or mouse recombinant SPARC treated cells was determined using RT-qPCR as previously described in this section using 20 μ M SPARC specific primers (Qiagen #QT00018620). β -actin was amplified using an Invitrogen primer set with the following sequences, sense: CGACAACGGCTCCGGCATGT, anti-sense: TGCCGTGCTCGATGGGGTACT, under the same cycling parameters. β -actin expression was determined relative to the untreated control using a standard curve generated from β -actin standards. Expression data was graphed and statistical analysis performed using Graphpad PRISM v5.01 (GraphPad Software).

Statistics

All data was analyzed using GraphPad PRISM v5.01 software (GraphPad Software). Statistical analysis for mRNA expression was performed using a 1-way ANOVA and Dunnett's Multiple Comparison *post hoc* test. Statistical significance determined for all results using $p < 0.05$ significance level.

Results

SPARC mRNA and Secreted Protein Expression in SPARC⁺ UROtsa Parent, Cd #1, and Cd #1-SPARC Cell Lines

SPARC mRNA and protein expression were verified prior to *in vivo* studies to ensure SPARC was still being stably expressed in the Cd #1-SPARC transfected cell line. RT-qPCR analysis in Figure IV-1 (A), revealed significantly higher expression of SPARC in the Cd #1-SPARC cell line compared to the non-transfected Cd #1 cell line. There did not appear to be a significant difference in SPARC expression between the

positive control UROtsa parent cell line and the Cd #1-SPARC cell line. This was slightly different from previous results in Slusser et al. (2016) which indicated a significant increase in expression following stable SPARC transfection. However, these results showed that the Cd #1-SPARC cell line is still expressing SPARC mRNA at relatively high levels.

To verify this further, protein expression was analyzed using Western Blot analysis. Initially, cell lysate was used to examine protein expression; however, results did not indicate protein expression that was similar to mRNA expression (data not shown). This was strikingly different from results reported in Slusser et al. (2016). Through a series of troubleshooting experiments, it was concluded that it was possible the Cd #1-SPARC cells were producing SPARC but quickly secreting it; therefore, expression was not being captured in the cell lysate fraction.

Subsequent Western Blot analysis then verified secreted protein expression using SPARC protein precipitated from the tissue culture media. Figure IV-1 (B) indicates ample quantities of secreted SPARC expression in both 24h and 48h post confluency media from Cd #1-SPARC tissue culture flasks. Additionally, these results show substantial secreted SPARC in the UROtsa parent cell line. There also appears to be some SPARC expression in the Cd #1 samples when the blot is overexposed. This could be due to the Cd #1 cells making and secreting minimal amounts of SPARC protein that are undetectable at the mRNA level. It is also possible that the band for Cd #1 is falsely intensified due to bleed over from the extreme amount of SPARC from the UROtsa parent sample as well as the high amounts of SPARC from the Cd #1-SPARC sample.

Overall, these results indicate SPARC is still being stably expressed in the Cd #1-SPARC cell line at drastically higher levels than the Cd #1 transformed cell line.

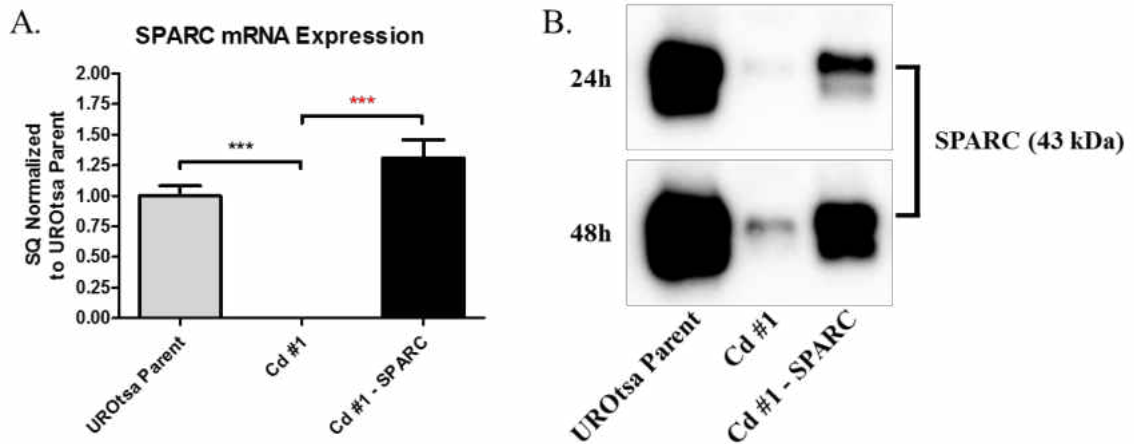


Figure IV-1. SPARC mRNA and Secreted Protein Expression in SPARC⁺ UROtsa Parent, Non-SPARC Expressing Cd #1, and Cd #1-SPARC Transfected Cells. (A) Relative SPARC mRNA expression with starting quantity (SQ) determined relative to UROtsa parent. Experiment was run in triplicate with statistical analysis determined using a one way ANOVA with Dunnett’s Multiple Comparison *post hoc* test. ***($p \leq 0.001$). (B) Western blot analysis showing secreted SPARC protein expression in tissue culture media collected at 24h and 48h post confluency.

Immunofluorescent Microscopy of SPARC Expression in SPARC⁺ UROtsa Parent, Cd #1, and Cd #1-SPARC Cell Lines

Immunofluorescent microscopy was utilized to visualize SPARC protein expression within UROtsa parent, Cd #1, and Cd #1-SPARC cells. Western blot analysis of cell lysate revealed SPARC expression only in the UROtsa parent cell line. However, SPARC expression was expected in the Cd #1-SPARC cell line. Figure IV-2 shows representative immunofluorescent images of SPARC expression within UROtsa parent (A), Cd #1 (B), and Cd #1-SPARC (C) cells. All cell lines were also stained with secondary antibody only, as a control (D, E, and F, respectively). UROtsa parent cells show SPARC expression within the cytoplasm of the cells. There does not appear to be a blur of staining throughout the cytoplasm, but rather, staining puncta; likely visualizing

SPARC-containing vesicles. Cd #1 cells do not appear to be expressing SPARC when compared to the UROtsa parent cells and the secondary antibody only control. This was expected as these cells show very little, if any, mRNA or protein expression with RT-qPCR or Western Blot analysis, respectively. Immunofluorescent microscopy revealed SPARC expression within Cd #1-SPARC cells that was not strongly observed with Western Blot analysis of cell lysate. The staining profile was similar to that seen in the UROtsa parent cells, showing staining puncta, indicating SPARC-containing vesicles. This experiment, in conjunction with Western Blot analysis of secreted SPARC, indicates SPARC expression in both UROtsa parent cells and malignant Cd #1-SPARC cells. Therefore, the Cd #1 and Cd #1-SPARC cells could be used in the *in vivo* studies to examine SPARC's role in tumor initiation and progression.

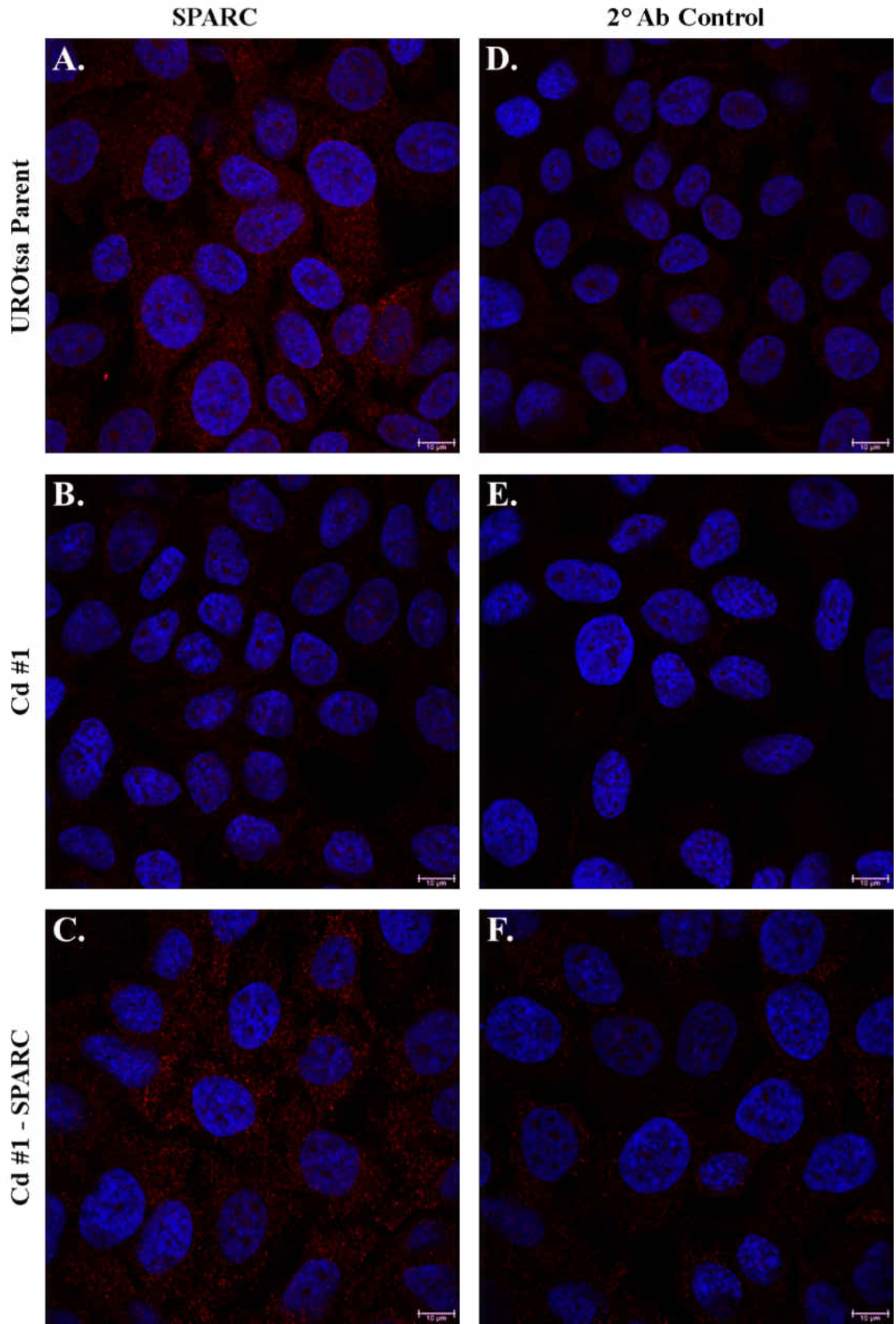


Figure IV-2. Visualization of SPARC Expression in UROtsa Parent, Cd #1, and Cd #1-SPARC using Confocal Microscopy. Representative images of SPARC expression (red) in UROtsa parent (A and D), Cd #1 (B and E), and Cd #1-SPARC (C and F) cell lines with a secondary antibody only control for each cell line. Cells were counterstained with DAPI (blue) for nuclear staining. Images were taken at 63x with scale bars shown at 10 μ m.

Immunohistochemical Localization of SPARC Protein Expression in Serial Heterotransplants

SPARC expression in serial heterotransplant tumor tissue was determined using immunohistochemistry. This experiment consisted of serial inoculations of mechanically dissociated tumor tissue to determine SPARC's role in tumor initiation and progression. Three mice were inoculated from each of the 4 groups: Cd #1 cell line, Cd #1 Urosphere, Cd #1-SPARC cell line, and Cd #1-SPARC Urosphere. At least one mouse from each group, at each tumor inoculation, had tumor formation and subsequent injection into another mouse. Therefore, serial transplantation could be assessed in regards to SPARC expression. Figure IV-3 illustrates representative immunohistochemical images from each group and each tumor formation event, in addition to human high grade invasive bladder carcinoma tumor tissue used as a control. This data is further summarized in Table 3.

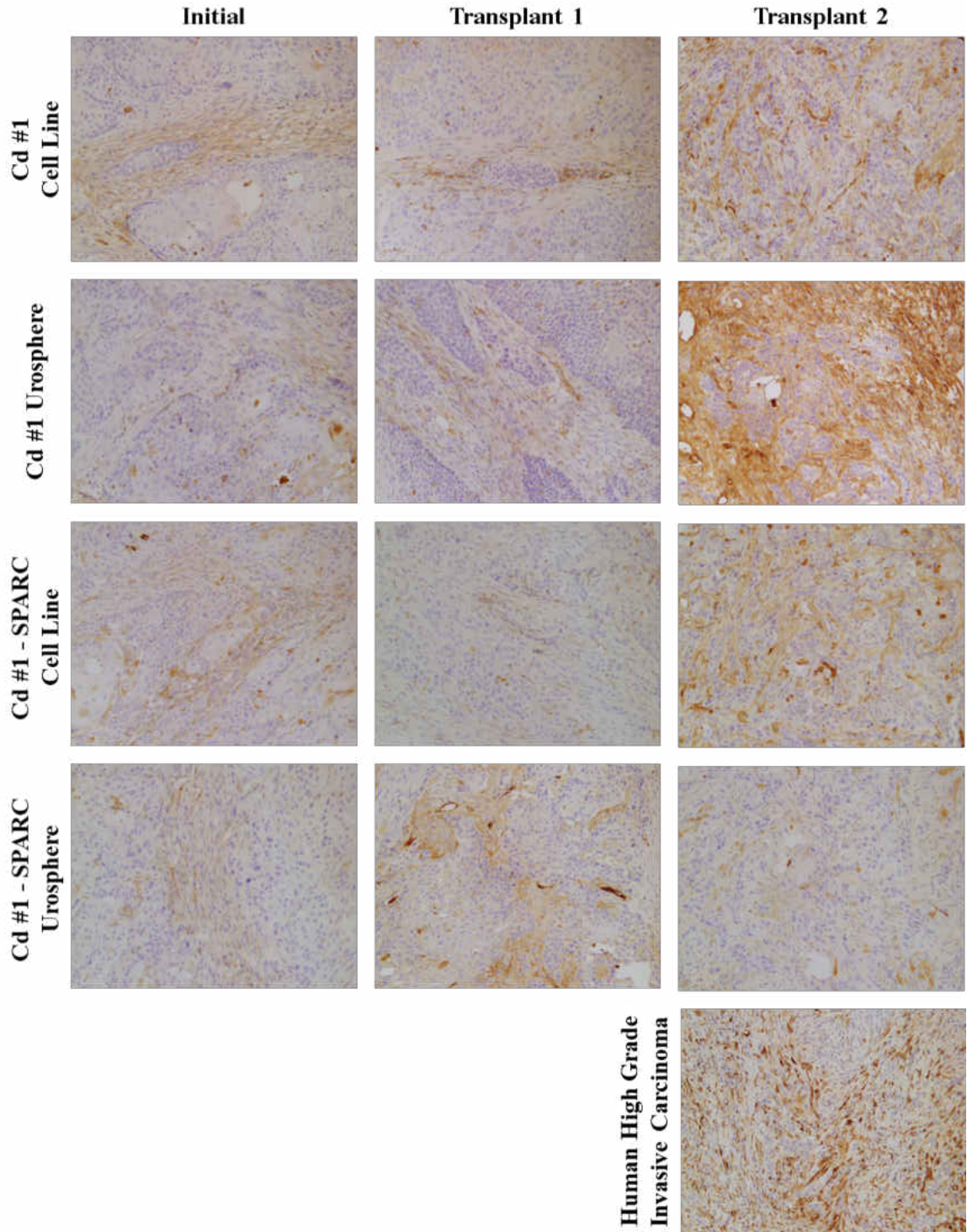


Figure IV-3. Immunohistochemistry Images of SPARC Expression in Serial Bladder Heterotransplant Tumors. Representative images of Initial, Transplant 1, and Transplant 2 serial bladder heterotransplants generated from Cd #1 cell line, Cd #1 Urosphere, Cd #1-SPARC cell line, and Cd #1-SPARC Urosphere populations. Human high grade invasive bladder carcinoma used as a control. All images taken at 200x.

Table 3. Summary of Immunohistochemistry Staining for SPARC Expression in Serial Bladder Heterotransplant Tumors.

SPARC Expression in mouse SC serial heterotransplants					
Group	Tumor #	Tumor		Stroma	
		Int	%	Int	%
Cd #1 Cell Line	Initial	-		2+	20
Cd #1 Cell Line	Transplant 1	-		2+	10
Cd #1 Cell Line	Transplant 2	-		2-3+	70
Cd #1 Urosphere	Initial	-		1-2+	10
Cd #1 Urosphere	Transplant 1	-		2-3+	40
Cd #1 Urosphere	Transplant 2	2-3+	40	2-3+	80
Cd #1 - SPARC Cell Line	Initial	2+	10	2+	10
Cd #1 - SPARC Cell Line	Transplant 1	-		1+	5
Cd #1 - SPARC Cell Line	Transplant 2	1+	10	2-3+	60
Cd #1 - SPARC Urosphere	Initial	-		1-2+	5
Cd #1 - SPARC Urosphere	Transplant 1	-		2-3+	30
Cd #1 - SPARC Urosphere	Transplant 2	-		1+	5
Human High Grade Inv Ca.		-		3+	80

Table summarizing immunohistochemistry staining of serial heterotransplant tumors generated from: Cd #1 cell line, Cd #1 Urosphere, Cd #1-SPARC cell line, and Cd #1-SPARC Urosphere populations. Tumor # shows three tumors for each group: Initial, Transplant 1, and Transplant 2. For both tumor and stroma, staining intensity (Int) is determined on a scale of 0-3+ and % indicates the percent of tumor or stroma showing SPARC staining. Int and % interpreted by pathologist. SC: subcutaneous, Inv Ca.: invasive carcinoma.

Results indicate an increase in intensity as well as percentage of tissue stained for SPARC expression in the supporting stromal tissue, from the initial tumor to the final transplant 2 tumor in 3 of the 4 groups. Cd #1 cell line initial tumor showed low to moderate SPARC staining in approximately 20% of the supporting stromal tissue which did not increase in the second transplant 1 tumor. However, there was a marked increase in stromal SPARC expression in the final Cd #1 transplant 2 tumor; showing moderate to strong staining in approximately 70% of the tumor. The tumors derived from the Cd #1 Urosphere population showed similar results; however, there was a substantial increase in

staining intensity and percentage of stroma stained from the initial tumor (low to moderate in 10% of tumor) to the second transplant 1 tumor (moderate to strong in 40% of tumor). This group also continued another substantial increase in stromal SPARC expression in the transplant 2 tumor; showing moderate to strong staining in approximately 80% of the tumor.

Cd #1-SPARC initial tumor showed moderate stromal SPARC staining in a low percentage of the tumor which did not increase in the second transplant 1 tumor. However, similar to the Cd #1 cell line tumor, there was a substantial increase in stromal SPARC expression in the Cd #1-SPARC cell line transplant 2 tumor; showing moderate to strong staining in 60% of the tumor. The Cd #1-SPARC Urosphere tumors did not show the same increase in stromal SPARC expression as the other three groups. There was an increase in stromal SPARC expression from the initial tumor (low to moderate staining in 5% of tumor) to the transplant 1 tumor (moderate to strong staining in 30% of tumor). However, this increase was not maintained to the final transplant 2 tumor, which showed staining intensity less than that of the initial tumor in only approximately 5% of the tumor. Interestingly, the human high grade invasive bladder carcinoma tumor also showed strong stromal SPARC expression in 80% of the tumor. Additionally, all tumor samples showed strong α -smooth muscle actin (α -SMA) staining in the supporting stroma (data not shown) indicating the presence of cancer-associated fibroblasts (CAFs).

Results also showed that SPARC expression did not increase nor was it maintained in the tumor cells from the initial tumor to the final transplant 2 tumor. Figure IV-4 illustrates immunohistochemistry images of the three tumor samples showing SPARC expression within the tumor cells. Cd #1 cell line tumors as well as Cd #1-

SPARC Urosphere tumors did not show any SPARC expression in the tumor cells of any of the three tumors. Interestingly, the Cd #1 Urosphere transplant 2 tumor showed moderate to strong SPARC staining in approximately 40% of the cancer cells comprising the tumor. However, neither the initial tumor nor the transplant 1 tumor displayed any SPARC expression within the tumor cells. Additionally, the Cd #1-SPARC cell line initial and transplant 2 tumors showed low to moderate SPARC staining in approximately 10% of the cancer cells comprising the tumor. However, it appeared the overall intensity of the tumor cell staining decreased from the initial tumor to the transplant 2 tumor; and, the transplant 1 tumor did not show any SPARC staining in the tumor cells. Therefore, again, it does not appear that SPARC is maintained within the tumor cells.

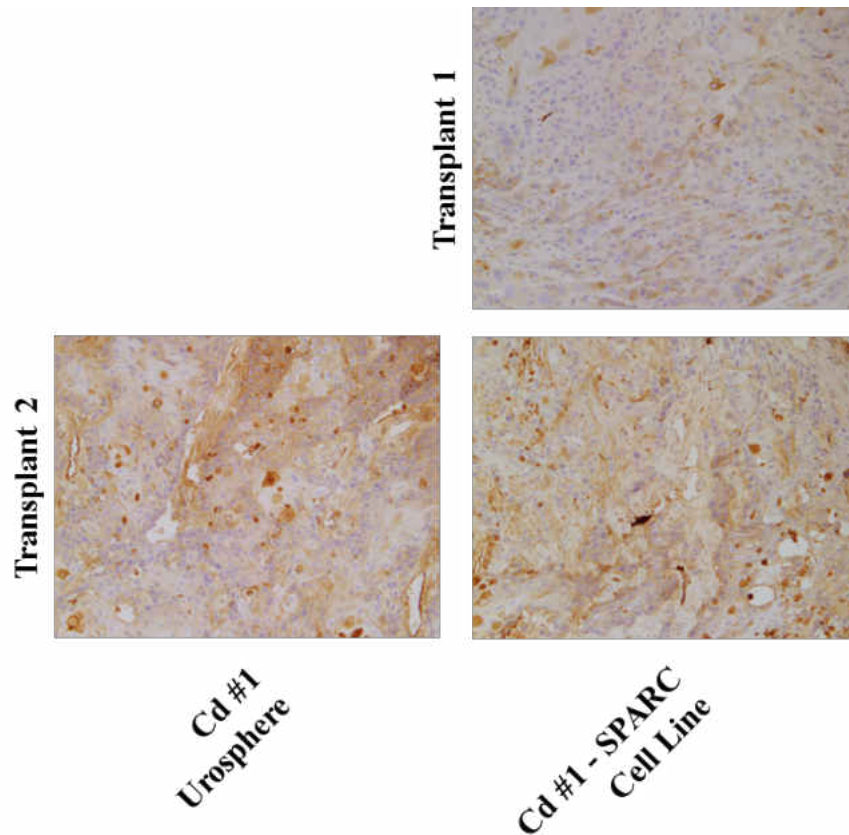


Figure IV-4. Immunohistochemistry Images of SPARC Expression within Tumor cells of Serial Bladder Heterotransplant Tumors. Images of three serial heterotransplant tumors: Cd #1 Urosphere transplant 2 tumor, in addition to Cd #1-SPARC cell line transplant 1 and transplant 2 tumors, expressing SPARC in the tumor

cells. Human high grade invasive bladder carcinoma used as a control (shown in Figure IV-3). All images taken at 200x.

Overall, these results suggest that SPARC expression is not maintained nor increased in serial heterotransplant tumor cells. However, results do indicate an increase in stromal SPARC expression in serially transplanted bladder tumors.

Immunohistochemistry observation suggests an increase in disorganization of tumor tissue, potentially indicating tumor progression; however, this was not substantiated in the pathology results. Additionally, staining intensity, as well as distribution of staining in the serial heterotransplants, was most similar between 3 of 4 final transplant 2 tumors and the human high grade invasive bladder carcinoma. Therefore, further studies are needed to address the increase in stromal SPARC expression and its impact on tumor progression.

Human SPARC and Mouse SPARC mRNA Expression in Serial Heterotransplants

The stromal SPARC expression observed in the immunohistochemistry experiment prompted further investigation into the origin of the SPARC being expressed. SPARC is a secreted extracellular matrix protein that acts in the extracellular space. Therefore, it was necessary to determine if the tumor cells were making human SPARC and secreting it into the surrounding support tissue; or, if the supporting mouse stromal tissue was expressing host SPARC. Results indicate high expression of mouse SPARC with no human SPARC detected in the majority of the tumor samples. Figure IV-5 (A) illustrates at least a 10-fold reduction in human SPARC expression across all serial heterotransplant samples compared to the UROtsa parent cell line control. Interestingly, only the initial, transplant 1, and transplant 2 Cd #1-SPARC cell line tumors and the initial Cd #1-

SPARC Urosphere tumor showed any human SPARC mRNA expression; however, expression was not significantly different compared to the mouse brain negative control.

In contrast, Figure IV-5 (B) shows a substantial increase in mouse SPARC expression in all of the serial heterotransplant samples compared to the mouse brain positive control. Additionally, as expected, the human UROtsa cell line did not express any mouse SPARC. All samples showed at least a 1.5-fold increase in mouse SPARC expression, with the transplant 1 Cd #1-SPARC cell line tumor showing a 5-fold increase in expression. The initial and transplant 2 Cd #1-SPARC Urosphere tumors showed the lowest mRNA expression of mouse SPARC and also showed two of the lowest intensities of stromal staining in the immunohistochemistry results. Additionally, the apparent increase in stromal SPARC staining from the initial tumor to transplant 2 tumor, observed via immunohistochemistry, was not as evident with mouse SPARC mRNA expression analysis. This may be due to the overall high mouse SPARC mRNA expression compared to the mouse brain positive control, making changes in already high expression not obvious. Although there were slight discrepancies between mRNA expression and protein expression, identified via immunohistochemistry, overall, the stromal SPARC expression observed in the serial heterotransplant tumors was clearly identified to be of mouse and not human origin. These results suggest a complex interplay between tumor and stroma.

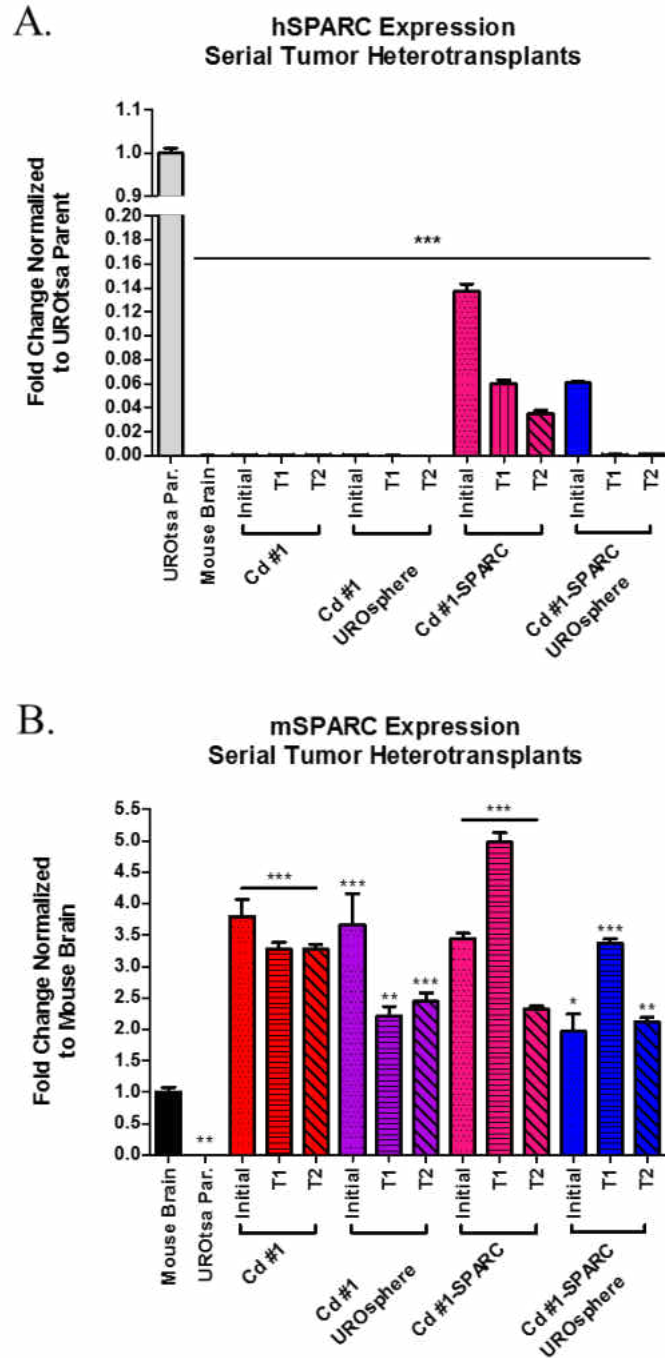


Figure IV-5. Human and Mouse SPARC mRNA Expression in Serial Bladder Heterotransplant Tumors. (A) Human and (B) mouse SPARC mRNA expression in serial heterotransplant tumor samples. For human SPARC expression, UROtsa parent cell line used as a positive control and mouse brain used as a negative control. For mouse SPARC expression, mouse brain used as a positive control and UROtsa parent cell line used as a negative control. Statistical analysis determined using one-way ANOVA with Dunnett's Multiple Comparison *post hoc* test, represented as mean \pm SEM. *($p \leq 0.05$), **($p \leq 0.01$), and ***($p \leq 0.001$).

SPARC mRNA Expression in Cd #1-SPARC Cell Line Following Recombinant SPARC Treatment

Experiments to further investigate how exogenous SPARC expression affects endogenous SPARC expression led to exposing the Cd #1-SPARC cell line, which was utilized to generate heterotransplant tumors, to varying amounts of exogenous, recombinant human SPARC or mouse SPARC. Preliminary experiments determined effective amounts of exogenous SPARC that resulted in a decrease in endogenous SPARC expression (data not shown). A subsequent time course study determined the greatest effect at 36h post exposure (data not shown). Therefore, Cd #1-SPARC cells were exposed to 0.002 μ g – 2.0 μ g rhSPARC in 10-fold increments and 0.002 μ g – 20.0 μ g rmSPARC in 10-fold increments. The extra dose of rmSPARC was to account for crossing species from mouse to human. Results in Figure IV-6 (A) illustrate a significant decrease in endogenous SPARC expression with 0.2 μ g rhSPARC. Interestingly, there was a significant increase in endogenous SPARC expression with 0.002 μ g rhSPARC. Overall, there appears to be a significant decrease in expression with an attempt to return to baseline expression levels. This is similar to an inverted cytokine-like curve showing maximal activation followed by a return to baseline when receptors become saturated.

Exposure of Cd #1-SPARC cells to 0.02 μ g, and 2.0 μ g recombinant mouse SPARC also resulted in a significant decrease in endogenous SPARC expression, as seen in Figure IV-6 (B). Interestingly, this source of exogenous source did not show a significant increase in SPARC expression with the lowest dose, but rather, endogenous SPARC expression showed a slight, non-significant, decrease. Additionally, endogenous expression returned to baseline with 0.2 μ g rmSPARC and even showed a slight, non-significant, increase above baseline at the highest exposure of 20.0 μ g. This also shows a

general bell-shaped curve, like that observed with receptor activation. Overall, it appears that exogenous sources of SPARC can contribute to endogenous repression of SPARC.

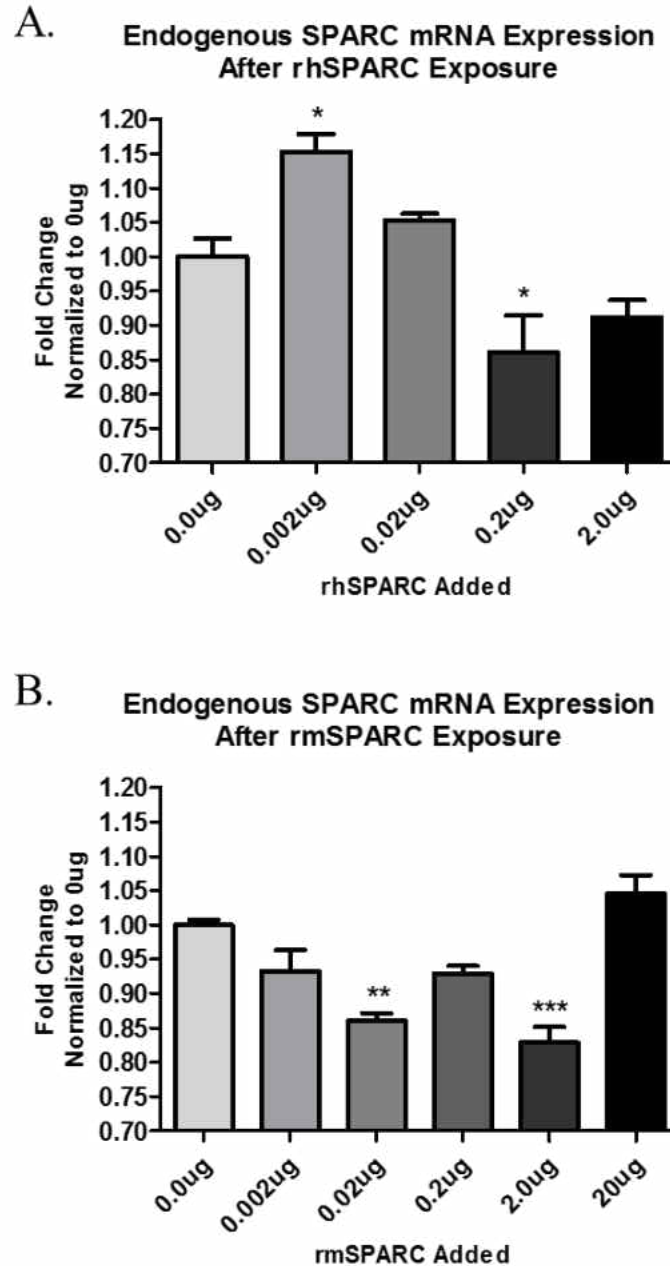


Figure IV-6. SPARC mRNA Expression in Cd #1-SPARC Cells Exposed to Recombinant hSPARC or Recombinant mSPARC. Human endogenous SPARC mRNA expression in Cd #1-SPARC cells after 36h exposure to (A) rhSPARC and (B) rmSPARC. Expression normalized to untreated 0.0µg control. Statistical analysis determined using one-way ANOVA with Dunnett’s Multiple Comparison *post hoc* test, represented as mean ±SEM. *(p≤0.05), **(p≤0.01), and ***(p≤0.001).

Discussion

SPARC expression has been studied in various cancer types; showing tissue-specific expression and function. Complicating these results, some tumor cells do not express SPARC; but, the supporting stromal cells express high levels of SPARC. Most often, in these instances, high stromal SPARC expression has been associated with a poorer patient outcome (Vaz et al., 2015). Additionally, increasing SPARC expression within tumor cells of some cancers has been associated with a more advanced stage (Vaz et al., 2015). Some mechanistic studies have elucidated proposed pathways involved in the roles of SPARC in various cancer types; however, the majority of studies are focused on SPARC expression and subsequent functional consequences of alterations in expression. SPARC expression in some cancers is better characterized than others. Overall, SPARC expression and function in bladder cancer remains to be fully characterized. This study aimed to determine SPARC expression in bladder urothelial serial heterotransplant tumors.

Previous results showed significant down regulation of SPARC in malignantly transformed cell lines and heterotransplant tumors (Larson et al., 2010, Slusser et al., 2016). It was found that heterotransplant tumors downregulated SPARC expression; even after stable SPARC transfection in cadmium-transformed cell lines used to generate the tumors (Slusser et al., 2016). This was an interesting finding because the SPARC open reading frame was transfected into the cells under the control of a strong cytomegalovirus (CMV) promoter. Therefore, this observed significant downregulation of SPARC expression supports the hypothesis that SPARC is a tumor suppressor-like molecule in bladder urothelial carcinoma. Interestingly, the human high grade invasive carcinoma

tumor sample also showed repression of SPARC within the tumor cells; further supporting a tumor suppressor role for SPARC within tumor cells. Serial transplantation of tumor cells was used in this study to determine if SPARC expression could increase with successive tumor inoculations; or, if tumor initiation potential decreased with increasing SPARC expression within tumor cells. Immunohistochemical analysis revealed no increase nor maintenance of tumor cell SPARC expression, but an increase in stromal SPARC expression in three of the four groups. Additionally, the final serial tumor showed stromal SPARC staining similar to that of the human high grade invasive carcinoma.

Importantly, the SPARC antibody used for this study was the same antibody used in previous SPARC studies performed in this lab, as described in Larson et al. (2010) and Slusser et al. (2016). It is a human-specific antibody; however, it appears to be staining the mouse fibroblast cells in the supporting stroma. There is a large degree of SPARC sequence and structure homology that has been conserved as species have evolved (Brekken and Sage, 2001). Therefore, it is likely that the SPARC antibody is recognizing both human and mouse SPARC. Antibody specificity as well as experimental methodology can be a complicating factor in studies and result in muddling the literature. Tai and Tang (2008) addressed differences in antibody usage resulting in slight discrepancies regarding ovarian cancer cell SPARC expression in the literature. This same argument can be made for SPARC expression in other cancer types as well, reinforcing the use of good, consistent antibodies.

It was determined in this study that the stromal SPARC observed in the tumor samples was of mouse and not human origin. It is imperative to decipher between tumor

cell- and stromal cell-derived SPARC in order to accurately determine expression as well as a functional role for SPARC in cancer. As discussed earlier, SPARC has tissue specific expression and function (Brekken and Sage, 2001). Therefore, stromal SPARC could be supporting tumor growth and progression while tumor cell SPARC expression has an inhibitory role. Overall, SPARC expression levels are downregulated in bladder cancer cells (Said and Theodorescu, 2013). However, one study proposed an increase in SPARC expression within the tumor cells, coinciding with an increase in MMP-2 expression (Yamanaka et al., 2001). Importantly, tumors in this study were not devoid of stroma and it was not discussed if the SPARC observed was derived from tumor or stroma (Yamanaka et al., 2001). Therefore, it is possible that the increase in SPARC expression is, in fact, an increase in stromal, rather than tumor cell, SPARC expression associated with increasing bladder tumor grade and aggressiveness.

Interestingly, mechanisms of action for SPARC have been proposed for these cancer types; however, the majority of the proposed mechanisms described are attributed to functional consequences of changes in SPARC expression within the tumor cells and not the stromal cells (Tai and Tang, 2008). Two important roles that have been proposed for stromal SPARC are its involvement in matrix modulation as well as dysregulation of growth factor functions; both of which can have severely detrimental downstream cellular effects (Brekken and Bradshaw, 2010). While the tumor cells themselves may show variable expression of SPARC, the supporting stroma appears to be highly positive for SPARC expression in pancreatic, ovarian, and bladder cancers (Vaz et al., 2015, Brown et al., 1999, Larson, et al., 2010). The results from this study are similar. It is possible the variable tumor cell SPARC expression observed is random and hence not

consistent. It is also possible that stromal-derived SPARC is being internalized by a subset of tumor cells and eliciting its effects inside the cell. However, Chlenski et al. (2011) determined that internalized SPARC is quickly shuttled back into the extracellular matrix. This provides further evidence of a potential role for SPARC in matrix modulation and growth factor regulation, ultimately leading to tumor progression.

Additionally, SPARC has been shown to have limited intracellular roles; however, some include: inducing cell cycle arrest via cyclin and inhibitor molecule dysregulation, promoting apoptosis via direct interaction with pro-caspase 8, and potentially involvement in matrix modulation via intracellular chaperoning of molecules important for collagen fibrillogenesis (Mao et al., 2014, Tang and Tai, 2007, Emerson et al., 2006, Brekken and Bradshaw, 2010). It is plausible that stromal SPARC is being internalized by the bladder tumor cells, as the RT-PCR results did not reveal any substantial increase in human SPARC expression.

The increase in stromal SPARC expression observed in 3 of the 4 groups, along with exogenous recombinant SPARC treatment in SPARC-expressing malignant cells, indicates a potential tumor-promoting role for stromal SPARC. An important role for SPARC is in matrix modulation (Brekken and Bradshaw, 2010). Furthermore, SPARC has been shown to be involved in a positive feedback loop with matrix metalloproteinases, specifically, MMP-2 and MMP-9 (Arnold et al., 2008). Activation of MMP-2 by SPARC has been observed in breast cancer cell lines (Gilles et al., 1998). In turn, MMP-2 has been shown to proteolytically cleave SPARC increasing its collagen-binding affinity (Sasaki et al., 1998). This becomes important for SPARC's ability to modulate the matrix environment. It is possible that the observed increase in stromal

SPARC expression in the serial bladder heterotransplant tumors is increasing MMP-2 activation, as well as other matrix metalloproteinases, thereby increasing SPARC's ability to promote tumor progression and invasion. MMP-2 cleavage of SPARC could result in matrix composition changes as well as a decrease in matrix strength promoting invasion and migration. Although there were no characteristic features identified by the pathologist, from the initial tumor to the final transplant 2 tumor, that indicated disease progression; it is possible increases in stromal SPARC expression may indicate early signs of bladder urothelial carcinoma progression. Alternatively, increased stromal SPARC expression could contribute to changes in the microenvironment increasing susceptibility to tumor recurrence.

Stromal SPARC could also be regulating growth factor interaction with the bladder cancer cells. SPARC has been described to interact both directly and indirectly with several growth factors including: VEGF, PDGF, FGF, and TGF- β (Brekken and Sage, 2001). These growth factors are necessary for normal cell function, making them ideal targets for dysregulation contributing to tumor initiation and/or progression. Importantly, SPARC has been shown to inhibit PDGF, VEGF, basic (b)FGF, and TGF- β -stimulated proliferation in various cells (Motamed et al., 2002, Kupprion et al., 1998, Sage et al., 1995, Schiemann et al., 2003). Additionally, SPARC was shown to reduce the migration of bovine aortic endothelial cells via bFGF (Hasselaar and Sage, 1992). In this study, it is possible that tumor cell SPARC is, in fact, contributing to the inhibition of cell proliferation via growth factor regulation; therefore, requiring SPARC repression. Alternatively, stromal SPARC may be contributing to tumor initiation and progression via its feedback mechanism involving TGF- β .

Studies show that increased SPARC expression results in increased TGF- β expression in mesangial cells and vice versa in dental pulp cells and keratinocytes (Francki et al., 1999, 2004, Shiba et al., 1998, Ford et al., 1993). Interestingly, TGF- β has been shown to be important for pancreatic ductal adenocarcinoma (PDAC) as well as invasive mammary adenocarcinoma progression (Ungefroren et al., 2011). Like SPARC, TGF- β plays multiple roles in various cancers (Drabsch and Dijke, 2011, Truty and Urrutia, 2007). While all roles are important, here, more relevant roles may include TGF- β induction of epithelial to mesenchymal transition (EMT) as well as immune evasion. Although the bladder tumor cells significantly repress SPARC expression, it is plausible that the CAFs in the surrounding stroma show up-regulated TGF- β concomitant with the observed increase in stromal SPARC expression, based on various studies suggesting a positive feedback loop (Brekken and Sage, 2001). In the stroma, enhanced TGF- β expression, via increased SPARC expression, could continue to stimulate fibroblast conversion to CAFs as well as promote EMT at the leading edge of the tumor (Ungefroren et al., 2011, Drabsch and Dijke, 2011). Additionally, once a cancer has been established, TGF- β can promote tumor progression via immune evasion (Flavell et al., 2010). TGF- β functions as an immunosuppressive molecule in the microenvironment by reducing the activity of anti-tumor immune cells such as: natural killer (NK) cells, dendritic cells, macrophages, and neutrophils; as well as, recruiting pro-tumorigenic immune cells such as: regulatory T cells, alternatively activated M2 macrophages, immature dendritic cells, and tumor associated macrophages (TAMS), among others (Flavell et al., 2010). This, in conjunction with the physical barrier created from matrix modulation by CAFs in the stroma, indicate a potential indirect role for stromal SPARC,

via TGF- β upregulation, in contributing to immune evasion and successful tumor initiation and progression (Ziani et al., 2018).

It is possible that, in humans, SPARC expression in the stroma surrounding the bladder urothelial carcinoma tumor is contributing to the SPARC repression observed within the tumor cells, and, up-regulating TGF- β to promote: tumor cell EMT, CAF conversion, as well as immune evasion. This change in the microenvironment could ultimately lead to tumor progression and/or increased risk of recurrence, which is a significant problem in bladder urothelial carcinoma. Unfortunately, upregulation of SPARC in the supporting stroma has been associated with poor patient outcome in a variety of cancers (Vaz et al., 2015). Overall, results from this study indicate SPARC repression, within the bladder tumor cells. Whether the decrease in SPARC expression is needed for initial tumor cell survival and growth is unknown; however, it is clear that expression of endogenous SPARC is not needed and/or required for continued tumor cell growth and survival. Therefore, with more research, SPARC could be a target of diagnostic and/or prognostic value for bladder urothelial carcinoma.

CHAPTER V

DISCUSSION

This study aimed to determine a role for SPARC in an *in vitro* model of heavy metal cadmium-induced bladder urothelial carcinoma. Bladder cancer has a strong link to environmental toxicant exposure (Inamura, 2018), making our *in vitro* system a relevant model to study bladder urothelial carcinoma. Previous long-term, low-dose exposure to cadmium, led to UROtsa bladder cell transformation, and ultimately, seven independent malignant cell populations (Sens et al., 2004, Somji et al., 2010). This transformation resulted in a number of genes showing differential expression compared to the untransformed UROtsa parent cell line (Garrett et al., 2014). SPARC showed a strikingly significant repression in all seven independent cadmium malignantly transformed cell lines (Larson et al., 2010, Garrett et al., 2014). Heterotransplant tumors generated from these cell lines along with archived human bladder cancer tumors showed significant repression of SPARC within tumor cells (Larson et al., 2010). Heterotransplant tumors generated from Cd²⁺-transformed cells stably transfected with SPARC, still lacked any detectable SPARC expression (Slusser et al., 2016). Furthermore, tumors generated from the proposed tumor initiating cell subpopulation, Urospheres, showed 5-20% focal SPARC expression, which was an increase from the previous tumors; however, still an overall decrease in tumor cell SPARC expression (Slusser et al., 2016). This consistent repression in: malignant cell lines, heterotransplant tumors, and archived human bladder cancer tumors, in conjunction with, literature suggesting SPARC repression in bladder

cancer, motivated further research into SPARC expression and function in our model system. This study focused on three central hypotheses: 1) SPARC plays a critical role in urothelial cell proliferation, migration, attachment, and spreading; 2) Cadmium transformation significantly decreases SPARC expression by silencing the promoter early in the malignant transformation process; and 3) that in urothelial tumors generated from Cd²⁺-transformed cell lines, SPARC is prohibitive to tumor initiation.

Previous studies investigated SPARC's role in proliferation, migration, and invasion of malignantly transformed UROtsa cells (Larson et al., 2010, Slusser et al., 2016). Results showed no clear cell biological explanation for SPARC's absence in bladder tumors (Larson et al., 2010, Slusser et al., 2016). Chapter II details investigation into SPARC's role in several cell biological processes, focusing mainly on cell attachment and spreading. These are both necessary for cell survival and SPARC has been implicated to play a role in them (Chen et al., 1997, Bradshaw and Sage, 2001). Some studies measure either attachment or spreading (Lee et al., 2017). Several studies do measure both attachment and spreading, but the experimental time points extend several hours (Sage et al., 1989, Everitt and Sage, 1992, Motamed and Sage, 1998, Hudson et al., 2005, Delostrinos et al., 2006, Zhang et al., 2011). Additionally, all of the referenced studies added exogenous SPARC to the cell cultures. Our study was unique from the aforementioned studies by assessing both attachment and spreading on collagen I, in the presence or absence of only cell-derived SPARC, with a single assay during the active initial attachment phase. Furthermore, when heterotransplant injections are made subdermally, as detailed in chapter IV, the matrix molecule encountered at the highest concentration is collagen I. The SPARC binding site on collagen I has been shown to

overlap with the cell surface discoidin domain receptor (DDR) and integrin receptor binding sites (Giudici et al., 2008); therefore, it is possible that SPARC is competing for collagen binding and ultimately interfering with cell attachment. Here, results did not show a significant decrease in cell attachment, as was expected. Preliminary results did show a decrease in cell attachment to a collagen I matrix; however, subsequent experimental troubleshooting required a decrease in the number of cells plated in order to accurately and efficiently count and classify cells. Therefore, it is possible that by reducing the cell number, the concentration of secreted SPARC was also decreased far enough to abrogate its effect on cell attachment. The lack of sufficient SPARC in the surrounding media may have resulted in a number of integrin receptor binding sites left available on the collagen I fibers, leading to adequate cell attachment. It is also possible that the initial cell attachment stimulates SPARC secretion into the matrix; therefore, not affecting cell attachment but rather affecting cell spreading.

Experimental results did show a significant increase in cell spreading in the presence of SPARC during the active cell attachment phase. SPARC has been described in several systems as a de-adhesive protein, inducing cell rounding by abrogating focal adhesions (Bradshaw and Sage, 2001). However, these experiments were performed on confluent monolayers and newly attached cells in alternative systems with exogenous SPARC added to cultures (Bradshaw and Sage, 2001). One study found increased cell spreading of SPARC-transfected murine F9 embryonal carcinoma stem cells when cultured in a Ca^{2+} -deficient environment (Everitt and Sage, 1992). Our system does show increased cell spreading in SPARC expressing cells; but, there is sufficient calcium

present in the medium. Therefore, this is likely not contributing to the results found in this study.

Limited studies have assessed urothelial cell spreading in regards to SPARC expression. However, two studies found that exogenous SPARC inhibited spreading of urothelial cells (Hudson et al., 2005, Delostrinos et al., 2006, Zhang et al., 2011). Unique to our study, cell spreading was analyzed every 15 minutes, up to 1 hour on collagen I; and, only endogenous, urothelial cell-derived SPARC was present in cultures.

Experimental results showed a contradictory role for endogenous SPARC in promoting cell spreading of a newly attached cell; that, with siRNA knockdown of SPARC expression was abrogated. Integrin $\alpha_2\beta_1$ was found to bind to collagen I fibrils and promote cell spreading as well as formation of extended cellular projections of $\alpha_2\beta_1$ - transfected Chinese hamster ovary cells and $\alpha_2\beta_1$ - transfected human osteosarcoma Saos-2 cells (Jokinen et al., 2004). Therefore, SPARC may be preferentially competing with alternative integrin and discoidin domain receptors for binding to collagen I, leaving available $\alpha_2\beta_1$ integrin binding sites. Furthermore, without the addition of exogenous SPARC in the extracellular environment, there may be inadequate competition for binding with the integrin-binding sites on collagen I fibrils; ultimately leading to proper cell attachment and quicker subsequent spreading.

Also unique to this study was the analysis methodology utilized for attachment and spreading assay quantitation. Several methods have been used to analyze cell attachment and spreading, including simple observation quantified using a rounding index (RI) by Lane and Sage, 1990. Initial experiments in this study utilized observation and a similar classification method. However, the experimental set up made this method

extremely time consuming as well as harbored a level of human bias in classification of cells. Therefore, implementation of software analysis was necessary to make attachment and spreading analysis more efficient and to reduce the human bias associated with observational classification.

Several studies have worked to implement software analysis into experimental methods for counting cells as well as analyzing cell morphology (Costa and Yang, 2009, Dehlinger et al., 2013, Ambühl et al., 2012, Carpenter et al., 2006, Garvey et al., 2016). However, expense and user friendliness were challenges associated with these programs. This study implemented the freely available Fiji software for the initial pre-processing of attachment and spreading images, which reduced the halo effect using the PHANTAST plugin (Jaccard et al., 2014a), and created more contrast between the cells and the background. Many of the software analysis programs also had trainable classification systems that categorized cells based on morphology (Jaccard et al., 2014b, Jaccard et al., 2015, Theriault et al., 2012). But, again, user friendliness was an issue. Intriguingly, Leica Microsystems, Inc. had a software package, LASX, with analysis capabilities and the advantage of being user friendly. However, this software was made for fluorescent images rather than gray-scale phase contrast images. The pre-processing performed in Fiji allowed the two programs to be used in conjunction resulting in successful attachment and spreading analysis. The software classification reduced the impact of human bias by using the same trained classifier for every image as well as provided a level of consistency throughout the analysis. To the author's knowledge, this is the first study utilizing Leica LASX software for analysis of non-fluorescent images that have been pre-processed using Fiji.

Overall, it appears that SPARC plays a role in promoting spreading of newly attached urothelial and SPARC-transfected urothelial carcinoma cells. This is a potential role that is necessary to shut down in order to promote tumor initiation and progression. The Cd²⁺-transformed urothelial carcinoma cells lack any detectable SPARC expression (Larson et al., 2010) and the Cd #1 cell line showed delayed cell spreading. Interestingly, all cell lines, SPARC expressing and non-SPARC expressing, show no significant morphological differences at confluency; with all lines showing an epithelial cell morphology (Rossi et al., 2001, Somji et al., 2010, Slusser et al., 2016). Therefore, it is possible the non-SPARC expressing cells are using an alternative molecule or molecules, such as SPARC family members, to aid in cell spreading; however, this process may not be as efficient as in the presence of SPARC. Additionally, the alternative molecules may not have as many diverse roles and therefore, may not be as prohibitive to bladder urothelial tumor initiation and progression.

The significant repression found after cadmium transformation of UROtsa cells, warranted investigation into the mechanism behind the downregulation of SPARC. Previous studies in the lab examined the methylation status of the SPARC promoter as it had been described to be hypermethylated in several cancer types (Larson et al., 2010, Brekken and Bradshaw, 2010). However, results indicated no significant differences in the DNA methylation status of the SPARC promoter between the UROtsa parent cells and the Cd²⁺-transformed cells (Larson et al., 2010). Additionally, previous analysis of several miRNAs did not reveal any significant difference in miRNA expression in the transformed cell lines that may be contributing to SPARC repression (unpublished data). This motivated investigation into an alternative mechanism for regulation of the SPARC

promoter, as detailed in Chapter III, with the hypothesis that cadmium transformation significantly decreases SPARC expression by silencing the promoter early in the malignant transformation process. The decrease in SPARC expression within UROtsa parent cells can be observed within the first 24 hours following cadmium exposure and continues through the process of cell transformation (Larson et al., 2010). These results indicated a role for cadmium in SPARC repression early in the malignant transformation process. However, cadmium does not directly bind to DNA, likely making its involvement in SPARC downregulation indirect.

Cadmium has been shown to replace zinc in zinc-finger transcription factors, rendering them inactive (Bertin and Averbeck, 2006). Kothinti et al. (2010b) showed that human recombinant Sp1 exposed to Cd^{2+} lost its DNA binding affinity. Further experiments showed that Cd^{2+} replacement of zinc in Sp1 zinc-fingers resulted in structural changes with less favorable side chain - DNA base pair interactions; and, that there may be preferential targeting of Cd^{2+} to Zn^{2+} within unbound Sp1 (Kothinti et al., 2010b). Preliminary results performed in our lab indicated potential alterations in transcription factor expression in the Cd^{2+} -transformed cell lines. Additionally, Sp1 and Sp3 zinc-finger transcription factors have been implicated in binding to the SPARC promoter activating gene transcription (Chamboredon et al., 2003, Vial et al., 2000, Xu et al., 2010). Alternatively, SOX5 transcription factor has been implicated in binding to the SPARC promoter inhibiting gene transcription (Huang et al., 2008). Therefore, this study focused on alteration of transcription factor binding to the SPARC promoter, induced by cadmium malignant transformation.

Results from chromatin immunoprecipitation (ChIP) experiments showed Sp1 and Sp3 binding to the SPARC promoter in the UROtsa parent cells; however, there did not appear to be any binding of these transcription factors to the SPARC promoter in the Cd #1 cells. Furthermore, there appeared to be enhanced binding of the SOX5 transcription factor to the SPARC promoter in the Cd #1 cells compared to the UROtsa parent cells. Preliminary experiments showed downregulation of Sp1 and Sp3 following exposure to cadmium (unpublished data). However, mRNA and protein expression analysis in this study indicated no significant difference in transcription factor expression between non-transformed UROtsa parent cells and transformed Cd #1 cells. Transcription factor expression is tightly regulated to prevent aberrant gene transcription and abnormal cell behavior. Therefore, it is possible that cadmium is initially replacing zinc in the Sp1 and Sp3 transcription factors, inactivating them and promoting their degradation. These transcription factors have thousands of gene targets and knocking out both of them is lethal. Therefore, following transformation, and removal of cadmium, it is likely the cells continue to express functional Sp1 and Sp3 transcription factors. However, they may be preferentially binding to higher affinity targets. SPARC does not contain a typical TATA box and therefore requires co-factors for proper gene transcription (Vizcaíno et al., 2015). However, there is a GGA-rich motif that is known to be a binding site for Sp1 and Sp3 transcription factors (Vial et al., 2000); therefore, SPARC could be a lower order gene target for these ubiquitous transcription factors, resulting in its repression.

Alternatively, cadmium is known to indirectly induce oxidative stress and subsequent DNA damage (Rani et al., 2014, Bertin and Averbeck, 2006). SPARC promoter may be a target of DNA damage thus resulting in its repression. This could

become permanent if the repression is advantageous to the cell's survival. For example, repression of a secreted protein may result in beneficial energy saving for a malignant cell requiring extra energy and nutrients for survival. Additionally, as stated earlier, SPARC repression inside tumor cells may be advantageous by decreasing SPARC's pro-apoptotic activity as well as its regulation of cell cycle progression (Tang and Tai, 2007, Said, 2016). In the case of the serial heterotransplant study, SPARC, with potential tumor promoting activities, is abundantly found in the supporting stroma which could further contribute to its permanent repression within tumor cells.

The link between cadmium and the SOX5 transcription factor is not as obvious as that with Sp1 and Sp3, in part because it is not a zinc-finger transcription factor. Reports in the literature have shown that Sp1 recruits chromatin remodeling complexes to the promoter region for gene transcription (Li and Davie, 2010). One study found Sp1 co-localized with Brg-1 ATPase to the SPARC promoter region activating gene transcription (Xu et al., 2010). Without Brg-1 ATPase and chromatin remodeling complex recruitment to the promoter, SPARC gene transcription was repressed (Xu et al., 2010). Therefore, if cadmium is initially replacing zinc in the Sp1 and/or Sp3 transcription factors, they cannot bind the DNA. Subsequently, the chromatin remodeling complexes will not be associated with the promoter region resulting in gene repression due to inaccessible chromatin. Additionally, chromatin accessibility changes, resulting from cadmium exposure, may result in preferential availability of SOX5 binding sites on the SPARC promoter, further contributing to gene repression. The initial SPARC repression in UROtsa parent cells, following cadmium exposure (Larson et al., 2010), may be

advantageous; therefore, requiring subsequent mechanisms to aid in the permanent SPARC repression observed in the Cd²⁺-transformed cells.

Following ChIP experiments, further experimentation assessed SPARC expression after siRNA knockdown of Sp1, Sp3, or SOX5 transcription factors. Sp3 transcription factor showed the most consistent knockdown in both the UROtsa parent cells and Cd #1 cells without knockdown in the control samples. Additionally, knockdown of Sp3 resulted in a significant reduction of SPARC expression in the UROtsa parent cells. Alternatively, SOX5 knockdown resulted in a significant increase in SPARC expression in Cd #1 cells. There did appear to be variability in control samples that could be the result of stress from transfection. These results indicate potential necessary transcription factors for activation of SPARC expression in the UROtsa parent cells as well as inhibition of SPARC expression in Cd #1 cells.

This study addressing cadmium regulation of the endogenous SPARC promoter is somewhat separate from the other two studies described here. Our *in vitro* system presented an ideal model to investigate the endogenous SPARC promoter in UROtsa parent cells that express SPARC as well as in Cd #1 cells that significantly repress SPARC expression. The Cd #1-SPARC transfected cells do express SPARC; however, only the SPARC open reading frame was transfected into the cells under the control of the strong CMV promoter rather than the endogenous SPARC promoter (Slusser et al., 2016). This enables a more stable expression of a gene that is significantly repressed, otherwise. Therefore, the Cd #1-SPARC cell line could not be used for this study. Overall, it was determined that cadmium exposure may be altering transcription factor binding to the SPARC promoter; therefore, contributing to SPARC repression. It is clear

this repression is happening early in the malignant transformation process; however, the exact mechanism remains to be determined. It is likely the significant repression is the result of a combination of mechanisms working together; as evidenced by human urothelial carcinoma tumors also showing significant repression of SPARC. Further research may provide insight into the direct or indirect role cadmium is playing to contribute to the permanent repression of SPARC in our model system of cadmium induced bladder urothelial carcinoma.

Chapter IV outlines, in detail, the examination into SPARC's expression and function in bladder urothelial tumor initiation and progression. Previous results from Larson et al. (2010) and Slusser et al. (2016) led to the hypothesis that in urothelial tumors generated from Cd²⁺-transformed cell lines, SPARC is prohibitive to tumor initiation. The goal for this study was to determine if serially transplanted heterotransplant tumors showed an increase in SPARC expression; and, additionally, if tumor initiation potential decreased with increased tumor cell SPARC expression. Results from the serial heterotransplant study showed an overall repression of human SPARC expression within the tumor cells; but, increased mouse SPARC expression in the supporting stromal tissue. The expression of SPARC in the stroma of the heterotransplant tumors was similar to that observed in Larson et al. (2010). The literature presents conflicting results regarding SPARC in cancer. It has been shown to be overexpressed in some cancers, including melanomas and gliomas; but, repressed in others, such as ovarian, pancreatic, and prostate cancers (Nagarju et al., 2014). This is further complicated by the intricate dynamics between tumor and host. Increased SPARC expression within supporting stromal cells has been reported to be associated with poor

patient prognosis in several cancers (Vaz et al., 2015). Many studies examine tumor SPARC expression or stromal SPARC expression; however, few distinguish between the two sources, or address both sources of SPARC. It is necessary to consider tumor and stromal SPARC to better understand the impact one source versus the other has on tumorigenesis and progression. This is especially important because of SPARC's well described tissue-specific expression and proposed function.

Although there were no characteristic signs of progression observed in this experiment, the serial heterotransplant experimental results do suggest an inherent need for SPARC to be repressed within tumor cells for tumor initiation and possibly progression. The tumor microenvironment has been shown to provide a physical barrier between the tumor and the immune system, promoting immune evasion (Ziani et al., 2018). Therefore, the increased SPARC expression in the surrounding stroma may serve to help disguise the tumor with an environment showing SPARC expression similar to that of normal tissue promoting immune evasion. Subsequently, the increased SPARC in the stroma could be altering the microenvironment in such a way as to promote tumor recurrence by matrix modulation and prolonged indirect immune suppression via TGF- β regulation. SPARC has been shown to interact with and regulate several extracellular matrix molecules (Yan and Sage, 1999), creating a complex web of direct and indirect interactions; all of which could contribute to tumor initiation and progression.

Additional experiments in this study showed that recombinant SPARC added to Cd #1-SPARC transfected cell cultures resulted in a decrease in endogenous SPARC expression. Interestingly, there was a trend toward a return to baseline expression observed in untreated cells, similar to an inverted cytokine response indicating decreased

activity due to receptor saturation. These results further show a potential paracrine role for SPARC that may contribute to tumor cell repression of SPARC. The concentration of recombinant SPARC used may not have been high enough; or, an additional mechanism may be necessary to achieve a stronger repression within tumor cells. It is possible that the high concentration of SPARC in surrounding stromal cells is enough to elicit a more significant repression, as was seen within the serial heterotransplant tumor cells. It is also plausible that the high stromal SPARC expression is sufficient for proper and/or enhanced tumor cell function, allowing the tumor cells to stop expending energy producing and secreting SPARC.

Reports in the literature suggest that addition of recombinant SPARC to cell cultures induces cell rounding and anti-spreading characteristics (Sage et al., 1989, Everitt and Sage, 1992, Hudson et al., 2005, Delostrinos et al., 2006). This provides a potential link between: the serial heterotransplant, recombinant SPARC, and the cell attachment and spreading experiments in this study. It is possible that the increase in stromal SPARC expression observed in the serial heterotransplant study is contributing, via paracrine action, to the downregulation of SPARC within the tumor cells and potentially leading to delayed cell spreading and promotion of tumor initiation and progression. Although there did not appear to be any rounding of the Cd #1-SPARC cells in response to recombinant SPARC exposure, the concentrations used in this study may not have been high enough. Hudson et al. (2005) found rounding of cells at rSPARC concentrations of 10 $\mu\text{g/mL}$ or higher. However, as stated earlier, there was a decrease in SPARC expression with recombinant SPARC exposure. Furthermore, siRNA knockdown of SPARC in Cd #1-SPARC cells resulted in delayed cell spreading and a larger portion

of the cell population displaying a rounded or early spreading phenotype. Together, these results suggest a potential necessary repression of endogenous SPARC prior to obtaining changes in morphology.

The Cd #1 cells that do not express SPARC, do not show any differences in morphology when compared to the UROtsa parent and Cd #1-SPARC transfected cells at confluency (Rossi et al., 2001, Somji et al., 2010, Slusser et al., 2016). It is plausible that alternative proteins and/or mechanisms are in place to aid in cell attachment and spreading; however, slightly delayed from that promoted by SPARC. In the case of the serial heterotransplant experiment, the extracellular environment has several components for cells to bind to when compared to the *in vitro* cell attachment and spreading study using only collagen I. Therefore, SPARC may also indirectly affect cell spreading through regulation of cell interaction with other extracellular matrix molecules. Overall, it appears that SPARC is necessary to be shut down within tumor cells for proper tumor initiation and progression.

Although the mechanism for its significant repression remains to be determined; the lack of SPARC expression in serially transplanted tumor cells indicates a strong tumor suppressor-like role for tumor cell-derived SPARC. Few intracellular roles have been proposed for SPARC; however, it is possible that SPARC acts intracellularly within bladder urothelial tumor cells to potentially inhibit cell cycle progression and promote apoptosis, as described in Said (2016) and Tang and Tai (2007). This could explain the low levels of SPARC protein observed in the cell lysate of Cd #1-SPARC cells, and the higher levels of secreted SPARC from the same cells. Stromal SPARC may exert a more oncogenic activity on the tumor cells via differential regulation of growth factors to

promote angiogenesis and immune system evasion as well as matrix modulation to promote invasion and metastasis.

With bladder cancer's strong link to environmental toxicant exposure, our *in vitro* system is a relevant model to study various characteristics of bladder cancer. A significant number of genes were differentially expressed following cadmium malignant transformation; however the one gene consistently repressed among the transformed cell lines was SPARC (Larson et al., 2010, Garrett et al., 2014). SPARC also shows significant repression among the majority of human bladder urothelial tumors (Larson et al., 2010, Said, 2016). However, conflicting results are present in the literature due to lack of differentiation between tumor cell-derived SPARC and stromal SPARC expression, as well as poor antibody quality for specifically recognizing human SPARC.

Although transgenic mice have been developed that lack SPARC expression and it does not appear to be a lethal mutation, the high level of sequence conservation throughout evolution points to an important role for this extracellular matrix protein (Brekken and Bradshaw, 2010). The differential expression of SPARC in various cancers also suggests important tissue-specific roles for SPARC that make it an ideal target to up- or downregulate for tumor initiation and progression. However, this variability in expression and function also make it a more difficult molecule to target in clinical applications; which, is the ultimate goal. Bladder cancer is the most expensive cancer to treat per patient lifetime (Kaffenberger et al., 2018, Jung et al., 2018), pointing to a desperate need for prognostic and/or diagnostic tools to reduce this burden and increase patient quality of life.

There is still more research to be done to better understand the role SPARC plays in bladder urothelial carcinoma; which, requires differentiation between tumor-derived SPARC and stromal SPARC, as well as an understanding of the complex interplay between tumor and host. Overall, results from this study determined a potential role for SPARC in cadmium-induced bladder urothelial carcinoma that may require suppression for proper tumor initiation. Additionally, the observed increase in stromal SPARC expression and overall decrease in tumor cell SPARC expression in serial heterotransplant tumors, indicates a substantial change in the microenvironment that may promote tumor progression as well as prime the microenvironment for subsequent tumor recurrence. SPARC is a molecule of considerable interest that with further insight into its specific mechanism of action, could be a target for future bladder urothelial carcinoma diagnosis or treatment.

REFERENCES

- Abdal Dayem, A., Choi, H. Y., Kim, J. H., & Cho, S. G. (2010). Role of oxidative stress in stem, cancer, and cancer stem cells. *Cancers*, *2*(2), 859-884.
- Agarwal, G., Kovac, L., Radziejewski, C., & Samuelsson, S. J. (2002). Binding of discoidin domain receptor 2 to collagen I: An atomic force microscopy investigation. *Biochemistry*, *41*(37), 11091-11098.
- Ahir, B. K., & Lakka, S. S. (2019). Elucidating the microRNA-203 specific biological processes in glioblastoma cells from comprehensive RNA-sequencing transcriptome profiling. *Cellular Signalling*, *53*, 22-38.
- Ajjimaporn, A., Botsford, T., Garrett, S. H., Sens, M. A., Zhou, X. D., Dunlevy, J. R., Somji, S. (2012). ZIP8 expression in human proximal tubule cells, human urothelial cells transformed by Cd⁺² and As⁺³ and in specimens of normal human urothelium and urothelial cancer. *Cancer Cell International*, *12*(16).
- Ambühl, M. E., Brepsant, C., Meister, J. J., Verkhovskiy, A. B., & Sbalzarini, I. F. (2012). High-resolution cell outline segmentation and tracking from phase-contrast microscopy images. *Journal of Microscopy*, *245*(2), 161-170.
- American Cancer Society. (2019). Cancer Facts & Figures 2019.
- American Cancer Society. (2016). Treating Bladder Cancer.
- Arnold, S. a., & Brekken, R. a. (2009). SPARC: a matricellular regulator of tumorigenesis. *Journal of Cell Communication and Signaling*, *3*(3-4), 255-273.
- Arnold, S., Mira, E., Muneer, S., Korpanty, G., Beck, A. W., Holloway, S. E., Brekken, R. A. (2008). Forced Expression of MMP9 Rescues the Loss of Angiogenesis and Abrogates Metastasis of Pancreatic Tumors Triggered by the Absence of Host SPARC. *Experimental Biology and Medicine*, *233*(7), 860-873.
- Barth, I., Schneider, U., Grimm, T., Karl, A., Horst, D., Gaisa, N. T., Garczyk, S. (2018). Progression of urothelial carcinoma in situ of the urinary bladder: a switch from luminal to basal phenotype and related therapeutic implications. *Virchows Archiv*, *472*(5), 749-758.

- Bernard, A. (2008). Cadmium & its adverse effects on human health. *Indian Journal of Medical Research*, 128(4), 557-564
- Bernhoft, R. A. (2013). Cadmium Toxicity and Treatment. *The Scientific World Journal*, 2013, 1-7.
- Bertin, G., & Averbeck, D. (2006). Cadmium: cellular effects, modifications of biomolecules, modulation of DNA repair and genotoxic consequences (a review). *Biochimie*, 88(11), 1549-1559.
- Bornstein, P. (1995). Diversity of function is inherent in matricellular proteins: An appraisal of thrombospondin 1. *Journal of Cell Biology*, 130(3), 503-506.
- Bornstein, P., & Sage, E. H. (2002). Matricellular proteins: Extracellular modulators of cell function. *Current Opinion in Cell Biology*, 14, 608-616.
- Bradshaw, A. D. (2012). Diverse biological functions of the SPARC family of proteins. *The International Journal of Biochemistry & Cell Biology*, 44(3), 480-488.
- Bradshaw, A. D. (2009). The role of SPARC in extracellular matrix assembly. *Journal of Cell Communication and Signaling*, 3(3-4), 239-246.
- Bradshaw, A. D., Puolakkainen, P., Dasgupta, J., Davidson, J. M., Wight, T. N., & Sage, E. H. (2003). SPARC-null mice display abnormalities in the dermis characterized by decreased collagen fibril diameter and reduced tensile strength. *Journal of Investigative Dermatology*, 120(6), 949-955.
- Bradshaw, A. D., & Sage, E. H. (2001). SPARC, a matricellular protein that functions in cellular differentiation and tissue response to injury. *Journal of Clinical Investigation*, 107(9), 1049-1054.
- Brekken, R. A., & Sage, E. H. (2001). SPARC, a matricellular protein: At the crossroads of cell-matrix communication. *Matrix Biology*, 19(8), 815-827.
- Brekken, R. A., & Bradshaw, A. D. (2010). The function of SPARC in tumor cell biology: SPARC as a modulator of cell-extracellular matrix interaction. In *Cell-Extracellular Matrix Interactions in Cancer* (pp. 171-189).
- Brekken, R. A., Puolakkainen, P., Graves, D. C., Workman, G., Lubkin, S. R., & Sage, E. H. (2003). Enhanced growth of tumors in SPARC null mice is associated with changes in the ECM. *Journal of Clinical Investigation*, 111(4), 487-495.
- Briggs, J., Chamboredon, S., Castellazzi, M., Kerry, J. A., & Bos, T. J. (2002). Transcriptional upregulation of SPARC, in response to c-Jun overexpression, contributes to increased motility and invasion of MCF7 breast cancer cells. *Oncogene*, 21(46), 7077-7091.

- Brown, T. J., Shaw, P. A., Karp, X., Huynh, M. H., Begley, H., & Ringuette, M. J. (1999). Activation of SPARC expression in reactive stroma associated with human epithelial ovarian cancer. *Gynecologic Oncology*, *75*(1), 25-33.
- Capper, D., Mittelbronn, M., Goeppert, B., Meyermann, R., & Schittenhelm, J. (2010). Secreted protein, acidic and rich in cysteine (SPARC) expression in astrocytic tumour cells negatively correlates with proliferation, while vascular SPARC expression is associated with patient survival. *Neuropathology and Applied Neurobiology*, *36*(3), 183-197.
- Chamboredon, S., Briggs, J., Vial, E., Hurault, J., Galvagni, F., Oliviero, S., Castellazzi, M. (2003). v-Jun downregulates the SPARC target gene by binding to the proximal promoter indirectly through Sp1/3. *Oncogene*, *22*(26), 4047-4061.
- Chen, C. S., Mrksich, M., Huang, S., Whitesides, G. M., & Ingber, D. E. (1997). Geometric control of cell life and death. *Science*, *276*(5317), 1425-1428.
- Chen, Q. Y., & Costa, M. (2017). A comprehensive review of metal-induced cellular transformation studies. *Toxicology and Applied Pharmacology*, *331*, 33–40.
- Chen, Z. Y., Zhang, J. L., Yao, H. X., Wang, P. Y., Zhu, J., Wang, W., Liu, Y. C. (2014). Aberrant methylation of the SPARC gene promoter and its clinical implication in gastric cancer. *Scientific Reports*, *4*.
- Cheng, M. L., & Iyer, G. (2018). Novel biomarkers in bladder cancer. *Urologic Oncology: Seminars and Original Investigations*, *36*(3), 115-119.
- Chiodoni, C., Colombo, M. P., & Sangaletti, S. (2010). Matricellular proteins: From homeostasis to inflammation, cancer, and metastasis. *Cancer and Metastasis Reviews*, *29*(2), 295-307.
- Chioran, A., Duncan, S., Catalano, A., Brown, T. J., & Ringuette, M. J. (2017). Collagen IV trafficking: The inside-out and beyond story. *Developmental Biology*, *431*(2), 124-133.
- Cirri, P., & Chiarugi, P. (2012). Cancer-associated-fibroblasts and tumour cells: A diabolic liaison driving cancer progression. *Cancer and Metastasis Reviews*, *31*(1-2), 195-208.
- Clark, B. Z., Onisko, A., Assylbekova, B., Li, X., Bhargava, R., & Dabbs, D. J. (2019). Breast cancer global tumor biomarkers: a quality assurance study of intratumoral heterogeneity. *Modern Pathology*, *32*(3), 354-366.
- Clark, C. J., & Sage, E. H. (2008). A prototypic matricellular protein in the tumor microenvironment - Where there's SPARC, there's fire. *Journal of Cellular Biochemistry*, *104*(3), 721-732.

- Costa, C. M., & Yang, S. (2009). Counting pollen grains using readily available, free image processing and analysis software. *Annals of Botany*, *104*(5), 1005-1010.
- Dehlinger, D., Suer, L., Elsheikh, M., Peña, J., & Naraghi-Arani, P. (2013). Dye free automated cell counting and analysis. *Biotechnology and Bioengineering*, *110*(3), 838-847.
- Delostrinos, C. F., Hudson, A. E., Feng, W. C., Kosman, J., & Bassuk, J. A. (2006). The C-terminal Ca²⁺-binding domain of SPARC confers anti-spreading activity to human urothelial cells. *Journal of Cellular Physiology*, *206*(1), 211-220.
- Dillekås, H., & Straume, O. (2019). The link between wound healing and escape from tumor dormancy. *Surgical Oncology*, *19*, 50-56.
- Dobruch, J., Daneshmand, S., Fisch, M., Lotan, Y., Noon, A. P., Resnick, M. J., Boorjian, S. A. (2016). Gender and Bladder Cancer: A Collaborative Review of Etiology, Biology, and Outcomes. *European Urology*, *69*(2), 300-310.
- Drabsch, Y., & Ten Dijke, P. (2011). TGF- β signaling in breast cancer cell invasion and bone metastasis. *Journal of Mammary Gland Biology and Neoplasia*, *16*(2), 97-108.
- Dvorak, H. F. (1986). Tumors: Wounds That Do Not Heal. *New England Journal of Medicine*, *315*(26), 1650-1659.
- Emerson, R. O., Sage, E. H., Ghosh, J. G., & Clark, J. I. (2006). Chaperone-like activity revealed in the matricellular protein SPARC. *Journal of Cellular Biochemistry*, *98*(4), 701-705.
- Environmental Protection Agency. (2014). Priority Pollutant List.
- Everitt, E. A., & Sage, E. H. (1992). Overexpression of SPARC in stably transfected F9 cells mediates attachment and spreading in Ca²⁺-deficient medium. *Biochemistry and Cell Biology*, *70*(12), 1368-1379.
- FDA-NIH Biomarker Working Group. (2016). BEST (Biomarkers, EndpointS, and other Tools) Resource.
- Flavell, R. A., Sanjabi, S., Wrzesinski, S. H., & Licona-Limón, P. (2010). The polarization of immune cells in the tumour environment by TGF- β . *Nature Reviews Immunology*, *10*(8), 554-567.
- Ford, R., Wang, G., Jannati, P., Adler, D., Racanelli, P., Higgins, P. J., & Staiano-Coico, L. (1993). Modulation of SPARC expression during butyrate-induced terminal differentiation of cultured human keratinocytes: Regulation via a TGF- β -dependent pathway. *Experimental Cell Research*, *206*(2), 261-275.

- Francki, A., Bradshaw, A. D., Bassuk, J. A., Howe, C. C., Couser, W. G., & Sage, E. H. (1999). SPARC regulates the expression of collagen type I and transforming growth factor- β 1 in mesangial cells. *Journal of Biological Chemistry*, 274(45), 32145-32152.
- Francki, A., McClure, T. D., Brekken, R. A., Motamed, K., Murri, C., Wang, T., & Sage, E. H. (2004). SPARC regulates TGF-beta1-dependent signaling in primary glomerular mesangial cells. *Journal of Cellular Biochemistry*, 91(5), 915-925.
- Funk, S. E., & Sage, E. H. (1993). Differential effects of SPARC and cationic SPARC peptides on DNA synthesis by endothelial cells and fibroblasts. *Journal of Cellular Physiology*, 154(1), 53-63.
- Galmozzi, F., Rubagotti, A., Romagnoli, A., Carmignani, G., Perdelli, L., Gatteschi, B., & Boccardo, F. (2006). Prognostic value of cell cycle regulatory proteins in muscle-infiltrating bladder cancer. *Journal of Cancer Research and Clinical Oncology*, 132(12), 757-764.
- Gao, J., Song, J., Huang, H., Li, Z., Du, Y., Cao, J., Gong, Y. (2010). Methylation of the SPARC gene promoter and its clinical implication in pancreatic cancer. *Journal of Experimental and Clinical Cancer Research*, 29(1).
- Garrett, S. H., Park, S., Sens, M. A., Somji, S., Singh, R. K., Namburi, V. B. R. K., & Sens, D. A. (2005). Expression of metallothionein isoform 3 is restricted at the post-transcriptional level in human bladder epithelial cells. *Toxicological Sciences*, 87(1), 66-74.
- Garrett, S. H., Somji, S., Sens, D. A., & Zhang, K. K. (2014). Prediction of the number of activated genes in multiple independent Cd⁺²- And As⁺³-induced malignant transformations of human urothelial cells (UROtsa). *PLoS ONE*, 9(1).
- Garvey, C. M., Spiller, E., Lindsay, D., Chiang, C. Te, Choi, N. C., Agus, D. B., Mumenthaler, S. M. (2016). A high-content image-based method for quantitatively studying context-dependent cell population dynamics. *Scientific Reports*, 6.
- Gilles, C., Bassuk, J. A., Pulyaeva, H., Sage, E. H., Foidart, J. M., & Thompson, E. W. (1998). SPARC/osteonectin induces matrix metalloproteinase 2 activation in human breast cancer cell lines. *Cancer Research*, 58(23), 5529-5536.
- Gilmour, D. T., Lyon, G. J., Carlton, M. B. L., Sanes, J. R., Cunningham, J. M., Anderson, J. R., Colledge, W. H. (1998). Mice deficient for the secreted glycoprotein SPARC/osteonectin/BM40 develop normally but show severe age-onset cataract formation and disruption of the lens. *EMBO Journal*, 17(7), 1860-1870.

- Giudici, C., Raynal, N., Wiedemann, H., Cabral, W. A., Marini, J. C., Timpl, R., Tenni, R. (2008). Mapping of SPARC/BM-40/osteonectin-binding sites on fibrillar collagens. *Journal of Biological Chemistry*, 283(28), 19551-19560.
- Gohring, W., Sasaki, T., Heldin, C. H., & Timpl, R. (1998). Mapping of the binding of platelet-derived growth factor to distinct domains of the basement membrane proteins BM-40 and perlecan and distinction from the BM-40 collagen-binding epitope. *European Journal of Biochemistry*, 255(1), 60-66.
- Grimm, D., Bauer, J., Wise, P., Krüger, M., Simonsen, U., Wehland, M., Corydon, T. J. (2019). The role of SOX family members in solid tumours and metastasis. *Seminars in Cancer Biology*.
- Hafner, M., Zimmermann, K., Pottgiesser, J., Krieg, T., & Nischt, R. (1994). A purine-rich sequence in the human BM-40 gene promoter region is a prerequisite for maximum transcription. *Matrix Biology*, 14(9), 733-741.
- Hanahan, D., & Weinberg, R. A. (2000). The hallmarks of cancer. *Cell*, 100(1), 57-70.
- Hanahan, D., & Weinberg, R. A. (2011). Hallmarks of cancer: the next generation. *Cell*, 144(5), 646-674.
- Harley, V. R., Lovell-badge, R., & Goodfellow, P. N. (1994). Definition of a consensus DNA binding site for SRY. *Nucleic Acids Research*, 22(8), 1500-1501.
- Hasselaar, P., & Sage, E. H. (1992). SPARC antagonizes the effect of basic fibroblast growth factor on the migration of bovine aortic endothelial cells. *Journal of Cellular Biochemistry*, 49(3), 272-283.
- Hoggarth, Z. E., Osowski, D. B., Freeberg, B. A., Garrett, S. H., Sens, D. A., Sens, M. A., Somji, S. (2018). The urothelial cell line UROtsa transformed by arsenite and cadmium display basal characteristics associated with muscle invasive urothelial cancers. *PLoS ONE*, 13(12).
- Hohenester, E., Maurer, P., Hohenadl, C., Timpl, R., Jansonius, J. N., & Engel, J. (1996). Structure of a novel extracellular Ca²⁺-binding module in BM-40. *Nature Structural Biology*, 3(1), 67-73.
- Hohenester, E., Maurer, P., & Timpl, R. (1997). Crystal structure of a pair of follistatin-like and EF-hand calcium-binding domains in BM-40. *EMBO Journal*, 16(13), 3778-3786.
- Hu, J., Tian, J., Zhu, S., Sun, L., Yu, J., Tian, H., Shang, Z. (2018). Sox5 contributes to prostate cancer metastasis and is a master regulator of TGF- β -induced epithelial mesenchymal transition through controlling Twist1 expression. *British Journal of Cancer*, 118(1), 88-97.

- Huang, D. Y., Lin, Y. T., Jan, P. S., Hwang, Y. C., Liang, S. T., Peng, Y., Lin, C. T. (2008). Transcription factor SOX-5 enhances nasopharyngeal carcinoma progression by down-regulating SPARC gene expression. *Journal of Pathology*, 214(4), 445-455.
- Hudson, A. E., Feng, W. C., Delostrinos, C. F., Carmean, N., & Bassuk, J. A. (2005). Spreading of embryologically distinct urothelial cells is inhibited by SPARC. *Journal of Cellular Physiology*, 202(2), 453-463.
- IARC. (1993). Cadmium and certain cadmium compounds. *IARC Monographs on the Evaluation of the Carcinogenic Risk of Chemicals to Humans. Beryllium, Cadmium, Mercury and Exposures in the Glass Manufacturing Industry*, 58, 1-119.
- Inamura, K. (2018). Bladder cancer: New insights into its molecular pathology. *Cancers*, 10(4).
- Infante, J. R., Matsubayashi, H., Sato, N., Tonascia, J., Klein, A. P., Riall, T. A., Goggins, M. (2007). Peritumoral fibroblast SPARC expression and patient outcome with resectable pancreatic adenocarcinoma. *Journal of Clinical Oncology*, 25(3), 319-325.
- Jaccard, N., Szita, N., & Griffin, L. D. (2015). Segmentation of phase contrast microscopy images based on multi-scale local Basic Image Features histograms. *Computer Methods in Biomechanics and Biomedical Engineering: Imaging and Visualization*, 5(5), 359-367.
- Jaccard, N., Griffin, L. D., Keser, A., Macown, R. J., Super, A., Veraitch, F. S., & Szita, N. (2014a). Automated method for the rapid and precise estimation of adherent cell culture characteristics from phase contrast microscopy images. *Biotechnology and Bioengineering*, 111(3), 504-517.
- Jaccard, N., Macown, R. J., Super, A., Griffin, L. D., Veraitch, F. S., & Szita, N. (2014b). Automated and Online Characterization of Adherent Cell Culture Growth in a Microfabricated Bioreactor. *Journal of Laboratory Automation*, 19(5), 437-443.
- Jacobs, B. L., Lee, C. T., & Montie, J. E. (2010). Bladder cancer in 2010: how far have we come? *CA: A Cancer Journal for Clinicians*, 60(4), 244-272.
- Jokinen, J., Dadu, E., Nykvist, P., Käpylä, J., White, D. J., Ivaska, J., Heino, J. (2004). Integrin-mediated cell adhesion to type I collagen fibrils. *Journal of Biological Chemistry*, 279(30), 31956-31963.
- Jung, A., Nielsen, M. E., Crandell, J. L., Palmer, M. H., Bryant, A. L., Smith, S. K., & Mayer, D. K. (2019). Quality of life in non-muscle-invasive bladder cancer survivors: A systematic review. *Cancer Nursing*, 42(3), E21-E33.

- Jutooru, I., Chadalapaka, G., Sreevalsan, S., Lei, P., Barhoumi, R., Burghardt, R., & Safe, S. (2010). Arsenic trioxide downregulates specificity protein (Sp) transcription factors and inhibits bladder cancer cell and tumor growth. *Experimental Cell Research*, *316*(13), 2174-2188.
- Kaffenberger, S. D., Miller, D. C., & Nielsen, M. E. (2018). Simplifying treatment and reducing recurrence for patients with early-stage bladder cancer. *JAMA - Journal of the American Medical Association*, *319*(18), 1864-1865.
- Kaṭnik-Prastowska, I., Lis, J., & Matejuk, A. (2014). Glycosylation of uroplakins. Implications for bladder physiopathology. *Glycoconjugate Journal*, *31*(9), 623–636.
- Kelm, R. J., & Mann, K. G. (1991). The collagen binding specificity of bone and platelet osteonectin is related to differences in glycosylation. *Journal of Biological Chemistry*, *266*(15), 9632-9639.
- Kent WJ, Sugnet CW, Furey TS, Roskin KM, Pringle TH, Zahler AM, Haussler D. (2002). The human genome browser at UCSC. *Genome Res.*, *12*(6), 996-1006.
- Khalili, A. A., & Ahmad, M. R. (2015). A Review of cell adhesion studies for biomedical and biological applications. *International Journal of Molecular Sciences*, *16*(8), 18149-18184.
- Kirkali, Z., Chan, T., Manoharan, M., Algaba, F., Busch, C., Cheng, L., Weider, J. (2005). Bladder cancer: epidemiology, staging and grading, and diagnosis. *Urology*, *66*(6 Suppl 1), 4-34.
- Knowles, M. A., & Hurst, C. D. (2015). Molecular biology of bladder cancer: New insights into pathogenesis and clinical diversity. *Nature Reviews Cancer*, *15*(1), 25-41.
- Kothinti, R. K., Blodgett, A. B., Petering, D. H., & Tabatabai, N. M. (2010a). Cadmium down-regulation of kidney Sp1 binding to mouse SGLT1 and SGLT2 gene promoters: Possible reaction of cadmium with the zinc finger domain of Sp1. *Toxicology and Applied Pharmacology*, *244*(3), 254-262.
- Kothinti, R., Blodgett, A., Tabatabai, N. M., & Petering, D. H. (2010b). Zinc finger transcription factor Zn3-Sp1 reactions with Cd²⁺. *Chemical Research in Toxicology*, *23*(2), 405–412.
- Kupprion, C., Motamed, K., & Sage, E. H. (1998). SPARC (BM-40, osteonectin) inhibits the mitogenic effect of vascular endothelial growth factor on microvascular endothelial cells. *Journal of Biological Chemistry*, *273*(45), 29635-29640.

- Kyriakides, T. R., & Bornstein, P. (2003). Matricellular proteins as modulators of wound healing and the foreign body response. *Thrombosis and Haemostasis*, 90(6), 986-992.
- Lane, T. F., & Sage, E. H. (1994). The biology of SPARC, a protein that modulates cell-matrix interactions. *FASEB Journal : Official Publication of the Federation of American Societies for Experimental Biology*, 8(2), 163-173.
- Lane, T. F., & Sage, E. H. (1990). Functional mapping of SPARC: Peptides from two distinct Ca²⁺-binding sites modulate cell shape. *Journal of Cell Biology*, 111(6 II), 3065-3076.
- Lane, T. F., Iruela-Arispe, M. L., Johnson, R. S., & Sage, E. H. (1994). SPARC is a source of copper-binding peptides that stimulate angiogenesis. *Journal of Cell Biology*, 125(4), 929-943.
- Lankat-Buttgereit, B., Mann, K., Deutzmann, R., Timpl, R., & Krieg, T. (1988). Cloning and complete amino acid sequences of human and murine basement membrane protein BM-40 (SPARC, osteonectin). *FEBS Letters*, 236(2), 352-356.
- Larabee, J. L., Hocker, J. R., & Hanas, J. S. (2005). Cys redox reactions and metal binding of a Cys2His2 zinc finger. *Archives of Biochemistry and Biophysics*, 434(1 SPEC. ISS.), 139-149.
- Larson, J. L. (2012). *The UROtsa Bladder Cell Model for Heavy Metal Carcinogenesis: Characterization with Respect to the Role of Beclin-1 and SPARC Expression* (Doctoral Dissertation, University of North Dakota, 2012). Ann Arbor, MI: ProQuest LLC.
- Larson, J., Yasmin, T., Sens, D. A., Zhou, X. D., Sens, M. A., Garrett, S. H., Somji, S. (2010). SPARC gene expression is repressed in human urothelial cells (UROtsa) exposed to or malignantly transformed by cadmium or arsenite. *Toxicology Letters*, 199(2), 166-172.
- Ledda, M. F., Adris, S., Bravo, A. I., Kairiyama, C., Bover, L., Chernajovsky, Y., Podhajcer, O. L. (1997). Suppression of SPARC expression by antisense RNA abrogates the tumorigenicity of human melanoma cells. *Nature Medicine*, 3(2), 171-176.
- Lee, P., Yeo, G. C., & Weiss, A. S. (2017). A cell adhesive peptide from tropoelastin promotes sequential cell attachment and spreading via distinct receptors. *FEBS Journal*, 284(14), 2216-2230.
- Lefebvre, V., Li, P., & De Crombrughe, B. (1998). A new long form of Sox5 (L-Sox5), Sox6 and Sox9 are coexpressed in chondrogenesis and cooperatively activate the type II collagen gene. *EMBO Journal*, 17(19), 5718-5733.

- Lefebvre, V., Dumitriu, B., Penzo-Méndez, A., Han, Y., & Pallavi, B. (2007). Control of cell fate and differentiation by Sry-related high-mobility-group box (Sox) transcription factors. *International Journal of Biochemistry and Cell Biology*, 39(12), 2195-2214.
- Lewis, S. A. (2000). Everything you wanted to know about the bladder epithelium but were afraid to ask. *American Journal of Physiology-Renal Physiology*, 278(6), F867–F874.
- Li, L., & Davie, J. R. (2010). The role of Sp1 and Sp3 in normal and cancer cell biology. *Annals of Anatomy*, 192(5), 275-283.
- Liu, T., Qiu, X., Zhao, X., Yang, R., Lian, H., Qu, F., Guo, H. (2018). Hypermethylation of the SPARC promoter and its prognostic value for prostate cancer. *Oncology Reports*, 39(2), 659-666.
- Luevano, J., & Damodaran, C. (2014). A review of molecular events of cadmium-induced carcinogenesis. *Journal of Environmental Pathology, Toxicology and Oncology : Official Organ of the International Society for Environmental Toxicology and Cancer*, 33(3), 183-194.
- Ma, Z., Shah, R. C., Chang, M. J., & Benveniste, E. N. (2004). Coordination of Cell Signaling, Chromatin Remodeling, Histone Modifications, and Regulator Recruitment in Human Matrix Metalloproteinase 9 Gene Transcription. *Molecular and Cellular Biology*, 24(12), 5496-5509.
- Ma, Z., Chang, M. J., Shah, R., Adamski, J., Zhao, X., & Benveniste, E. N. (2004). Brg-1 is required for maximal transcription of the human matrix metalloproteinase-2 gene. *Journal of Biological Chemistry*, 279(44), 46326-46334.
- Mantoni, T. S., Schendel, R. R. E., Rodel, F., Niedobitek, G., Al-Assar, O., & Masamune, A. (2008). Stromal SPARC expression and patient survival after chemoradiation for non-resectable pancreatic adenocarcinoma. *Cancer Biology and Therapy*, 7(11), 1807-1816.
- Mao, Z., Ma, X., Fan, X., Cui, L., Zhu, T., Qu, J., Wang, X. (2014). Secreted protein acidic and rich in cysteine inhibits the growth of human pancreatic cancer cells with G1 arrest induction. *Tumor Biology*, 35(10), 10185-10193.
- Martinek, N., Shahab, J., Sodek, J., & Ringuette, M. (2007). Is SPARC an evolutionary conserved collagen chaperone? *Journal of Dental Research*, 86(4), 296-305.
- Mason, I. J., Taylor, A., Williams, J. G., Sage, H., & Hogan, B. L. (1986). Evidence from molecular cloning that SPARC, a major product of mouse embryo parietal endoderm, is related to an endothelial cell 'culture shock' glycoprotein of Mr 43,000. *The EMBO Journal*, 5(7), 1465-1472.

- Maurer, P., Göhring, W., Sasaki, T., Mann, K., Timpl, R., & Nischt, R. (1997). Recombinant and tissue-derived mouse BM-40 bind to several collagen types and have increased affinities after proteolytic activation. *Cellular and Molecular Life Sciences*, 53(5), 478-484.
- Maurer, P., Hohenadl, C., Hohenester, E., Göhring, W., Timpl, R., & Engel, J. (1995). The C-terminal portion of BM-40 (SPARC/osteonectin) is an autonomously folding and crystallisable domain that binds calcium and collagen IV. *Journal of Molecular Biology*, 253(2), 347-357.
- Mayeux, R. (2004). Biomarkers: Potential Uses and Limitations. *NeuroRx*, 1(2), 182-188.
- McVey, J. H., Nomura, S., Kelly, P., Mason, I. J., & Hogan, B. L. M. (1988). Characterization of the mouse SPARC/osteonectin gene. Intron/exon organization and an unusual promoter region. *Journal of Biological Chemistry*, 263(23), 11111-11116.
- Midwood, K. S., Williams, L. V., & Schwarzbauer, J. E. (2004). Tissue repair and the dynamics of the extracellular matrix. *International Journal of Biochemistry and Cell Biology*, 36(6), 1031-1037.
- Miremami, J., & Kyprianou, N. (2014). The promise of novel molecular markers in bladder cancer. *International Journal of Molecular Sciences*, 15(12), 23897-23908.
- Mok, S. C., Chan, W. Y., Wong, K. K., Muto, M. G., & Berkowitz, R. S. (1996). SPARC, an extracellular matrix protein with tumor-suppressing activity in human ovarian epithelial cells. *Oncogene*, 12(9), 1895-1901.
- Morrissey, M. A., Jayadev, R., Miley, G. R., Blebea, C. A., Chi, Q., Ihara, S., & Sherwood, D. R. (2016). SPARC Promotes Cell Invasion In Vivo by Decreasing Type IV Collagen Levels in the Basement Membrane. *PLoS Genetics*, 12(2).
- Motamed, K., Funk, S. E., Koyama, H., Ross, R., Raines, E. W., & Sage, E. H. (2002). Inhibition of PDGF-stimulated and matrix-mediated proliferation of human vascular smooth muscle cells by SPARC is independent of changes in cell shape or cyclin-dependent kinase inhibitors. *Journal of Cellular Biochemistry*, 84(4), 759-771.
- Motamed, K., & Sage, E. H. (1998). SPARC inhibits endothelial cell adhesion but not proliferation through a tyrosine phosphorylation-dependent pathway. *Journal of Cellular Biochemistry*, 70(4), 543-552.
- Munk, R., Martindale, J. L., Yang, X., Yang, J. H., Grammatikakis, I., Germanio, C. Di, Panda, A. C. (2019). Loss of miR-451a enhances SPARC production during myogenesis. *PLoS ONE*, 14(3), 1-14.

- Murphy-Ullrich, J. E., Schultz-Cherry, S., & Hook, M. (1992). Transforming growth factor-beta complexes with thrombospondin. *Molecular Biology of the Cell*, 3(2), 181-188.
- Murphy-Ullrich, J. E., Lightner, V. A., Aukhil, I., Yan, Y. Z., Erickson, H. P., & Höök, M. (1991). Focal adhesion integrity is downregulated by the alternatively spliced domain of human tenascin. *Journal of Cell Biology*, 115(4), 1127-1136.
- Murphy-Ullrich, J. E., & Sage, E. H. (2014). Revisiting the matricellular concept. *Matrix Biology*, 37, 1-14.
- Nagaraju, G. P., Dontula, R., El-Rayes, B. F., & Lakka, S. S. (2014). Molecular mechanisms underlying the divergent roles of SPARC in human carcinogenesis. *Carcinogenesis*, 35(5), 967-973.
- Negrete, H. O., Lavelle, J. P., Berg, J., Lewis, S. A., & Zeidel, M. L. (1996). Permeability properties of the intact mammalian bladder epithelium. *American Journal of Physiology - Renal Fluid and Electrolyte Physiology*, 271(4), F886-F894.
- Nordberg, G. F. (2009). Historical perspectives on cadmium toxicology. *Toxicology and Applied Pharmacology*, 238(3), 192-200.
- Norose, K., Clark, J. I., Syed, N. A., Basu, A., Heber-Katz, E., Sage, E. H., & Howe, C. C. (1998). SPARC deficiency leads to early-onset cataractogenesis. *Investigative Ophthalmology and Visual Science*, 39(13), 2674-2680.
- Ogasawara, M. A., & Zhang, H. (2009). Redox Regulation and Its Emerging Roles in Stem Cells and Stem-Like Cancer Cells. *Antioxidants & Redox Signaling*, 11(5), 1107-1122.
- Page, A. L., Chang, A. C., & El-Amamy, M. (1987). Cadmium Levels in Soils and Crops in the United States. *Lead, Mercury Cadmium and Arsenic in the Environment*, 119-146.
- Patthy, L. (1991). Exons – original building blocks of proteins? *BioEssays*, 13(4), 187-192.
- Pawlina, W. (2016). Urinary System. In *Histology A Text and Atlas, With Correlated Cell and Molecular Biology* (7th ed., pp. 698-741). Philadelphia, PA: Wolters Kluwer Health.
- Pei, X. H., Lv, X. Q., & Li, H. X. (2014). Sox5 induces epithelial to mesenchymal transition by transactivation of Twist1. *Biochemical and Biophysical Research Communications*, 446(1), 322-327.

- Petzoldt, J. L., Leigh, I. M., Duffy, P. G., & Masters, J. R. W. (1994). Culture and characterisation of human urothelium in vivo and in vitro. *Urological Research*, 22(2), 67-74.
- Petzoldt, J. L., Leigh, I. M., Duffy, P. G., Sexton, C., & Masters, J. R. W. (1995). Immortalisation of human urothelial cells. *Urological Research*, 23(6), 377-380.
- Pickup, M. W., Mouw, J. K., & Weaver, V. M. (2014). The extracellular matrix modulates the hallmarks of cancer. *EMBO Reports*, 15(12), 1243-1253.
- Podhajcer, O. L., Benedetti, L. G., Girotti, M. R., Prada, F., Salvatierra, E., & Llera, A. S. (2008). The role of the matricellular protein SPARC in the dynamic interaction between the tumor and the host. *Cancer and Metastasis Reviews*, 27(4), 691-705.
- Pottgiesser, J., Maurer, P., Mayer, U., Nischt, R., Mann, K., Timpl, R., Engel, J. (1994). Changes in calcium and collagen IV binding caused by mutations in the EF hand and other domains of extracellular matrix protein BM-40 (SPARC, osteonectin). *Journal of Molecular Biology*, 238(4), 563-574.
- Prada, F., Benedetti, L. G., Bravo, A. I., Alvarez, M. J., Carbone, C., & Podhajcer, O. L. (2007). SPARC endogenous level, rather than fibroblast-produced SPARC or stroma reorganization induced by SPARC, is responsible for melanoma cell growth. *Journal of Investigative Dermatology*, 127(11), 2618-2628.
- Prenzel, K. L., Warnecke-Eberz, U., Xi, H., Brabender, J., Baldus, S. E., Bollschweiler, E., Schneider, P. M. (2006). Significant overexpression of SPARC/osteonectin mRNA in pancreatic cancer compared to cancer of the papilla of Vater. *Oncology Reports*, 15(5), 1397-1401.
- Puolakkainen, P. A., Brekken, R. A., Muneer, S., & Sage, E. H. (2004). Enhanced Growth of Pancreatic Tumors in SPARC-Null Mice Is Associated With Decreased Deposition of Extracellular Matrix and Reduced Tumor Cell Apoptosis. *Molecular Cancer Research*, 2(4), 215-224.
- Rani, A., Kumar, A., Lal, A., & Pant, M. (2014). Cellular mechanisms of cadmium-induced toxicity: A review. *International Journal of Environmental Health Research*, 24(4), 378-399.
- Reid, L. M., Leav, I., Kwan, P. W. L., Merk, F. B., & Russell, P. (1984). Characterization of a Human, Sex Steroid-responsive Transitional Cell Carcinoma Maintained as a Tumor Line (R198) in Athymic Nude Mice. *Cancer Research*, 44(10), 4560-4573.
- Ristic, L., Vucevic, D., Radovic, L., Djordjevic, S., Nikacevic, M., & Colic, M. (2014). Corrosive and cytotoxic properties of compact specimens and microparticles of Ni-Cr dental alloy. *Journal of Prosthodontics*, 23(3), 221-226.

- Rossi, M. R., Masters, J. R. W., Park, S., Todd, J. H., Garrett, S. H., Sens, M. A., Sens, D. A. (2001). The immortalized UROtsa cell line as a potential cell culture model of human urothelium. *Environmental Health Perspectives*, 109(8), 801-808.
- Sage, E. H. (2003). Purification of SPARC/Osteonectin. *Current Protocols in Cell Biology*, 17(1), 10.11.1-10.11.23.
- Sage, E. H., Bassuk, J. A., Yost, J. C., Folkman, M. J., & Lane, T. F. (1995). Inhibition of endothelial cell proliferation by SPARC is mediated through a Ca²⁺-binding EF-hand sequence. *Journal of Cellular Biochemistry*, 57(1), 127-140.
- Sage, H., Johnson, C., & Bornstein, P. (1984). Characterization of a novel serum albumin-binding glycoprotein secreted by endothelial cells in culture. *Journal of Biological Chemistry*, 259(6), 3993-4007.
- Sage, H., Vernon, R. B., Funk, S. E., Everitt, E. A., & Angello, J. (1989). SPARC, a secreted protein associated with cellular proliferation, inhibits cell spreading in vitro and exhibits Ca²⁺-dependent binding to the extracellular matrix. *Journal of Cell Biology*, 109(1), 341-356.
- Said, N., Socha, M. J., Olearczyk, J. J., Elmarakby, A. A., Imig, J. D., & Motamed, K. (2007). Normalization of the Ovarian Cancer Microenvironment by SPARC. *Molecular Cancer Research*, 5(10), 1015-1030.
- Said, N. (2016). Roles of SPARC in urothelial carcinogenesis, progression and metastasis. *Oncotarget*, 7(41), 67574-67585.
- Said, N., Frierson, H. F., Sanchez-Carbayo, M., Brekken, R. A., & Theodorescu, D. (2013). Loss of SPARC in bladder cancer enhances carcinogenesis and progression. *Journal of Clinical Investigation*, 123(2), 751-766.
- Said, N., Najwer, I., & Motamed, K. (2007). Secreted protein acidic and rich in cysteine (SPARC) inhibits integrin-mediated adhesion and growth factor-dependent survival signaling in ovarian cancer. *American Journal of Pathology*, 170(3), 1054-1063.
- Said, N., & Theodorescu, D. (2013). Secreted Protein Acidic and Rich in Cysteine (SPARC) in Cancer. *Journal of Carcinogenesis & Mutagenesis*, 4(3).
- Sangaletti, S., Stoppacciaro, A., Guiducci, C., Torrisi, M. R., & Colombo, M. P. (2003). Leukocyte, Rather than Tumor-produced SPARC, Determines Stroma and Collagen Type IV Deposition in Mammary Carcinoma. *The Journal of Experimental Medicine*, 198(10), 1475-1485.
- Sasaki, T., Göhring, W., Mann, K., Maurer, P., Hohenester, E., Knäuper, V., Timpl, R. (1997). Limited cleavage of extracellular matrix protein BM-40 by matrix

- metalloproteinases increases its affinity for collagens. *Journal of Biological Chemistry*, 272(14), 9237-9243.
- Sasaki, T., Hohenester, E., Göhring, W., & Timpl, R. (1998). Crystal structure and mapping by site-directed mutagenesis of the collagen-binding epitope of an activated form of BM-40/SPARC/osteonectin. *EMBO Journal*, 17(6), 1625-1634.
- Satarug, S., Garrett, S. H., Sens, M. A., & Sens, D. A. (2010). Cadmium, environmental exposure, and health outcomes. *Environmental Health Perspectives*, 118(2), 182-190.
- Sato, N., Fukushima, N., Maehara, N., Matsubayashi, H., Koopmann, J., Su, G. H., Goggins, M. (2003). SPARC/osteonectin is a frequent target for aberrant methylation in pancreatic adenocarcinoma and a mediator of tumor-stromal interactions. *Oncogene*, 22(32), 5021-5030.
- Schiemann, B. J. (2003). SPARC Inhibits Epithelial Cell Proliferation in Part through Stimulation of the Transforming Growth Factor- β -Signaling System. *Molecular Biology of the Cell*, 14(10), 3977-3988.
- Schultz, C., Lemke, N., Ge, S., Golembieski, W. A., & Rempel, S. A. (2002). Secreted protein acidic and rich in cysteine promotes glioma invasion and delays tumor growth in vivo. *Cancer Research*, 62(21), 6270-6277.
- Schwarzbauer, J. E., Musset-Bilal, F., & Ryan, C. S. (1994). Extracellular calcium-binding protein SPARC/osteonectin in *Caenorhabditis elegans*. *Methods in Enzymology*, 245(C), 257-270.
- Sens, D. A., Park, S., Gurel, V., Sens, M. A., Garrett, S. H., & Somji, S. (2004). Inorganic cadmium- and arsenite-induced malignant transformation of human bladder urothelial cells. *Toxicological Sciences*, 79(1), 56-63.
- Shariat, S. F., Ashfaq, R., Sagalowsky, A. I., & Lotan, Y. (2006). Correlation of cyclin D1 and E1 expression with bladder cancer presence, invasion, progression, and metastasis. *Human Pathology*, 37(12), 1568-1576.
- Shi, Q., Bao, S., Song, L., Wu, Q., Bigner, D. D., Hjelmeland, A. B., & Rich, J. N. (2007). Targeting SPARC expression decreases glioma cellular survival and invasion associated with reduced activities of FAK and ILK kinases. *Oncogene*, 26(28), 4084-4094.
- Shiba, H., Fujita, T., Doi, N., Nakamura, S., Nakanishi, K., Takemoto, T., Kato, Y. (1998). Differential effects of various growth factors and cytokines on the syntheses of DNA, type I collagen, laminin, fibronectin, osteonectin/secreted protein, acidic and rich in cysteine (SPARC), and alkaline phosphatase by human pulp cells in culture. *Journal of Cellular Physiology*, 174(2), 194-205.

- Slusser-Nore, A., Larson-Casey, J. L., Zhang, R., Zhou, X. D., Somji, S., Garrett, S. H., Dunlevy, J. R. (2016). SPARC Expression Is Selectively Suppressed in Tumor Initiating Urospheres Isolated from As⁺³- and Cd⁺²-Transformed Human Urothelial Cells (UROtsa) Stably Transfected with SPARC. *PLoS ONE*, *11*(1).
- Socha, M. J., Said, N., Dai, Y., Kwong, J., Ramalingam, P., Trieu, V., Motamed, K. (2009). Aberrant promoter methylation of SPARC in ovarian cancer. *Neoplasia*, *11*(2), 126-135.
- Somji, S., Sens, M. A., Lamm, D. L., Garrett, S. H., & Sens, D. A. (2001). Metallothionein isoform 1 and 2 gene expression in the human bladder: evidence for upregulation of MT-1X mRNA in bladder cancer. *Cancer Detection and Prevention*, *25*(1), 62-75.
- Somji, S., Garrett, S. H., Toni, C., Zhou, X. D., Zheng, Y., Ajjimaporn, A., Sens, D. A. (2011). Differences in the epigenetic regulation of MT-3 gene expression between parental and Cd⁺² or As⁺³ transformed human urothelial cells. *Cancer Cell International*, *11*(2).
- Somji, S., Zhou, X. D., Garrett, S. H., Sens, M. A., & Sens, D. A. (2006). Urothelial cells malignantly transformed by exposure to cadmium (Cd⁺²) and arsenite (As⁺³) have increased resistance to Cd⁺² and As⁺³-induced cell death. *Toxicological Sciences*, *94*(2), 293-301.
- Somji, S., Zhou, X. D., Mehus, A., Sens, M. A., Garrett, S. H., Lutz, K. L., Sens, D. A. (2010). Variation of keratin 7 expression and other phenotypic characteristics of independent isolates of cadmium transformed human urothelial cells (UROtsa). *Chemical Research in Toxicology*, *23*(2), 348-356.
- Strimbu, K., & Tavel, J. A. (2010). What are biomarkers? *Current Opinion in HIV and AIDS*, *5*(6), 463-466.
- Strobeck, M. W., DeCristofaro, M. F., Banine, F., Weissman, B. E., Sherman, L. S., & Knudsen, E. S. (2001). The BRG-1 Subunit of the SWI/SNF Complex Regulates CD44 Expression. *Journal of Biological Chemistry*, *276*(12), 9273-9278.
- Swaroop, A., Hogan, B. L., & Francke, U. (1988). Molecular analysis of the cDNA for human SPARC/osteonectin/BM-40: sequence, expression, and localization of the gene to chromosome 5q31-q33. *Genomics*, *2*(1), 37-47.
- Tabayoyong, W., & Kamat, A. M. (2018). Current Use and Promise of Urinary Markers for Urothelial Cancer. *Current Urology Reports*, *19*(12), 96.
- Tai, I. T., & Tang, M. J. (2008). SPARC in cancer biology: Its role in cancer progression and potential for therapy. *Drug Resistance Updates*, *11*(6), 231-246.

- Tang, M. J., & Tai, I. T. (2007). A novel interaction between procaspase 8 and SPARC enhances apoptosis and potentiates chemotherapy sensitivity in colorectal cancers. *Journal of Biological Chemistry*, 282(47), 34457-34467.
- Tardáguila-García, A., García-Morales, E., García-Alamino, J. M., Álvaro-Afonso, F. J., Molines-Barroso, R. J., & Lázaro-Martínez, J. L. (2019). Metalloproteinases in chronic and acute wounds: A systematic review and meta-analysis. *Wound Repair and Regeneration*.
- Termine, J. D., Kleinman, H. K., Whitson, S. W., Conn, K. M., McGarvey, M. L., & Martin, G. R. (1981). Osteonectin, a bone-specific protein linking mineral to collagen. *Cell*, 26(1 PART 1), 99-105.
- Terret, C., Fléchon, A., & Droz, J. P. (2010). Prostate cancer. *ESMO Handbook of Cancer in the Senior Patient*, 388(10061), 114-120.
- Therhault, D. H., Walker, M. L., Wong, J. Y., & Betke, M. (2012). Cell morphology classification and clutter mitigation in phase-contrast microscopy images using machine learning. In *Machine Vision and Applications*, 23(4), 659-673.
- Tremble, P. M., Lane, T. F., Sage, E. H., & Werb, Z. (1993). SPARC, a secreted protein associated with morphogenesis and tissue remodeling, induces expression of metalloproteinases in fibroblasts through a novel extracellular matrix-dependent pathway. *Journal of Cell Biology*, 121(6), 1433-1444.
- Truty, M. J., & Urrutia, R. (2007). Basics of TGF- β and pancreatic cancer. *Pancreatology*, 7(5-6), 423-435.
- Ungefroren, H., Sebens, S., Seidl, D., Lehnert, H., & Hass, R. (2011). Interaction of tumor cells with the microenvironment. *Cell Communication and Signaling*, 9(18).
- Vacchi-Suzzi, C., Kruse, D., Harrington, J., Levine, K., & Meliker, J. R. (2016). Is Urinary Cadmium a Biomarker of Long-term Exposure in Humans? A Review. *Current Environmental Health Reports*, 3(4), 450-458.
- Vaz, J., Ansari, D., Sasor, A., & Andersson, R. (2015). SPARC: A Potential Prognostic and Therapeutic Target in Pancreatic Cancer. *Pancreas*, 44(7), 1024-1035.
- Vial, E., Perez, S., & Castellazzi, M. (2000). Transcriptional control of SPARC by v-Jun and other members of the AP1 family of transcription factors. *Oncogene*, 19(43), 5020-5029.
- Vizcaíno, C., Mansilla, S., & Portugal, J. (2015). Sp1 transcription factor: A long-standing target in cancer chemotherapy. *Pharmacology and Therapeutics*, 152, 111-124.

- Waisberg, M., Joseph, P., Hale, B., & Beyersmann, D. (2003). Molecular and cellular mechanisms of cadmium carcinogenesis. *Toxicology*, *192*(2-3), 95-117.
- Wang, D., Han, S., Wang, X., Peng, R., & Li, X. (2015). SOX5 promotes epithelial–mesenchymal transition and cell invasion via regulation of Twist1 in hepatocellular carcinoma. *Medical Oncology*, *32*(2).
- Wang, H., Fertala, A., Ratner, B. D., Sage, E. H., & Jiang, S. (2005). Identifying the SPARC binding sites on collagen I and procollagen I by atomic force microscopy. *Analytical Chemistry*, *77*(21), 6765-6771.
- Wegner, M. (2010). All purpose Sox: The many roles of Sox proteins in gene expression. *International Journal of Biochemistry and Cell Biology*, *42*(3), 381-390.
- Wong, G. S., & Rustgi, A. K. (2013). Matricellular proteins: Priming the tumour microenvironment for cancer development and metastasis. *British Journal of Cancer*, *108*(4), 755-761.
- Wu, X. R., Kong, X. P., Pellicer, A., Kreibich, G., & Sun, T. T. (2009). Uroplakins in urothelial biology, function, and disease. *Kidney International*, *75*, 1153-1165.
- Xu, Y., Gurusiddappa, S., Rich, R. L., Owens, R. T., Keene, D. R., Mayne, R., Höök, M. (2000). Multiple binding sites in collagen type I for the integrins $\alpha_1\beta_1$ and $\alpha_2\beta_1$. *Journal of Biological Chemistry*, *275*(50), 38981-38989.
- Xu, Y. Z., Heravi, M., Thuraisingam, T., Marco, S. D., Muanza, T., & Radzioch, D. (2010). Brg-1 mediates the constitutive and fenretinide-induced expression of SPARC in mammary carcinoma cells via its interaction with transcription factor Sp1. *Molecular Cancer*, *9*(210).
- Xu, Y., Yang, L., Jiang, X., Yu, J., Yang, J., Zhang, H., Liu, F. (2013). Adenovirus-mediated coexpression of DCX and SPARC radiosensitizes human malignant glioma cells. *Cellular and Molecular Neurobiology*, *33*(7), 965-971.
- Yamanaka, M., Kanda, K., Li, N. C., Fukumori, T., Oka, N., Kanayama, H. O., & Kagawa, S. (2001). Analysis of the gene expression of SPARC and its prognostic value for bladder cancer. *The Journal of Urology*, *166*(6), 2495-2499.
- Yan, J., Zhang, J., Zhang, X., Li, X., Li, L., Li, Z., Zhang, M. (2018). SPARC is down-regulated by DNA methylation and functions as a tumor suppressor in T-cell lymphoma. *Experimental Cell Research*, *364*(2), 125-132.
- Yan, Q., Clark, J. I., Wight, T. N., & Sage, E. H. (2002). Alterations in the lens capsule contribute to cataractogenesis in SPARC-null mice. *Journal of Cell Science*, *115*(Pt 13), 2747-2756.

- Yan, Q., & Sage, E. H. (1999). SPARC, a matricellular glycoprotein with important biological functions. *Journal of Histochemistry and Cytochemistry*, 47(12), 1495-1505.
- Yang, H., & Shu, Y. (2015). Cadmium transporters in the kidney and cadmium-induced nephrotoxicity. *International Journal of Molecular Sciences*, 16(1), 1484-1494.
- Young, M. F., Findlay, D. M., Dominguez, P., Burbelo, P. D., McQuillan, C., Kopp, J. B., Termine, J. D. (1989). Osteonectin promoter. DNA sequence analysis and S1 endonuclease site potentially associated with transcriptional control in bone cells. *Journal of Biological Chemistry*, 264(1), 450-456.
- Zalups, R. K., & Ahmad, S. (2003). Molecular handling of cadmium in transporting epithelia. *Toxicology and Applied Pharmacology*, 186(3), 163-188.
- Zhang, D., Hudson, A. E., Delostrinos, C. F., Carmean, N., Eastman, R., Hicks, B., Bassuk, J. A. (2011). Dual sources of vitronectin in the human lower urinary tract: synthesis by urothelium vs. extravasation from the bloodstream. *American Journal of Physiology-Renal Physiology*, 300(2), F475-F487.
- Zhang, W. M., Käpylä, J., Puranen, J. S., Knight, C. G., Tiger, C. F., Pentikäinen, O. T., Gullberg, D. (2003). $\alpha_1\beta_1$ integrin recognizes the GFOGER sequence in interstitial collagens. *Journal of Biological Chemistry*, 278(9), 7270-7277.
- Ziani, L., Chouaib, S., & Thiery, J. (2018). Alteration of the antitumor immune response by cancer-associated fibroblasts. *Frontiers in Immunology*, 9(414).
- Zorretto, V. A., Silveira, G. G., Oliveira-Costa, J. P., Soave, D. F., Soares, F. A., & Ribeiro-Silva, A. (2013). The relationship between lymphatic vascular density and vascular endothelial growth factor A (VEGF-A) expression with clinical-pathological features and survival in pancreatic adenocarcinomas. *Diagnostic Pathology*, 8(1).